Performance Analysis and Interference Management in Underlay D2D Cellular Networks

A
Thesis Submitted
in Partial Fulfillment of the Requirements
for the Degree of

DOCTOR OF PHILOSOPHY

By

Mahari Berhe Tsegay

DEPARTMENT OF ELECTRONICS AND ELECTRICAL ENGINEERING
INDIAN INSTITUTE OF TECHNOLOGY GUWAHATI
GUWAHATI-781039, ASSAM, INDIA
August, 2023

Declaration

I hereby declare that the thesis entitled "**PERFORMANCE ANALYSIS AND INTERFERENCE MANAGEMENT IN UNDERLAY D2D CELLULAR NETWORKS**", submitted in the *Department of Electronics and Electrical Engineering*, *Indian Institute of Technology Guwahati, Assam, India*, for the award of the degree of **Doctor of Philosophy**, is a bonafide work carried out by me under the supervision of Prof. Ratnajit Bhattacharjee and Dr. Kalpana Dhaka. The content of this thesis, in full or in parts, have not been submitted to any other University or Institute for the award of any degree or diploma. I also wish to state that to the best of my knowledge and understanding nothing in this report amounts to plagiarism.

Mahari Berhe Tsegay
Research Scholar
Department of Electronics and Electrical Engineering
Indian Institute of Technology Guwahati
Guwahati-781039, Assam, India.

Date:

Place: Guwahati

Certificate

This is to certify that the thesis entitled "**PERFORMANCE ANALYSIS AND INTERFERENCE MANAGEMENT IN UNDERLAY D2D CELLULAR NETWORKS**", submitted by Mahari Berhe Tsegay (156102021), a research scholar in the *Department of Electronics and Electrical Engineering*, *Indian Institute of Technology Guwahati*, for the award of the degree of **Doctor of Philosophy**, is a record of an original research work carried out by him under our supervision and guidance. The thesis has fulfilled all requirements as per the regulations of the institute and in my opinion has reached the standard needed for submission. The results embodied in this thesis have not been submitted to any other University or Institute for the award of any degree or diploma.

Prof. Ratnajit Bhattacharjee
Professor
Department of Electronics and Electrical Engineering
Indian Institute of Technology Guwahati
Guwahati-781039, Assam, India.

Dr. Kalpana Dhaka
Associate Professor
Department of Electronics and Electrical Engineering
Indian Institute of Technology Guwahati
Guwahati-781039, Assam, India.

Date:
Place: Guwahati

Dedicated to
My beloved Wife
and
kids

Who always love me,
for their patience and encouragement
on this long journey and adventure,
specially this one

Acknowledgements

First and foremost, I would like to express my heartfelt gratitude to my supervisors Prof. Ratnajit Bhattacharjee and Dr. Kalpana Dhaka, Department of Electronics and Electrical Engineering, Indian Institute of Technology Guwahati, for their consistent support, inexhaustible patience, and positive guidance during my doctoral research. Without their full support and guidance, I would have never attained progress on my research and hardly completed it. I am thankful for their ethical beliefs and philosophy, which made me mature as a scientific researcher and a human. I would like to convey my deepest gratitude to my family, my wife, my daughter, and my son for their immense love, patience, understanding, and faith in me. Specifically, I am in debt, grateful to my wife for being strong, hardworking, and brave to support our family in the worst times of my people, the people of Tigray. I would also like to express my heartfelt thanks to my friends Dr. Mohammed A. Adem Cherinet Kejela, Dr. Amare Wubineh Mengste, and Achenf Fentaw for helping me, for making my stay at IITG unforgettable and for being good friends one can ever ask for. Last but not least, a huge thanks to the whole IITG community for being helpful, understanding, friendly and cooperative which makes my stay at IITG full of good memories with a number of good friends for life.

Sincerely
Mahari Berhe Tsegay

Abstract

With the advancement in technology, the demand for wireless data is growing explosively over years. The unprecedented rise in demand for higher data rates is attributed to factors such as an increase in the number of mobile applications, alarming growth in bandwidth-needy applications like video streaming, and the use of multiple devices by the same user. This has resulted in a push for an investigation of new architecture and technologies to satisfy the ever increasing demands and requirements of the wireless networks.

Data-based applications have gained immense popularity as a necessity in our day-to-day life. In order to connect the growing number of wireless devices, resources are reused in the cellular system. In the traditional cellular wireless network, the cellular user equipment (UE) communicates its data to the base station (BS) using uplink (UL) network resources. Similarly, the data at the BS is communicated to the cellular UE on employing downlink (DL) network resources. However, if the transmitting and receiving UEs are in close proximity to one another, the BS can allow with control/limited control the UEs to directly communicate with each other. This direct communication mode between the transmitting and receiving UEs is referred as the device-to-device (D2D) communications. The introduction of D2D communication in cellular wireless networks provides advantage in terms of proximity gain at crowded arenas like shopping places, carnivals and festivals, and office buildings. Thus, transmission is achieved with high data rate, lesser delays, and less power consumption. In underlaying D2D mode, the cellular resources are reused by D2D links and achieve a reuse gain as one of the advantages of D2D communications. D2D communication underlying cellular network offers an advantage in terms of improved spectral efficiency but at the cost of increase in interference due to sharing of resources.

The main challenge in allowing links using the same resources for the cellular DL or UL transmissions is the mutual interference between the D2D and cellular links. In order to manage the mutual interference an interference cancellation (IC) strategy is presented which considers orthogonal precoding vectors for links sharing the same resources. This IC strategy improves the outage probability and the overall capacity of cellular and D2D UEs sharing the same resources.

The channel model for communication in macro cell is generally considered as Rayeligh faded as it characterizes channel with scattered components. However, at high frequencies the communication distance is small and the channel constitutes of more specular components than scattered

components. Beaulieu-Xie (BX) fading model characterizes channels with multiple specular component when compared to the Ricean and generalized Ricean channel model used for line-of-sight (LOS) communication. The BX model has applications in high frequency wireless systems operating in millimeter-wave and terahertz band having small cell size. The model is also applicable for high speed vehicluar communication. The BX distribution is derived from the non-central chi distribution. Also it exhibits a seamless relationship to other fading models, such as the Ricean, generalized Ricean, Nakagami-m, Rayleigh fading models, and κ-μ distributions.

The need for Vehicle-to-Vehicle (V2V) communications rises from the idea of the growing intelligent transportation technologies for the next generation on vehicular communications. D2D communication technology can be an enabler for V2V applications as it offload a crowded cellular network and create a direct and localized communications without or with less involvement of the BS. In other words, V2V services has a localized nature which fits to the core idea of D2D communications. Furthermore, V2V services require a low latency which exactly fits to the reduced latency of D2D communications due to the hop gain. Finally, a high reliable communication which is one of the basic requirements of V2V applications and again fits right in to the D2D proximity gain advantage.

This thesis aims to analyze the D2D underlying cellular network performance and its application in V2V systems. The outage performance and ergodic capacity of a D2D underlying cellular network with multiple antenna at each node are analyzed. At the source node, orthogonal precoded data is communicated and decoding at the receiver cancels interference from some of the interfering links. The links are assumed to be Rayleigh faded. Considering equal power is transmitted at all the D2D nodes, the effects of the number of interferes, fraction of cellular to D2D power, and number of transmit and receive antennas on the systems' performance are shown. Further, we analyzed the performance of the relay-assisted D2D underlying cellular network with multiple antennas at each node. Considering cellular link majorly contributes to the interference as the power transmitted at the D2D source is small covering a smaller radius. The outage and symbol error probability (SEP) performance of the system are analyzed on considering interference mitigation techniques. The links are considered to be Rayleigh faded. The exact and the asymptotic expressions for the outage and SEP of the relay-assisted D2D underlying cellular network are also analyzed in the presence of a single interfering source when the links are BX faded. Each node of the system is considered to be equipped with a single antenna. The effect of channel parameters, relay placement, and modulation order on the system performance is observed. D2D-based V2V system with multiple antennas at each node is analyzed and expressions for the exact and asymptotic outage probability

are deduced. The diversity order of the system is also determined. Decode-and-forward (DF) protocol is assumed at the relay node to process the signal.

Contents

List of Figures

List of Tables

List of Acronyms

AF	Amplify and Forward
AWGN	Additive White Gaussian Noise
BEP	Bit Error Probability
BER	Bit Error Rate
BS	Base Station
BX	Beaulieu-Xie
CDF	Commulative Distribution Function
CMP	Conventional Multiple Input Multiple Output Precoding
CRS	Common Reference Signal
CSI	Channel State Information
CUE	Cellular User Equipment
DCOC	Device to Device Communication Operator controlled
DF	Decode and Forward
DFT	Discrete Fourier Transform
DL	Downlink
D2D	Device-to-Device
FD	Full duplex
FD-AF	Full Duplex Amplify and forward
FD-MIMO	Full Duplex Multiple Input Multiple Output
FFR	Fractional Frequency Reuse
FSO	Free Space Optical
IC	Interference Cancellation
INR	Interference Noise Ratio
LOS	Line of Sight
LTE	Long Term Evolution
MGF	Moment Generating Function
MIMO	Multiple Input Multiple Output
MRC	Maximum Ratio Combining
PDF	Probability Density Function
PMI	Precoding Matrix Indicator
PSD	Power Spectral Density
QoS	Quality of Service
RF	Radio Frequency
RRM	Radio Resource Management
RSI	Residual Self interference
RV	Random Variable
SEP	Symbol Error Probability
SER	Symbol Error Rate
SIC	Successive Interference Cancellation

SIMO	Single Input Multiple Output
SIR	Signal to Interference Ratio
SNR	Signal to Noise Ratio
SINR	Signal to Noise and Interference Ratio
TDD	Time Division Duplex
UE	User Equipment
UL	Up Link
VUE	Vehicle to User Equipment
V2D	Vehicle to Device
V2I	Vehicle to Infrastructure
V2N	Vehicle to Network
V2P	Vehicle to Pedestrian
V2V	Vehicle to Vehicle
V2X	Vehicle to Everything
3GPP	Third Generation Partnership Project

Chapter 1
Introduction

The volume of mobile data traffic demand has shown explosive growth and studies predict that the exponential growth will continue in the future. The growth is mainly with the introduction of a myriad of smart hand-held devices like smartphones and tablets [1, 2]. The unprecedented rise in bandwidth-needy device applications like video streaming, the use of multiple devices by the same user and multimedia files have resulted in a push for an investigation of new architectures and technologies. Over the years mobile broadband technologies have evolved and reached a certain level of maturity. Now, we are on the verge of a transition into state of fully connected society where high capacity is needed. Therefore incremental changes in the current systems and technologies are not enough to make this transition [3]. Future wireless technology is evolving to meet network challenges like scarce spectrum, demanding and diverse applications, reliability, ubiquitous coverage, and seamless indoor and outdoor operation. The device challenges include limitation on power, size and cost of the device, deploying multiple antennas at small handheld devices, multiradio integration, and coexistance of new technologies with the existing once. The future wireless system intend to provide extremely high-speed and high-capacity communication, enhanced coverage, extremely low power consumption, reduced cost, extremely low latency, more reliable communication, and massive connectivity [4]. The 6G technology will be supported by above 6 GHz bands, metasurfaces, optical wireless communication, and drone based communications. The applications will be diverse including tracking, autonomous vehicles, smart cities, ehealth, industrial automation,

wearables, artificial intelligence, holographic teleportation, unmanned aerial vehicles, wireless data centers, etc.

D2D communication has been recognized as one of the promising components to enable the explosive demand for mobile data. In this chapter, the concept of D2D communications, interference management, and wireless medium are discussed.

1.1 D2D Communication

In the traditional cellular network, the user equipment (UE) transmits its data to the base station using uplink (UL) network resources; then the BS forwards received data to the corresponding receiver using downlink (DL) network resources. However, if the transmitting UE and receiving UE are in close proximity to one another, the BS can allow the UEs to directly communicate with each other. This direct communication between the UEs is referred to as D2D mode.

D2D communication is a new paradigm in cellular networks [5]. UEs in close proximity uses direct link to communicate data instead of sending their signals all the way through core network [6, 7]. This offloading of information from the UL and DL of the core network offers advantage in the form of improved hop gain of the system. Since UEs are in close proximity of each other, D2D provides higher data rates, lesser delays, and lower power consumption [8, 9]. Further, sharing of radio resources by the cellular link and other D2D users in a cell improves reuse gain [10]. Some of the practical applications of D2D communication includes information sharing between UEs to transfer files and videos with higher data rates using unicast, groupcast or broadcast modes of transmission with way less energy than the conventional cellular users. D2D can operate even if the core network is paralyzed in a disaster hit areas. It offloads data and computation from the core network. Data at the BS can be offloaded to a UE with good connection so that other UEs can download the data. UEs with less processing capability can also offload computational heavy tasks to nearby capable UEs. D2D UEs can be used as relays to extend the coverage range and to create cooperative diversity which is relaying through multiple UEs. D2D communication optimizes resource utilization improving spectral efficiency of the network. Relaying assists the UEs to further enhance their performance and the coverage range. In underlay D2D communication, two closely placed UEs can communicate with each other over a licensed cellular bandwidth without or with

partial involvement of the BS. Some of the functionalities of D2D communication are exhibited by Bluetooth and Wi-Fi which work in unlicensed bandwidth having no control of the interference. Moreover, these systems do not provide the required QoS and security [8].

Depending on the involvement of BS, the following four types of D2D operation modes can be defined.

1. D2D communication with operator controlled link establishment: the transmitting UE and the receiving UE exchange data with each other and form a UE-to-UE direct link instead of UE-to-BS-UE link. In this mode, the BS establishes connection between D2D UEs using control channels. This enables the BS to manage interference among the devices.

2. D2D communication with device controlled link establishment: the UE-to-UE link is established without the involvement of BS. In addition, call set up, interference management, and resource allocation are handled by the devices themselves. The radio resources are used such that the interference to other devices in the D2D tier and at the micro and macro cell tiers is minimum.

3. Device relaying with operator controlled link establishment: a UE at the edge of a cell or device (in a poor coverage area) can communicate with the BS by relaying its data via other devices. This results in improving the battery life and achieves better Quality of Service (QoS). The base station has a partial or complete control and handles all the tasks of link establishment.

4. Device relaying with device controlled link establishment: the base station is not involved in the process of link establishment between the UE-to-UE and UE-to-relay-UE. The transmitting and receiving UEs are capable of and responsible for coordinating communication. This includes establishing relay-assisted link, interference management, resource allocation, and call set up.

D2D technology can operate on the cellular spectrum or on unlicensed spectrum. D2D communications can be classified into inband and outband communications. Inband D2D, the cellular spectrum is shared by both the cellular and D2D link. The use of cellular spectrum helps in controlling the interference. Inband D2D can operate either in underlay or overlay mode. In underlay

mode, the same resources are shared by both D2D UEs and cellular UEs. Due to the sharing of radio resources, interference between D2D links and conventional cellular links pose a threat, therefore interference management is necessary. In overlay mode, D2D links are allocated dedicated radio resources not interfering with each other but at a cost of reduced spectrum efficiency. Outband D2D uses unlicensed spectrum unlike the inband D2D, thus avoids the interference between D2D and cellular links. However, it gets additional interfaces from devices operating in unlicensed spectrum, like Bluetooth and Wi-Fi. Cellular technologies with two wireless interfaces like LTE and Wi-Fi can accommodate outband, thereby, cellular and D2D communications can happen at the same time [11]. Outband D2D can be controlled or uncontrolled.

Despite the numerous benefits of D2D communications, there are concerns in implementation of this technology. Interference management is one of the main concerns due to the sharing of resources between UEs in D2D and the cellular UEs. Other concerns include resource allocation, device discovery, security, mode selection, and power control.

1.2 Interference Management

An introduction of D2D into the traditional cellular network provides advantage in terms of reduced burden on the core network, improved overall throughput, enhanced battery life and increase in data rate [12, 13]. However, resource sharing between D2D communications and traditional cellular networks causes inter-tier interference [14]. The network resources assignment can be orthogonal or non-orthogonal. D2D and cellular UEs do not interfere on orthogonal resource assignment but requires additional resources. On the other hand, non-orthogonal network resource assignment improves spectrum efficiency at the cost of increased interference between D2D and traditional cellular links. The non-orthogonal assignment is more practical as it accommodates more users using the same resources. In underlay cellular networks, the interference between D2D links and cellular UEs and among D2D links sharing the same spectrum resources reduces capacity of the network [11, 15]. The most important challenges in underlay D2D system are radio resource management and interference management [10, 15]. Network densification enhances traffic volume and user data rate but results in increased co-channel interference due to increment in number of users and higher traffic volume. This is more severe at the cell edges. In fact, interference is one of the major factor that hinders further improvement of the cellular networks.

In order to improve the performance of D2D enabled cellular networks, extensive studies has been done. In [16], orthogonal time-frequency resource allocation schemes are adopted to avoid interference. Intelligent power control and link scheduling schemes are employed in [17, 18] to mitigate interference between D2D and cellular links. Advanced signal processing techniques are applied at transmitter and receiver of cellular links and D2D UE-to-UE links to cancel the interference in [19, 20]. In the IC techniques, the interference is first regenerated and then subsequently canceled from the desired signal. The following are the best known IC techniques: successive IC, parallel IC, and iterative IC.

1.3 Beaulieu-Xie (BX) fading

In the literature, various channel models that characterizes channels with scattered and line-of-sight (LOS) components are presented. In [21], the BX fading model that characterizes channels with multiple specular component when compared to the Ricean and generalized Ricean channel model used for LOS communication is presented. The BX model has applications in high frequency wireless systems operating in millimeter-wave and terahertz band having small cell size. The model is also applicable for high speed vehicluar communication. The BX distribution is derived from the non-central chi distribution. Also it exhibits a seamless relationship to other fading models, such as the Ricean, generalized Ricean, Nakagami-m, Rayleigh fading models, and κ-μ distributions.

1.4 D2D based Vehicle-to-Vehicle (V2V) Applications

D2D technology can be an enabler for V2V applications because of its very idea to offload a crowded network and create a direct and localized communications without or with less involvement of the BS. V2V services also have a localized nature which fits to the core idea of D2D communications. Furthermore, V2V services requires low latency which again is also offered in case of D2D due to the hop gain. Finally, a highly reliable communication link which is one of the basic requirements of V2V applications and again fits right into the D2D proximity gain advantage [22]. In fact, the D2D underlay mode of communications is proposed as a potential solution for V2V applications. The down side of using D2D underlay for V2V applications is the reuse of resources used by the traditional cellular network which results in system performance degradation due to interference.

Also, V2V communications requires a low latency and high reliability but yet again achieving these requirements is still a challenge to be resolved and investigated.

Autonomous driving is seen as the future for automobile industry. V2V communications is one of the future intelligent transportation technologies. In vehicular communication high reliability and low latency are the key components in order to avoid accidents. A low latency transmission is required in order to send ultra-fast warning messages within an extremely short time frame [23]. Newly emerging technologies uses higher frequency bands, that are in the range of 30 GHz and 300 GHz. At these frequencies, it is possible to achieve data rate close to 1 Tbps and latency less than 1 ms [24–26].

Vehicular-to-everything (V2X) consider all surrounding elements to enable vehicular communication like vehicles, roads, traffic lights, message signs, etc and uses this information to make them intelligent. V2X incorporates specific types of communication as vehicle to infrastructure (V2I), vehicle-to-device (V2D), vehicle-to-network (V2N), vehicle-to-pedestrian (V2P), and V2V.

1.5 Precoding

Multiple-input multiple-output (MIMO) offers a great deal of advantage in terms of overall throughput and data rate of the system. It has the ability to handle a number of parallel data streams that are transmitted on different antennas. Therefore, MIMO is considered necessary in 6G communication systems. There are close loop and open loop MIMO precoding methods and both can enhance systems performance. To be more specific, in the close loop multiple-input multiple-output (MIMO) precoding technique, the feedback of channel state information (CSI) is considered to be known at the source terminal. These systems can be designed on estimating CSI at the receiver and then feedback this CSI to the transmitter through a feedback link with a very limited capacity. Based on CSI, DL/UL data can be precoded before it is transmitted in order to improve signal-to-interference and noise ratio (SINR) at the receiving side and thereby improve the capacity of the overall system.

Precoding techniques transfers the systems complexity to the transmitter side or the BS side. The processing stage of the precoder is important in an LTE system as it make use of the computationally and power capabilities of the BS. Precoding at the transmitter reduces the performance

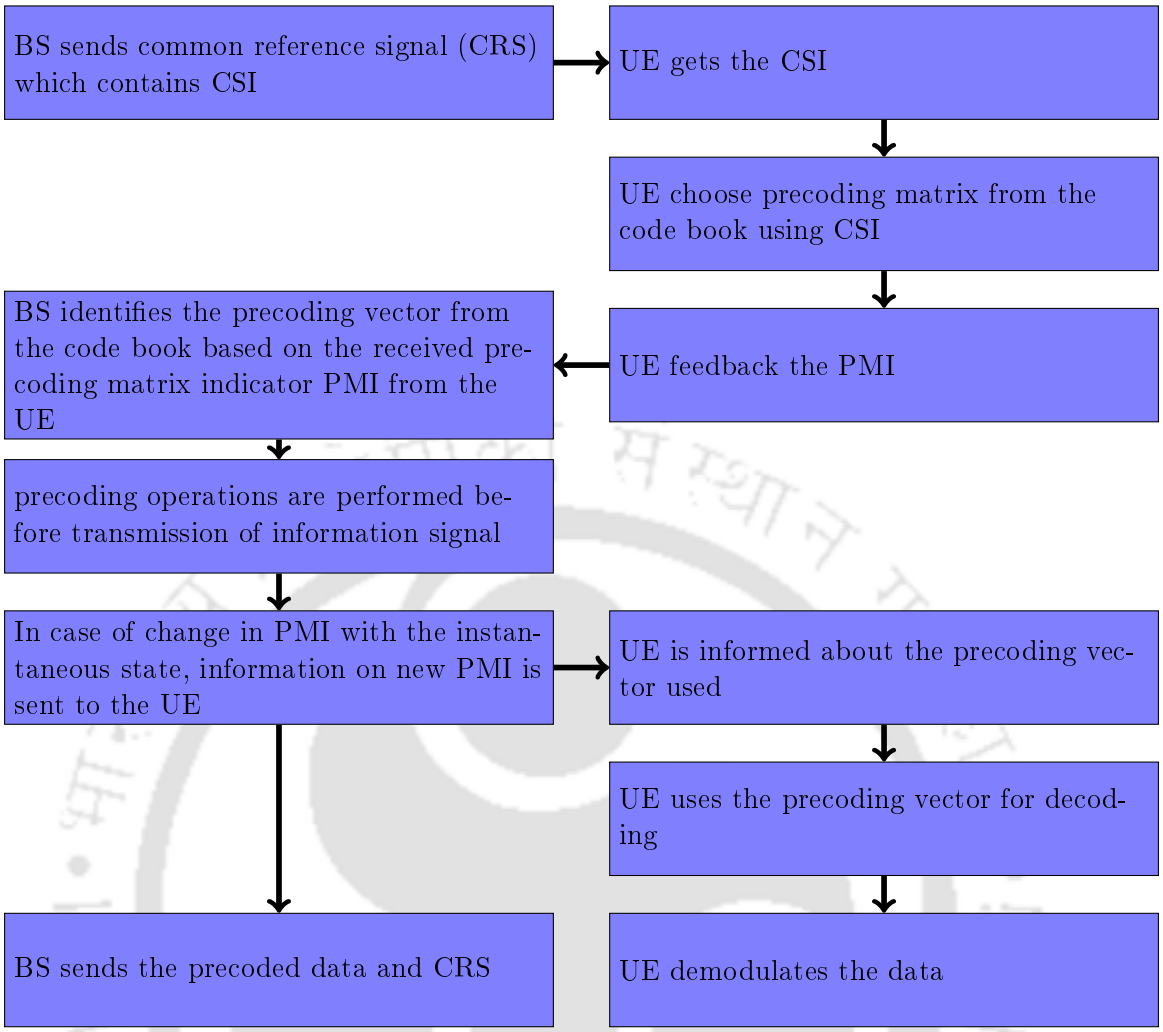

FIGURE 1.1: Mechanism for precoding matrix allocation

loss due to interference and channel fading. In the proposed technique, the interference is canceled on selecting orthogonal precoding vectors from the code book defined for LTE 3GPP standard. These vectors are selected in such a way that channel fading reduces and the magnitude square of the product of channel coefficients and the precoding matrix maximizes. Due to the impracticality of getting instantaneous CSI, a limited close loop feedback mechanism can be used. In this mechanism, the receiver informs the transmitting UE about the index of the precoding matrix from a code book in case of code book based precoding implementation. In this thesis, the code book based implementation is considered. The only difference is, in our case, the orthogonality among the precoding vectors for different links has to be maintained in order to reduce the interference when same resources are shared by different links. The precoding matrix used at the transmitter is required at the receiver for detecting the desired information signal. In the codebook based precoding, orthogonality is maintained as it assigns orthogonal vectors to the UEs sharing same

resources from the existing LTE based code book. Based on the number of transmitting antennas DFT or house holder based code books are used in LTE [27]. The precoding process considered in the thesis is summarized in the Table 1.1.

1.6 Challenges

A number of challenges arise due to the introduction of D2D into the traditional cellular networks. For D2D communications to be successful the challenges include peer discovery and link establishment. To accomplish the peer discovery process, the D2D UEs are required to broadcast their messages to search for potential peers and set up the D2D links [10]. In the case of network-assisted D2D communications, the BS helps D2D UEs to broadcast their messages as well as set up the D2D communication links [10, 28]. The fundamental challenge is synchronizing the peers and defining the role of BS in the link setup for an efficient peer discovery process [29]. After the D2D link establishment, interference and radio resource management becomes the next challenges [10, 15]. In underlying D2D communications, the spectrum resources are shared by both the D2D UEs and the cellular UEs and the sharing may result in mutual interference. In D2D communications, interference and resource management are crucial as they help in achieving the benefits of D2D communications [10, 15, 30, 31]. The challenges of interference management are considered in this thesis.

1.7 Literature Review

In this section, a survey on various interference cancellation techniques, interference alignment techniques, relay-assisted underlying D2D communication, BX-fading, and D2D-enabled V2V communication is presented.

1.7.1 Interference Management

The introduction of D2D communications links underlying classical cellular networks results in the following interference types.

- **Inter-tier Interference** also known as inter-cell interference is interference caused by users in different cells sharing the same resources.
- **Intra-tier interference** is interference caused by the BS and the other D2D users using the same resources within a cell.

In this thesis, intra-tier interference is considered. The inter-cell interference is ignored since it is negligible for coordinated transmissions among cells.

In the literature, the interference management techniques are based on power control mechanisms, IC strategy, and resource allocation techniques. In [32–34], the authors have developed methods to manage interference using power control mechanisms. The techniques to reduce interference with mode selection are presented in [31, 35]. Resource allocation methods to reduce interference are proposed in [36, 37]. Table 1.1 and 1.2 lists the interference cancellation and interference alignment techniques, respectively and their contributions in underlay D2D systems.

TABLE 1.1: Summary of interference cancellation schemes for underlying D2D cellular networks

Ref.	Interference type	Article's contributions	Performance measuring parameters	Remarks
[38]	Inter-tier D2D to DL, UL to D2D	Proposed practical and efficient scheme to generate awareness of the interference between cellular and D2D links at the BS. Achieved significant SINR gains and almost three-fold increase in capacity.	SINR, capacity	Used single transmit and receive antenna. Intra-tier in D2D links is ignored.
[39]	Inter-cell, intra-cell	Proposed a combined power control and link selection algorithm with temporary removal.	Outage probability, convergence rate	BS and UEs equipped with an omnidirectional antenna.
[40]	Inter-tier	Proposed a novel MIMO orthogonal precoding approach.	Outage probability, capacity	Considered single cellular UE and single D2D link each equipped with a single transmit and receive antenna.
[41]	Cellular to D2D	Proposed MIMO transmission approaches for cellular DL to avoid generating interference to D2D links sharing the same resources. Achieved substantial gains in SINR of the D2D links and increase in overall capacity gains.	SINR and capacity.	Considered cellular to D2D interference only. Inter-tier is ignored.

Continuation of Table 1.1

Ref.	Interference type	Article's contributions	Performance measuring parameters	Remarks
[19]	Cellular to D2D	Proposed three receive schemes for reliable demodulation of the D2D receiver while sharing the same resources with the cellular link. Achieved a remarkable outage enhancement using re-transmission receive mode.	Outage probability	Single cellular UE and single D2D link is considered. UEs are equipped with single transmit-receive antenna.
[42]	Cellular to D2D	Proposed an interference limited area to manage the cellular to D2D interference. achieved a capacity increase in D2D with a negligibly small loss in capacity of the cellular UEs.	Capacity	UEs equipped with single transmit-receive antenna. DL to D2D and D2D to cellular are not considered.
[32]	Cellular to D2D	Proposed a simple power control method to the D2D UEs which limits the SINR degradation of the cellular link to a certain degree.	SINR and cumulative distribution function (CDF)	Single cellular UE and single D2D pair. BS has no instantaneous CSI. Inter-tier interference not considered.
[43]	Inter-tier	Studied the performance of successive interference cancellation (SIC) in D2D enabled cellular networks using stochastic geometry. Derived successful transmission probabilities of D2D and cellular links.	Successful transmission probabilities	Used multiple D2D and cellular links. Considered both tiers.

TABLE 1.2: Summary of interference alignment schemes for underlying D2D cellular networks

Ref.	Interference type	Article's contributions	Performance measuring parameters	Remarks
[44]	Inter-tier and intra-tier	Proposed an interference mitigating scheme for underlying D2D and developed a D2D capacity maximizing optimization problem.	Capacity	Considered one cellular UE and multiple D2D links. Obtained decoding and precoding matrices.
[45]	Inter-cell, intra-cell, intra-tier	Proposed an approach for resource management and interference avoidance in multiple D2D underlying cellular links and optimized the system performance to achieve maximum throughput.	Throughput and number of UEs.	Considered two adjacent cells and assumed knowledge of interference level and CSI.

Continuation of Table 1.2

Ref.	Interference type	Article's contributions	Performance measuring parameters	Remarks
[46]	Inter-tier	Proposed interference aware power allocation of the cellular links following the resource allocation of D2D links and achieved decreased number of dropped cellular UEs due to severe interference.	Power transmission and number of dropped cellular UEs.	Considered single cell, single cellular UE and single D2D link.
[47]	Intra-tier and D2D inter-tier.	Proposed a fair and restricted resource allocation assignment to minimize system interference while maintaining system sum rate. Claimed their algorithm out performs other state of the art algorithms.	System sum rate and total system interference with respect to number of D2D UEs.	Considered multiple cellular UEs and D2D UEs.
[48]	Cellular to D2D multicast and intra-multicast D2D.	Presented a strategy to maximize the sum rate using a joint channel assignment and power allocation frame work. Frame work guarantees a rate above some specified outage for all UEs.	Outage probability and total rate.	Multicast D2D is considered. D2D UEs are equipped with single transmitter and multiple receiving antennas.
[49]	Inter-cell, intra-cell and D2D inter-tier.	Proposed an analytical approach to characterize the interference due to the coexistence of cellular and D2D links. Demonstrated system throughput increase through proper selection of underlay D2D UEs.	Throughput, SINR and effect of distance and device density.	UEs equipped with single transmit-receive antenna. Inter-cell interference is considered.
[50]	Inter-tier	Studied FFR in underlay D2D communication to mitigate the mutual interference. Introduced accessible and reusable regions to protect the outages of both cellular and D2d links.	SINR and Outage probability	Considered UL scenarios. D2D Inter-tier not considered.
[51]	D2D Inter-tier and DL-to- D2D.	Investigated interference coordination in underlaying D2D for FD MIMO. Proposed coordination techniques for D2D links to mitigate DL interference and interference between D2D links.	Throughput and number of active D2D links.	Considered single cell with FD MIMO and multiple D2D links.

1.7.2 Performance of relay-assisted underlay D2D communications system.

As performance measuring metrics, outage probability, ergodic capacity, outage capacity, and symbol error probability (SEP) are considered in this thesis. In this section, review of work done on performance analysis of relay-assisted underlay D2D communication system is presented in Table 1.3.

TABLE 1.3: Summary of underlay relay-assisted D2D cellular networks.

Ref.	**Interference type**	**Article's contributions**	**Performance measuring parameters**	**Remarks**
[52]	Residual self interference (RSI)	Analysed the FD-SM decode-and-forward (DF) relay system and obtained the closed form expressions of SEP. Proposed a simple power allocation algorithm to compensate the effect of RSI and improved SEP.	SEP Considered RSI only.	Done for single source-relay-destination system.
[53]	RSI	Proposed an effective power allocation approach for the FD relay node to minimize the effect of RSI. Claimed their scheme improved system performance.	Outage probability, Throughput, SEP and ergodic capacity.	Considered nodes with single transmit-receive antenna. Derived closed from expressions for single source-relay-destination node only.
[54]	Cellular to D2D and cellular to relay.	Presented D2D communication based on MIMO relay technology under imperfect channel estimation. Analysed channel estimation error and number of UE antennas and determined their effect on the system outage.	Outage probability.	Considered single cell, single cellular UE single D2D link relayed through a relay. Used relay to improve outage without interference handling approach.
[55]	...	Reviewed and highlighted research issues and challenges of relay assisted D2D communication. Proposed matching theory for relay allocation considering uncertainties due to relay mobility.	Outage probability.	Considered relay allocation problem and reviewed the rest of the challenges.
[56]	Cellular to D2D, cellular to relay and D2D to cellular.	Proposes an approach that integrates advantages of D2D and relay along with a technique to improve the spectral efficiency. Presented a way of choosing a better relay and improve relay throughput.	Outage probability and total rate.	D2D inter-tier is not considered. Cellular and D2D UEs equipped with single transmit-receive antenna.

Continuation of Table 1.3

Ref.	Interference type	Article's contributions	Performance measuring parameters	Remarks
[57]	Cellular to D2D-relay link.	Devised a power control approach at D2D and relay in order to maintain the QoS requirements of a prioritized cellular links. Indicated outage probability performance gain when relay is introduced.	Outage probability.	UEs equipped with single transmit-receive antenna. RSI is assumed to be canceled.
[58]	Cross-tier.	Investigated the coverage probability and transmission capacity of cellular and D2Dlinks using FD-AF relay. Derived closed form expressions of both parameters for both links.	SINR, coverage probability and transmission capacity.	Considered UL scenarios. D2D Inter-tier not considered. UEs and relay equipped with single transmit-receive antenna.
[59]	Cellular to D2D and D2D to cellular.	Proposed a game theory based algorithm in relay selection of D2D communications. Achieved improved distance coverage, reduced interruption probability and improved system throughput.	SINR, outage probability and Throughput.	Considered single cell scenario and ignored D2D inter-tier interference.

1.7.3 Performance of D2D enabled V2V communications.

In the literature, D2D-based V2V underlaying cellular network are analyzed to improve the performance measured in terms of average SEP and outage probability and optimize the resources at the nodes of the network. Different resource optimization techniques to enhance the overall performance of the system are discussed in [64, 93–96]. A power control strategy at the network nodes is presented in [64]. The techniques for radio resource management are presented in [93, 95]. The resource allocation techniques are described in [94, 96] for one way system and [18] for a two-way cellular network. The outage probability for a D2D-based V2V single-input multiple-output (SIMO) system in presence of co-channel interference and imperfect channel state information (CSI) are analyzed in [97]. The expressions for outage probability and the average symbol error rate (SER) of a dual-hop regenerative cooperative system are obtained in [98]. The bit error probability (BEP) of a V2V multi-hop system in a single crowded lane is examined in [99]. In

[100], the outage probability and the amount of fading for a signal hop multiple-input multiple-output (MIMO) system is analyzed in Rayleigh fading. The related literature on D2D-enabled V2V network and its contributions are listed in Table 1.4.

TABLE 1.4: Summary of D2D-enabled V2V communications.

Ref.	**Interference type**	**Article's contributions**	**Performance measuring parameters**	**Remarks**
[60]	Intra-cell interference.	Proposed to use the D2D underlay as a carrier for vehicle safety applications and used a location dependent resource allocation for mobile D2D UEs that will satisfy the requirements safety applications.	CDF and D2D capacity.	Single V-UE reuses the cellular spectrum resources. Used UL resources for reuse.
[61]	Intra-cell	Investigated spectrum resource management problem for D2D based V2V applications. Proposed separate power allocation and RB algorithm to deal with the problem.	CDF, sum rate of C-UE and average power of V-UE.	V-UE to V-UE interference is not considered.
[62]	Intra-cell	Investigated the RRM for V2X applications based on D2D communications. Proposed an efficient power control and resource allocation for V2X applications.	System throughput and RB utilisation.	Single V2I and V2V links share the same resources. Interference in multiple V2V is not considered.
[63]	Intra-cell	Investigated the spectrum sharing problem in V2I and V2V communications. Proposed two interference graph theory based resource sharing approaches to deal with the problem.	CDF and network sum rate.	Sub-optimal performance is obtained.
[22]	Between V2V and cellular transmissions.	Analysed mathematical model actual requirements for cellular and V2V communications. proposed a power allocation and RB algorithm to satisfy the requirements of V2V.	CDF	V-UEs use orthogonal RBs.
[64]	Cellular to V2V and inter-tier V2V.	Studied how to efficiently apply underlying D2D cellular systems to support V2V links. Proposed a D2D-V grouping to obtain optimal performance of the D2D-V system.	Sum rate, minimum rate and V2V density.	Neighbouring UEs in different grouping communicate through traditional cellular links.

Continuation of Table 1.4

Ref.	Interference type	Article's contributions	Performance measuring parameters	Remarks
[65]	Intra-cell	Focused on optimal power allocation in V2V communications with channel uncertainty. Proposed a novel optimization approach to handle reliable V2V in two tier communication links.	Real outage percentage and sum rate.	V-UEs and C-UEs are equipped with single transmitting and receiving antenna. All V2V links are differently faded
[66]	Co-channel between V2I and V2V, Co-channel between V2V and V2V	Investigated latency constrained resource allocation in V2V communications. Proved convergence of proposed resource allocation algorithm.	Sum rate and total number of V2V links	V-UEs equipped with single transmit receive antenna.

1.8 Motivations and Objectives

D2D communication has a huge potential to be a part of the future generations of the wireless technology as it offers improved spectral efficiency of the system. Intensive research is ongoing in both academia and industry to address the challenges of introducing D2D to the classical cellular networks. D2D provides efficient utilization of the limited spectrum. In case of broadcast and multicast, a single UE can connect to multiple nearby D2D capable UEs. In order to maximize the spectral efficiency by introducing D2D capabilities, the classical cellular resources are shared for communication among UEs. This improves the spectral efficiency but results in interference between users sharing the same resources. Therefore, interference management plays a vital role in improving the performance of the system. The interference related problems in D2D underlaying cellular network are addressed in this work. This thesis objectives are outlined as follows.

1. Analyze the expressions for the outage probability, ergodic capacity, outage capacity at the cellular and D2D receiver for a D2D underlaying cellular system. Here, the cellular and the D2D receiver observes interference due to the sharing of resources. Each node is assumed to be equipped with multiple antennas. The links are considered to be Rayleigh faded. The effect of the number of transmit and receive antennas on the performance of the system

is observed. The effect of number of interfering nodes is also determined considering the transmit power is same for all D2D UEs. Further, the transmit power at the cellular and the D2D UEs is varied to observe their effect on the performance.

2. Deduce the expressions for the end-to-end outage probability and SEP for a relay-assisted D2D communication system underlying a cellular network. Each node is assumed to have multiple antennas. The links connecting the nodes are Rayleigh faded. The signal received at the relay and the destination node observes interference from the cellular link (UL/DL) and D2D devices in the vicinity. The power of the signal transmitted over cellular link is high when compared to that sent over the D2D link, therefore the interference caused due to cellular link is comparatively larger. It is considered that the interference at the relay and destination due to cellular transmission is mitigated using interference mitigation techniques.

3. Consider BX fading channel model to observe the effect of interference in relay-assisted D2D underlaying cellular system. This channel model is more practical in system with dominant specular component. BX fading model is a generalized channel model therefore the parameters of each link can be varied and their effect on the performance can be observed. Each node is equipped with single antenna and only one interfering source is considered. In this work, the expression of the outage probability and the SEP are deduced. The effect of relay location, transmit power at source and relay, varying link parameters, and modulation on the end-to-end performance is analyzed.

4. Consider multi-antenna V2V underlaying cellular networks in rush hour multilane highway scenarios. The closed-form expressions for the outage probability are deduced for i) D2D-based V2V transmission and ii) relay-assisted V2V communication. The links are considered to be Rayleigh faded. The outage performance is analyzed in the presence of an interfering link sharing the resources. The effect of relay residual interference (RSI) at the relay node is also considered. The high signal-to-interference and noise ratio (SINR) approximations of the outage probability are derived. The diversity order of the system is determined.

1.9 Thesis Organization

The thesis is organized as follows.

- **Chapter 1** presents a brief overview on the need of underlay D2D in improving network capacity. D2D offloads traffic from the network and provides advantage such as improved performance, reduced latency, and reduced battery power consumption. However, due to underlaying D2D communication suffers interference as the resources are shared in a cell. The existing works on underlay D2D communication with IC are discussed. The work on orthogonal precoding techniques in literature is also mentioned. At high frequencies, channel fading model with specular components is more practical than that with shadowed fading, therefore BX fading is considered. The applications of underlay D2D in V2V communication are also presented. Towards the end of the chapter, the thesis contributions are summarized and a brief outline of the thesis is provided.

- **Chapter 2** focuses on analyzing performance of underlay D2D communication system where the resources assigned for cellular DL or UL transmissions are shared with D2D users. IC method is considered which allocates orthogonal precoding vectors in case of underlay D2D transmissions over the channel assigned for cellular communication. The expressions for the outage probability, ergodic capacity, outage capacity at the cellular and D2D receiver are deduced. Numerical results are plotted to observe the effect of the different parameters on the performance.

- **Chapter 3** presents the performance analysis of a relay assisted D2D communication underlaying cellular network. The interference due to cellular transmission at the relay and destination node of the relay-assisted D2D link are mitigated using interference mitigation technique. The exact expressions of the end-to-end outage probability and average SEP are deduced. Numerical results are plotted to observe the impact of number of transmit/receive antennas, power transmitted at the source and relay nodes, modulation order, and interference due to other D2D devices.

- In **Chapter 4**, the expression for performance analysis of a DF relay based D2D communication system is analyzed. The RF links connecting the nodes are considered to BX faded. The expressions for the end-to-end average SEP, outage probability, and outage capacity are derived. Further, plots to present the effect of RF link parameters on the optimal relay location.

- In **Chapter 5**, the performance of a direct and relayed D2D-based V2V underlay communications system is analyzed. Orthogonal precoding is consider to handle the interference at receiving nodes. A closed form expression for the end-to-end outage probability is derived for direct and relayed transmission.

- **Chapter 6** includes concluding remarks and possible directions for future work.

Chapter 2

Interference Cancellation in Multiple D2D Underlaying LTE Cellular Networks

2.1 Introduction

In the traditional cellular wireless network, the UE transmits its data to the BS using UL network resources. Similarly, the data at the BS is communicated to the UE on employing DL network resources. However, if the transmitting UE and receiving UE are in close proximity to one another, the BS can allow the UEs to directly communicate with each other. This direct communication mode between the UEs is referred to as the D2D mode. D2D communication in cellular wireless networks provides an advantage in terms of proximity gain as UEs are located close to each other. Thus it supports high rate data transmission, lesser delays, and low power consumption [8]. In underlay mode, the cellular resources are reused for D2D communication giving an advantage in terms of reuse gain [67]. The hop gain in D2D communication refers to using a single link in D2D communication mode instead of both UL and DL while communicating via the base station in cellular network mode.

In D2D communication, the BS station has different levels of involvement in network resource allocation. We consider D2D communication with operator controlled (DC-OC) link establishment. In DC-OC, transmitting and receiving UEs communicate and exchange data with each other without the need for an operator although it assists in link establishment and resource allocation. The major challenge in allowing D2D links to use the same resources as the cellular DL or UL is high mutual interference between the links. In comparison to the cellular DL or UL transmission in macro and micro cells, D2D UEs transmit low power. This makes D2D receivers more vulnerable to high interference caused due to simultaneous communication over cellular links. Further, the proximity of D2D UEs to the cellular receivers may result in potentially severe near-far problems. In [38], interference aware scheduling approach is used to coordinate transmission and handle high interference and near-far problems. Power control schemes for DL D2D communication are studied in [39]. An UL interference reducing scheme for D2D communication through combined power control and link selection has been studied in [39]. In [40], a novel IC scheme used to avoid interference between cellular DL and a single D2D link is presented. A novel interference avoiding precoding schemes for cellular DL transmissions in the presence of intracell D2D is proposed in [41]. An interference cancellation scheme for underlay D2D communication in cellular networks is developed using receive mode selection in [19].

In this chapter, we consider an interference cancellation technique for underlay D2D communication networks with multiple antennas at each node. This method is implemented by selecting orthogonal precoding vectors for the UEs using same resources. We have analyzed the performance of this IC scheme. The UL/ DL link resources are shared by a cellular UE and multiple D2D UEs. Due to the sharing of resources by a cellular UE and multiple D2D UEs, they interfere with each other. We have applied a power control mechanism used in [42] to analyze expressions for the outage probability and capacity of the system considered. To the best of our knowledge, the outage analysis on cancelling interference in D2D underlaying cellular network with each node equipped with multiple antennas is not reported in the literature.

2.2 System model

Consider the LTE TDD network scenario where the resources assigned for cellular UL/DL transmission are shared with K D2D user pairs. These shared resources cause interference for each

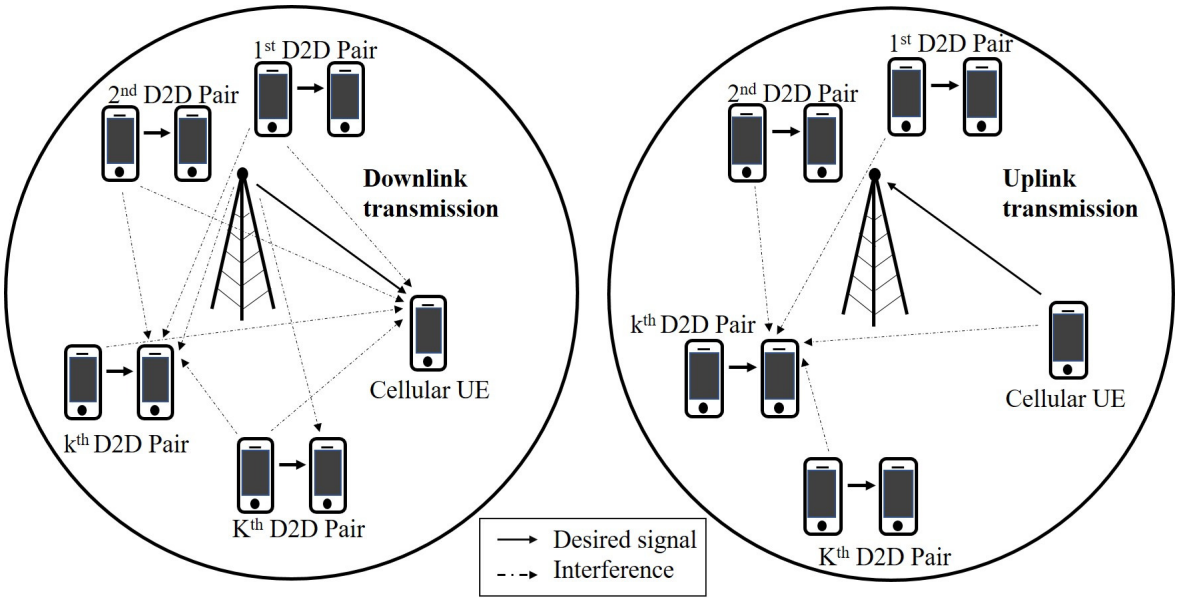

FIGURE 2.1: Uplink and downlink transmission in underlay D2D communication network with K D2D user pairs

other. That is communication over cellular link effect D2D transmissions and D2D devices pose interference to the cellular device and other D2D devices in the vicinity as shown in Fig. 2.1. We consider that interference at the BS due to low power D2D UEs is negligible and therefore it is ignored. However, cellular DL transmission is affected due to all D2D devices in the vicinity. Further, inter-cell interference is also ignored as it is negligible for coordinated transmissions among cells. Each communication pair has N_t transmit and N_r receive antennas and operates in half-duplex mode. A symbol vector $\boldsymbol{x}_k$ of dimension $N_t \times 1$ is transmitted with signal power P_k, where $k = 0$ for CUE and $k \in \{1, \ldots, K\}$ for kth D2D transmitter. The $N_r \times 1$ received signal vector at cellular UE $\boldsymbol{Y}_0$ and kth D2D receiver $\boldsymbol{Y}_k$ is given by

$$\boldsymbol{Y_k} = \sqrt{P_k}\boldsymbol{H}_k\boldsymbol{\phi}_k\boldsymbol{x}_k + \sum_{\substack{i=0 \\ i\neq k}}^{K} \sqrt{P_i}\boldsymbol{H}_i\boldsymbol{\phi}_i\boldsymbol{x}_i + \boldsymbol{n}_k\,, \quad k = 0, \ldots, K, \tag{2.1}$$

where $\boldsymbol{H}_0$ and $\boldsymbol{H}_k$, $k \in \{1, \ldots, K\}$ are $N_r \times N_t$ channel matrices corresponding to cellular link and kth D2D user pair link, respectively sharing the same resources. The (i, j)th element of matrix $\boldsymbol{H}_0$ and $\boldsymbol{H}_k$ represents complex gain from transmit antenna j to receive antenna i. The elements are independent and circularly symmetric complex Gaussian with zero mean and unit variance in each direction. Further, $\boldsymbol{\phi}_0$ and $\boldsymbol{\phi}_k$ are $N_t \times N_t$ precoding matrices used for interference mitigation at the BS and kth D2D pair transmitter, respectively. $\boldsymbol{n}_k$ is $N_r \times 1$ additive white Gaussian noise

(AWGN) having zero mean and covariance matrix $\sigma_n^2 \boldsymbol{I}_{N_r}$, where $\boldsymbol{I}_{N_r}$ denotes $N_r \times N_r$ identity matrix. In (2.1), $\sqrt{P_k}\boldsymbol{H}_k\boldsymbol{\phi}_k\boldsymbol{x}_k$ is the desired signal component and the second term corresponds to interference caused by the other devices using the same resources.

We consider signal at the receiver is combined using maximum ratio combining (MRC). Thus the weight vector considered at the kth receiver is given by $\boldsymbol{W}_k = \boldsymbol{H}_k\boldsymbol{\phi}_k$, for $k = 0, \ldots, K$. The signal received is $\widetilde{\boldsymbol{Y}}_k = \boldsymbol{W}_k^H \boldsymbol{Y}_k$, that is

$$\widetilde{\boldsymbol{Y}}_k = \sqrt{P_k}\boldsymbol{H}_k\boldsymbol{\phi}_k\boldsymbol{\phi}_k^H\boldsymbol{H}_k^H\boldsymbol{x}_k + \sum_{\substack{i=0 \\ i\neq k}}^{K} \sqrt{P_i}\boldsymbol{H}_i\boldsymbol{\phi}_i\boldsymbol{\phi}_k^H\boldsymbol{H}_k^H\boldsymbol{x}_i + \boldsymbol{\phi}_k^H\boldsymbol{H}_k^H\boldsymbol{n}_k\,. \tag{2.2}$$

Using (2.2), the signal-to-interference noise ratio (SINR) at the kth receiver is

$$\Gamma_k = \frac{||\boldsymbol{H}_k\boldsymbol{\phi}_k\boldsymbol{\phi}_k^H\boldsymbol{H}_k^H||^2}{\frac{N_0}{P_k}||\boldsymbol{\phi}_k^H\boldsymbol{H}_k^H||^2 + \sum_{\substack{i=0 \\ i\neq k}}^{K}\frac{P_i}{P_k}||\boldsymbol{H}_i\boldsymbol{\phi}_i\boldsymbol{\phi}_k^H\boldsymbol{H}_k^H||^2}\,, \tag{2.3}$$

where N_0 is noise power spectral density (PSD). The transmit precoding matrix $\boldsymbol{\phi}_k$ should be known at the transmitter and the receiver in order to precode and decode the information. It is difficult to have perfect channel state information known at the transmitter, therefore using a limited feedback mechanism the index of the precoding vector is communicated to the transmitter from a codebook $\boldsymbol{\Phi}$. In conventional MIMO precoding (CMP), $\boldsymbol{\phi}_k$ is chosen on adopting the following measure [40]

$$\arg\max_{\boldsymbol{\phi}_k \in \boldsymbol{\Phi}} ||\boldsymbol{H}_k\boldsymbol{\phi}_k||^2\,. \tag{2.4}$$

In (2.3), we assume K' terms in the denominator contributes to the interference and the precoding matrices selected using (2.4) are orthogonal for the remaining $(K+1-K')$ terms. The precoding vectors are orthogonal if $\boldsymbol{\phi}_i\boldsymbol{\phi}_k^H = \boldsymbol{0}$ for $i \neq k$, where $\boldsymbol{0}$ is the zero matrix of order $N_t \times N_t$. Using the Cauchy-Schwarz inequality that states $||\boldsymbol{\phi}_k\boldsymbol{H}_k||^2 \leq ||\boldsymbol{\phi}_k||^2||\boldsymbol{H}_k||^2$ and the property that $||\boldsymbol{\phi}_k||^2 = 1$, (2.3) is rewritten as

$$\Gamma_k \leq \frac{||\boldsymbol{H}_k||^2}{\frac{N_0}{P_k} + \sum_{\substack{i=0 \\ i\neq k}}^{K'}\frac{P_i}{P_k}||\boldsymbol{H}_i||^2}\,. \tag{2.5}$$

Let power transmitted at all the D2D UEs be the same, that is $P_1, \ldots, P_K = P_D$. Thus the ratio of power transmitted at the CUE to that at the D2D UE is constant, given by $P_0/P_D = \alpha$, $\alpha \geq 1$.

Further using high SINR approximations, (2.5) is simplified for cellular link and the D2D links as

$$\Gamma_0 \leq \frac{||\boldsymbol{H}_0||^2}{\frac{1}{\alpha}\sum_{i=1}^{K'}||\boldsymbol{H}_i||^2} \quad \text{and} \quad \Gamma_k \leq \frac{||\boldsymbol{H}_k||^2}{\alpha||\boldsymbol{H}_0||^2 + \sum_{\substack{i=1 \\ i\neq k}}^{K'}||\boldsymbol{H}_i||^2}\,, \tag{2.6}$$

respectively.

Let $X = ||\boldsymbol{H}_k||^2$ and $Y = \sum_{i=1}^{K'}||\boldsymbol{H}_i||^2$. The PDF of X is the sum of N_tN_r independent exponential distributed random variables which is given by a Gamma distribution [68]. That is [69, Eq. 6.45]

$$f_X(x) = \frac{x^{N_tN_r-1}}{\Gamma(N_tN_r)}\exp(-x)u(x)\,, \tag{2.7}$$

where $\Gamma(\cdot)$ is Gamma function and $u(\cdot)$ is a unit step function. Now, Y is the sum of K' independent Gamma distributed random variables. The PDF of Y is obtained using [70, Eq. 6.60] as

$$f_Y(y) = \frac{y^{K'N_tN_r-1}}{\Gamma(K'N_tN_r)}\exp(-y)u(y)\,. \tag{2.8}$$

Using (2.7) and (2.8), the PDF of $Z = X/Y$ is given by

$$\begin{aligned} f_Z(z) &= \int_0^\infty y f_{X,Y}(yz, y)dy \\ &= \int_0^\infty y\frac{(yz)^{N_tN_r-1}y^{K'N_tN_r-1}}{\Gamma(N_tN_r)\Gamma(K'N_tN_r)}\exp(-y(1+z))dy \\ &= \frac{\Gamma((K'+1)N_tN_r)}{\Gamma(N_tN_r)\Gamma(K'N_tN_r)}\frac{z^{N_tN_r-1}}{(1+z)^{(K'+1)N_tN_r}}\,. \end{aligned} \tag{2.9}$$

2.3 Outage Probability

In this section, we analyze an expression of the outage probability for transmission over both cellular and D2D links. The outage probability is CDF of SINR at γ_{th}, where γ_{th} is the minimum SINR required for reliable communication.

Using (2.6) and (2.9), the PDF of Γ_0 is given by

$$f_{\Gamma_0}(z) = \frac{\Gamma((K'+1)N_tN_r)}{\Gamma(N_tN_r)\Gamma(K'N_tN_r)}\frac{(\alpha^{K'}z)^{N_tN_r}}{z(\alpha+z)^{(K'+1)N_tN_r}} \tag{2.10}$$

and the corresponding CDF is

$$F_{\Gamma_0}(z) = \frac{\Gamma((K'+1)N_tN_r)}{\Gamma(N_tN_r+1)\Gamma(K'N_tN_r)}\left(\frac{z}{\alpha}\right)^{N_tN_r} {}_2F_1(N_tN_r,(K'+1)N_tN_r;N_tN_r+1,-z/a)\,, \quad (2.11)$$

where ${}_2F_1(\cdot)$ is an Gaussian hypergeometric function. Similarly, the PDF and CDF of Γ_k can be computed using (2.6), (2.7), and (2.8). On simplifying using [69, eq. (6.59)] and [70, eq. 3.351.3], the PDF is given as

$$\begin{aligned} f_{\Gamma_k}(z) &= \frac{z^{(N_tN_r-1)}}{\alpha^{N_tN_r}\Gamma(N_tN_r)}\Bigg((-1)^{(K'-1)N_tN_r}\sum_{j=1}^{N_tN_r}\binom{K'N_tN_r-j-1}{N_tN_r-j} \\ &\times \frac{\Gamma(N_tN_r+j)((1/\alpha)-1)^{j-K'N_tN_r}}{(j-1)!(z+(1/\alpha))^{N_tN_r+j}} + (-1)^{N_tN_r}\sum_{j=1}^{(K'-1)N_tN_r}\binom{K'N_tN_r-j-1}{N_tN_r-1} \\ &\times \frac{\Gamma(N_tN_r+j)(1-(1/\alpha))^{j-K'N_tN_r}}{(j-1)!(z+1)^{N_tN_r+j}}\Bigg)\,. \end{aligned} \quad (2.12)$$

Further, the CDF of (2.12) is obtained using [70, eq. 3.194.1] as

$$\begin{aligned} F_{\Gamma_k}(z) &= \frac{z^{N_tN_r}}{\alpha^{N_tN_r}\Gamma(N_tN_r+1)}\Bigg((-1)^{(K'-1)N_tN_r}\sum_{j=1}^{N_tN_r}\binom{K'N_tN_r-j-1}{N_tN_r-j}\frac{\Gamma(N_tN_r+j)}{(j-1)!} \\ &\times \frac{\alpha^{(N_tN_r+j)}\ {}_2F_1(N_tN_r+j,N_tN_r;N_tN_r+1;-\alpha z)}{((1/\alpha)-1)^{K'N_tN_r-j}} + (-1)^{N_tN_r} \\ &\times \sum_{j=1}^{(K'-1)N_tN_r}\binom{K'N_tN_r-j-1}{N_tN_r-1}\frac{\Gamma(N_tN_r+j)}{(j-1)!}\frac{{}_2F_1(N_tN_r+j,N_tN_r;N_tN_r+1;-z)}{(1-(1/\alpha))^{K'N_tN_r-j}}\Bigg)\,. \end{aligned} \quad (2.13)$$

Now, on substituting z as γ_{th} in (2.11) and (2.13), we get the expression of outage probability for cellular and D2D transmission, respectively.

2.4 Ergodic Capacity

In the previous section, we deduced an expression of PDF for the SINR. The PDFs can be used to analyze the ergodic capacity of the given system. The ergodic capacity in bps is given by

$$C = B\int_0^\infty \log_2(1+z)f_{\Gamma_k}(z)dz\,, \quad (2.14)$$

where B is bandwidth in Hz. For $k = 0$, the ergodic capacity is obtained on substituting (2.10) in (2.14), we get

$$\begin{aligned} C &= \frac{B}{\ln 2}\frac{\Gamma((K'+1)N_tN_r)}{\Gamma(N_tN_r)\Gamma(K'N_tN_r)}\int_0^\infty \frac{\ln(1+z)(\alpha^{K'}z)^{N_tN_r}}{z(\alpha+z)^{(K'+1)N_tN_r}}dz \\ &= \frac{1}{\ln 2}\frac{\Gamma((K'+1)N_tN_r)}{\Gamma(N_tN_r)\Gamma(K'N_tN_r)}\sum_{\ell=0}^{N_tN_r-1}\frac{(-1)^\ell}{(KN_tN_r+\ell)^2}\binom{N_tN_r-1}{\ell} \\ &\quad \times {}_2F_1(KN_tN_r+\ell, 1; KN_tN_r+\ell+1; 1-(1/\alpha))\,. \end{aligned} \tag{2.15}$$

Similarly, for $k = 1, \ldots, K$ ergodic capacity can be obtained on substituting (2.12) in (2.14). That is

$$\begin{aligned} C &= \frac{B}{\ln 2}\frac{1}{\alpha^{N_tN_r}\Gamma(N_tN_r)}\Bigg((-1)^{(K'-1)N_tN_r}\sum_{j=1}^{N_tN_r}\binom{K'N_tN_r-j-1}{N_tN_r-j}\frac{\Gamma(N_tN_r+j)}{((1/\alpha)-1)^{K'N_tN_r-j}} \\ &\quad \times\frac{1}{(j-1)!}\int_0^\infty \frac{\ln(1+z)z^{(N_tN_r-1)}}{(z+(1/\alpha))^{N_tN_r+j}}dz + (-1)^{N_tN_r}\sum_{j=1}^{(K'-1)N_tN_r}\binom{K'N_tN_r-j-1}{N_tN_r-1} \\ &\quad \times\frac{\Gamma(N_tN_r+j)}{(1-(1/\alpha))^{K'N_tN_r-j}}\frac{1}{(j-1)!}\int_0^\infty \frac{\ln(1+z)z^{(N_tN_r-1)}}{(z+1)^{N_tN_r+j}}dz\Bigg) \\ &= \frac{1}{\ln 2}\frac{1}{\alpha^{N_tN_r}\Gamma(N_tN_r)}\Bigg((-1)^{(K'-1)N_tN_r}\sum_{j=1}^{N_tN_r}\binom{K'N_tN_r-j-1}{N_tN_r-j}\frac{\Gamma(N_tN_r+j)}{((1/\alpha)-1)^{K'N_tN_r-j}} \\ &\quad \times\frac{1}{(j-1)!}\sum_{\ell=0}^{N_tN_r-1}(-1)^\ell\binom{N_tN_r-1}{\ell}\frac{\alpha^j}{(\ell+j)^2} + (-1)^{N_tN_r}\sum_{j=1}^{(K'-1)N_tN_r}\binom{K'N_tN_r-j-1}{N_tN_r-1} \\ &\quad \times\frac{\Gamma(N_tN_r+j)}{(1-(1/\alpha))^{K'N_tN_r-j}}\frac{1}{(j-1)!}\sum_{\ell=0}^{N_tN_r-1}(-1)^\ell\binom{N_tN_r-1}{\ell}\frac{1}{(\ell+j)^2}\Bigg)\,. \end{aligned} \tag{2.16}$$

2.5 Capacity with Outage

In ergodic capacity, averaging is done over the instantaneous SINR, therefore, the signal is expected to fade through all possible fading states. Thus observation interval is long. However, capacity with an outage is mainly applicable in slowly varying channels. That is, the instantaneous SINR is constant over a large number of transmissions. The outage capacity is given by

$$C_{out} = B(1-P_{out})\log_2(1+\gamma_{min})\,, \tag{2.17}$$

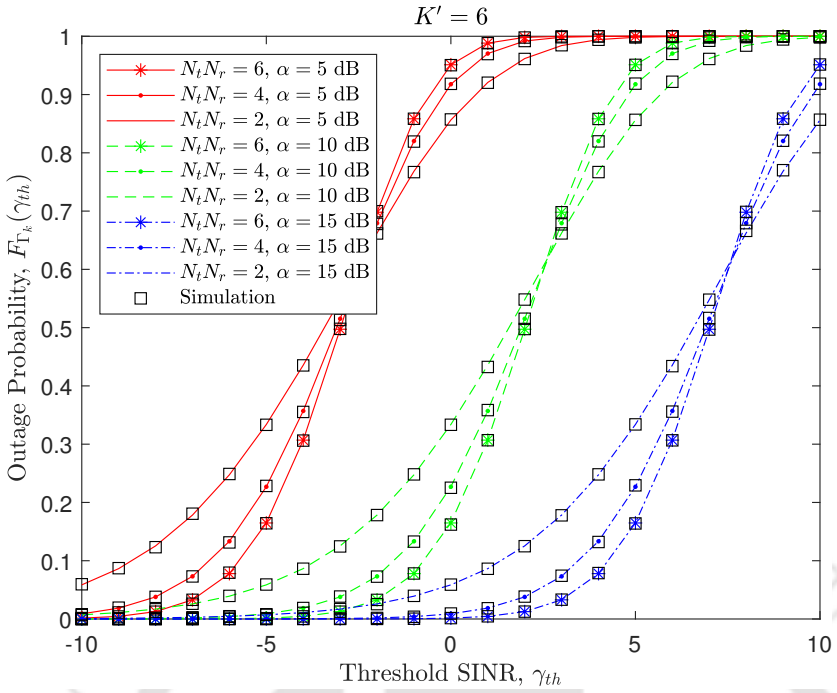

FIGURE 2.2: Plot of outage probability versus γ_{th} at cellular UE.

where P_{out} is outage probability obtained in Section 2.3 and γ_{min} is minimum SINR required for reliable communication.

2.6 Numerical Results and Discussion

In this section, numerical results for the outage probability, ergodic capacity, and outage capacity are plotted when SINR is observed at the i) cellular UE and ii) D2D UE. The precoding matrices considered at the transmitters are chosen according to the 3 GPP LTE specifications [71]. The simulation results are obtained using the Monte Carlo method considering perfect CSI at the receiver. Cellular nodes transmit signals with higher power when compared to D2D nodes. It is assumed that power transmitted at all the D2D nodes is the same. We considered 10^6 iterations to simulate each point on the plot.

In Figs. 2.2-2.5, numerical results for the outage probability are plotted with threshold SINR, γ_{th}. The outage probability with variation in N_tN_r and α for cellular UE is shown in Figs. 2.2 and 2.3 using (2.11) and for D2D UEs in Figs. 2.4 and 2.5 using (2.13). In Figs. 2.2 and 2.3, it is considered that 6 of the K precoding matrices are not orthogonal and thus cause interference. We observe that with the increase in α, the outage probability improves at the cellular receiver and degrades at

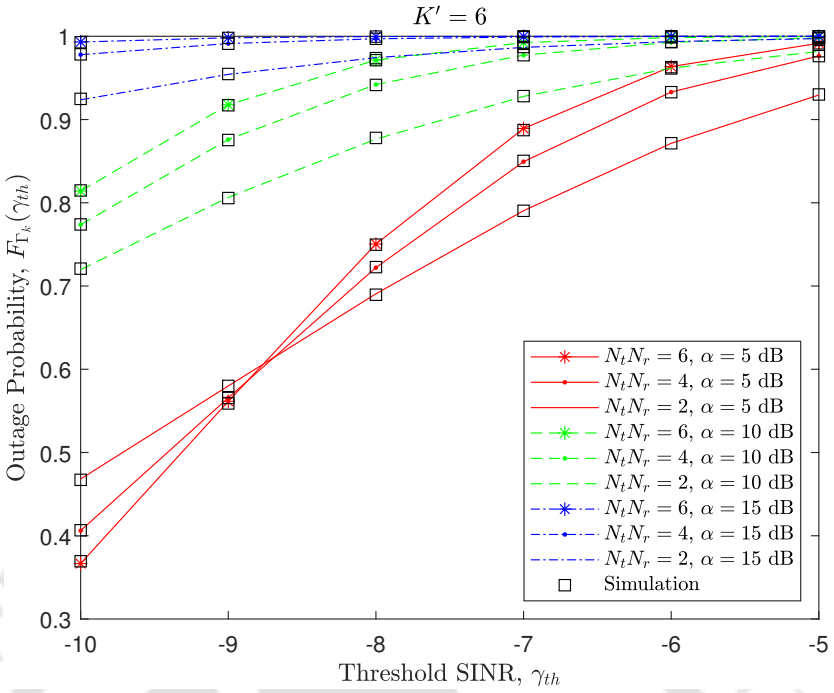

FIGURE 2.3: Plot of outage probability versus γ_{th} at D2D UE.

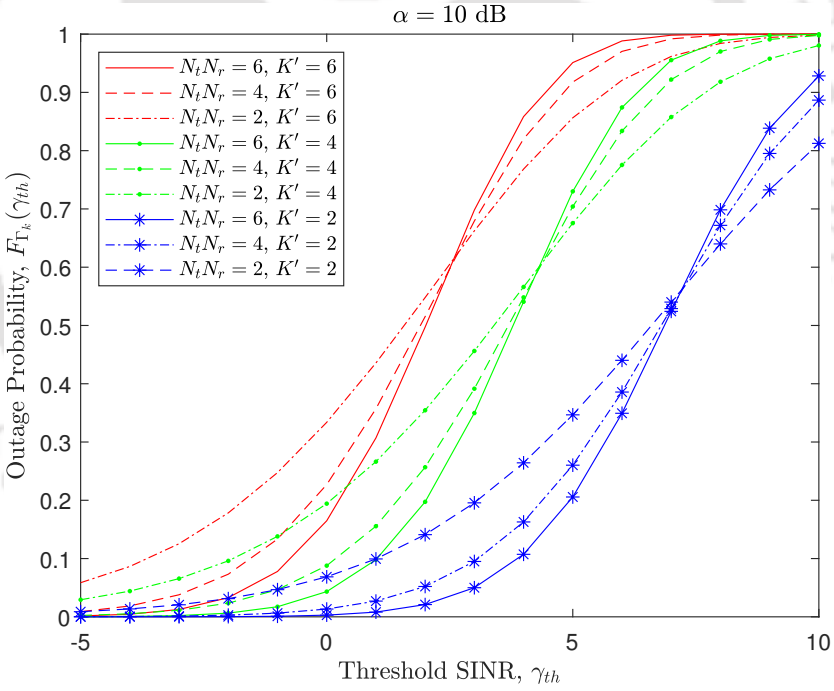

FIGURE 2.4: Plot of outage probability versus γ_{th} at cellular UE.

the D2D receiver. The effect of increase in the number of transmit or receive antennas represented using their product N_tN_r on outage probability is also shown. The crossovers in plots represent trade-off in the parameters. At low threshold SINR, the higher value of N_tN_r is preferred as it offers a diversity advantage and therefore improves the performance. However, at high threshold

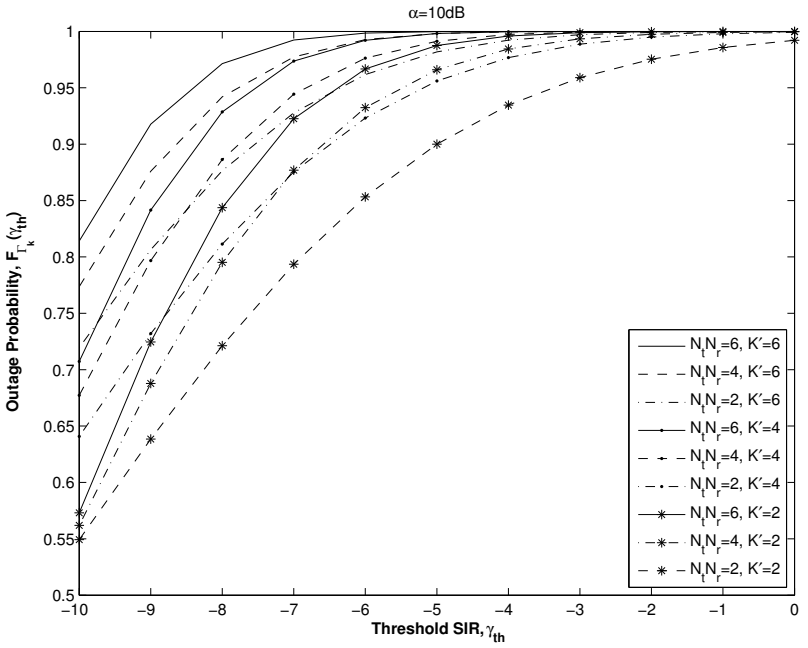

FIGURE 2.5: Plot of outage probability versus γ_{th} at D2D UE.

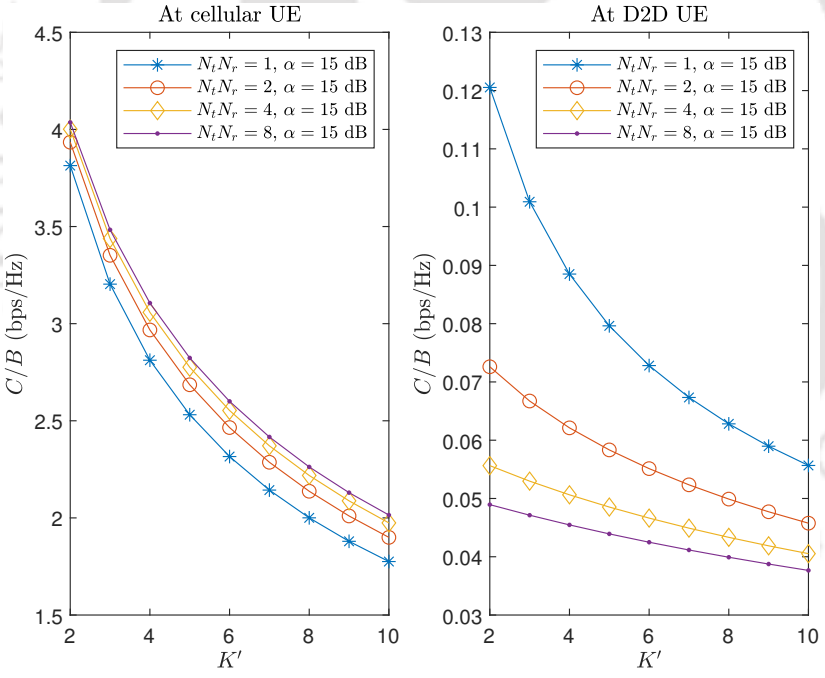

FIGURE 2.6: Plot of normalized ergodic capacity versus K'.

SINR, the links are more reliable therefore diversity is not very advantages and small values of N_tN_r are preferred. In Figs. 2.4 and 2.5, variation in outage probability with an increase in the number of interfering D2D UEs, K' (having non-orthogonal precoding matrix) is shown for $\alpha = 10$ dB. The outage probability degrades with an increase in K' but for some N_tN_r performance is better for higher K'. Thus, we can say an that loss in outage performance with increase in K'

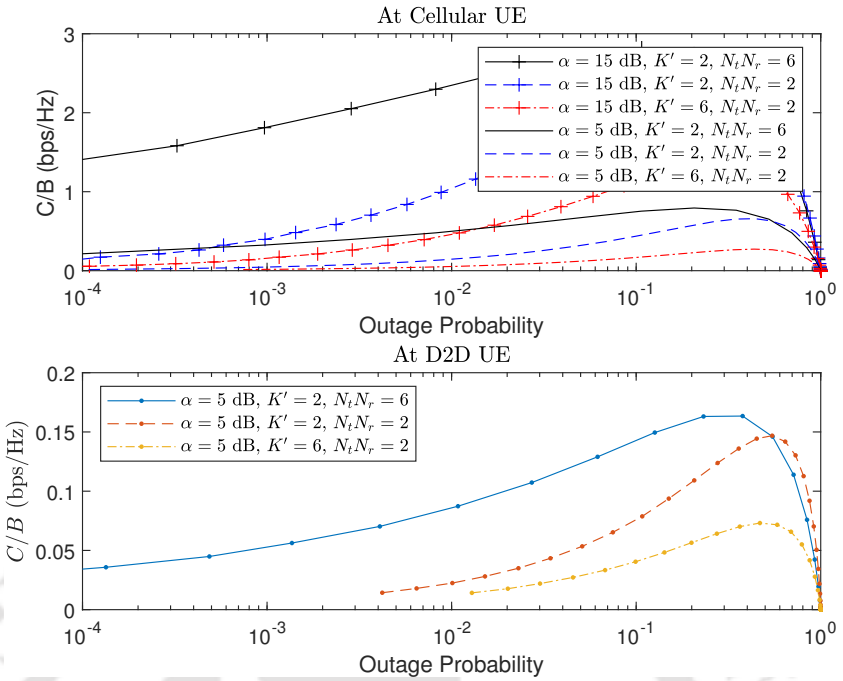

FIGURE 2.7: Plot of normalized outage capacity versus outage probability P_{out}.

can be improved by increasing N_tN_r. Further, it is also observed that for the same α, the outage probability is high when SINR is observed at the D2D UE. Numerical results are justified using the simulation plots.

The ergodic capacity at the cellular and D2D UEs are plotted in Fig. 2.6 using (2.16) and (2.17). It is observed that ergodic capacity degrades with gain in K'. Further, for the same α, ergodic capacity is better in case of communication over the cellular link than D2D transmission. With an increase in α ergodic capacity for cellular transmission improves. In Fig. 2.7, outage capacity is plotted using (2.17). It is seen that outage capacity improves with addition in N_tN_r and degrades with gain in interferers (K'). Further, the outage capacity for cellular link is high when more power is transmitted over the link.

2.7 Conclusion

In this chapter, we analyze performance on employing the IC method which allocates orthogonal precoding vectors in case of underlay D2D transmissions over the channel assigned for cellular communication. The expressions for the outage probability, ergodic capacity, outage capacity at the cellular and D2D receiver are deduced. Numerical results are plotted to observe the effect of

the different parameters on the performance. It is observed that outage probability at the cellular and D2D receivers reduce with an increase in the number of transmit or receive antennas. However, with gain in transmit power at cellular UE, the outage performance improves at cellular receiver and degrades at D2D receiver. Further, crossover in outage probability plots indicates tradeoff in parameters N_tN_r, α, and K'. The ergodic capacity and outage capacity at the cellular and D2D receivers are also obtained. It is observed that capacity improves with addition in transmit/receive antennas and degrades with growth in the number of interferers. Also, at the cellular receiver gain in capacity is observed for a larger difference between the transmit power at the cellular and D2D UEs.

Chapter 3

Performance Analysis of a Relay-Assisted D2D Underlay Cellular Network

3.1 Introduction

D2D communication underlying cellular network offers an advantage in terms of improved spectral efficiency but at the cost of the increase in interference due to sharing of resources [72, 73]. According to 3GPP standardized relay technology for LTE-A, the benefits of using a relay are improved reliability of the network, better cell edge performances, and expansion in cell edge coverage. These benefits of the relay technology can also be used to enhance the performance of D2D communications. Employing multiple antennas at the transmit and the receive nodes can further add to the performance of a communication system. The cellular link communicates signal with higher power over a longer distance when compared to power communicated over D2D link. Therefore, cellular link majorly contributes to interference. In our work, it is considered that interference caused by the cellular device can be removed using interference mitigation techniques and only the other D2D devices reusing the resources contribute to the interference.

The concept of relaying in wireless networks is widely explored in the literature. In D2D communication, relaying establish a connection when the two devices are not in line-of-sight and extends the range of reliable transmission. On underlying, interference disrupts the reliable transmission of the data to end user. Therefore, interference management techniques are considered in literature. In [45, 46], interference-aware power management techniques are presented where the transmit power at the source and the relay node is optimally decided in order to minimize the interference. Algorithm to achieve the target sum rate on sharing radio resource blocks is presented in [47]. A joint radio resource management and power allocation technique to maximize the sum rate is presented in [48]. Device spatial distribution is considered in [49] for interference management. The authors proposed a location-based interference mitigation technique in [50], where the D2D users in the inner region reuse resources assigned for cellular communication in the outer region and vice-a-versa. A method to derive the boundary of the accessible and reusable region is calculated. In [51], channel state information is used to mitigate interference caused by a cellular user equipment (CUE) to D2D pairs. Beamforming for interference management and interference cancellation techniques are presented in [74].

The outage probability for an underlay D2D system with single antenna at transmit and receive node is analyzed in [75]. A closed-form expression for the outage probability of a spatial modulation multiple-input multiple-output (MIMO) system with antenna selection is derived in [76]. In [52] and [77], closed-form expressions for the outage probability and symbol error probability (SEP) are obtained for different coherent and non-coherent modulation schemes. The SEP of a full duplex decode-and-forward (DF) relay system is obtained in [78]. In [79], authors have proposed an effective power allocation scheme to reduce the residual self-interference in a full-duplex relay system and found a closed expression of the outage, SEP and throughput. In [53], authors have analyzed the outage performance for D2D devices with perfect successive interference cancellation (SIC) and imperfect SIC. In [73], base station controls the maximum power transmitted by the D2D transmitter in order to mitigate interference caused at the neighbouring nodes.

In this chapter, we have analyzed the performance of a relay-assisted D2D communication system underlying a cellular network. The interference caused due to CUE is mitigated using decoding matrices. The expressions for the outage probability and SEP are deduced to analyze the impact of interference on the system. We assume each node to be equipped with N_t transmit and N_r receive antennas.

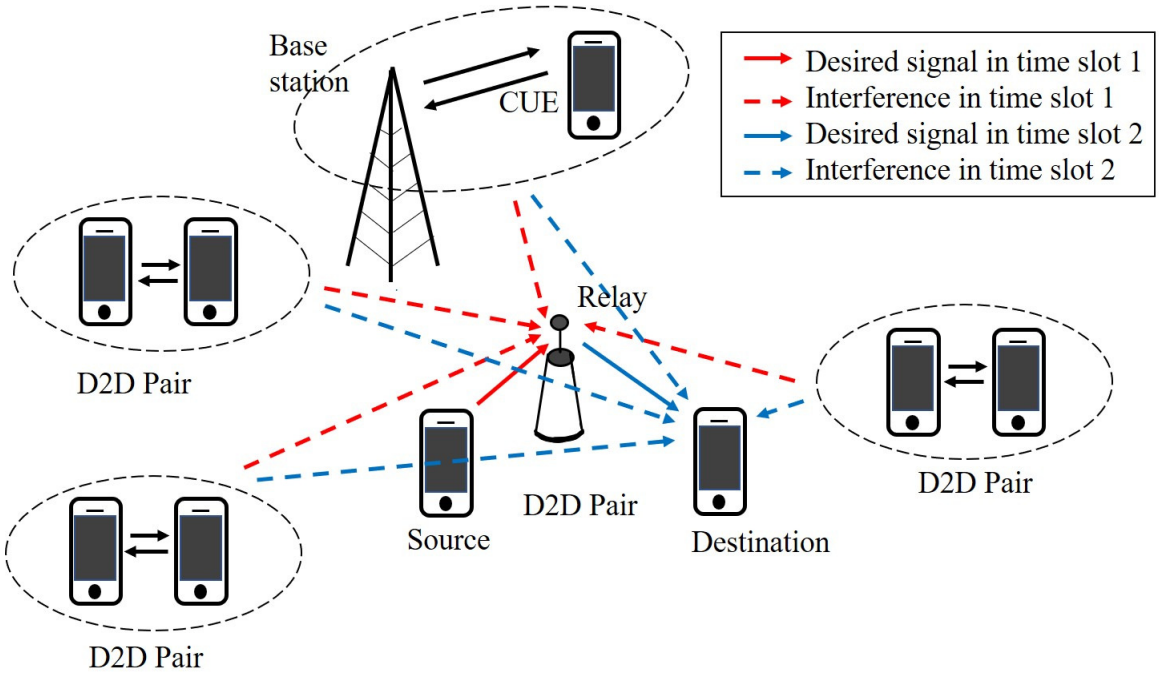

FIGURE 3.1: Relay-assisted underlay D2D communication network

3.2 System Model

We consider relay-assisted D2D communication underlaying a cellular network as shown in Fig. 3.1. The signal received at the relay observes interference from the transmission over the cellular link (UL/DL) and K D2D devices in the vicinity. Similarly, the signal received at the destination node observes interference due to transmission over cellular and L D2D relay nodes. Using different power control mechanisms, the interference caused by D2D user equipments (UEs) and relay due to the cellular link can be managed [76]. It is assumed that the inter-cell interference is negligible due to coordination among the cells [80]. However, interference at D2D UEs can be critical, thus requiring interference management strategies.

We assume that each communicating terminal is equipped with N_t transmit and N_r receive antennas. Additionally, it is considered that each device operates in half-duplex mode. The D2D source terminal S sends a $d \times 1$ symbol vector $\boldsymbol{x}_S$ with power P_S to the relay node R. The signal received at R in the first time slot is given by

$$\boldsymbol{y}_R = \sqrt{P_S}\boldsymbol{H}_{SR}\boldsymbol{\Phi}_S\boldsymbol{x}_S + \sqrt{P_C}\boldsymbol{H}_{CR}\boldsymbol{\Phi}_C\boldsymbol{x}_C + \sum_{i=1}^{K}\sqrt{P_{iR}}\boldsymbol{H}_{iR}\boldsymbol{\Phi}_i\boldsymbol{x}_i + \boldsymbol{n}_R\,, \tag{3.1}$$

where $\boldsymbol{\Phi}_\ell$ is the precoding matrix with dimension $N_t \times d$ employed at node ℓ and $\boldsymbol{H}_{\ell R}$ for $\ell \in \{S, C, 1, 2, \ldots, K\}$ are channel matrices of the link connecting nodes ℓ and R. The elements of $\boldsymbol{H}_{\ell R}$ are independent and circularly symmetric complex Gaussian distributed with zero mean and unit variance. $\boldsymbol{H}_{\ell R}$ are matrices with dimensions $N_r \times N_t$. $\boldsymbol{x}_C$ and $\boldsymbol{x}_i$ are $d \times 1$ symbol vectors transmitted over cellular and D2D link with power P_C and P_{iR}, respectively. $\boldsymbol{n}_R$ is $N_r \times 1$ additive white Gaussian noise (AWGN) at the relay. In (3.1), the first term corresponds to the desired signal component, the second term represents interference caused by the cellular transmission and the third term is the interference due to D2D devices communicating using the same cellular resources.

Consider DF protocol is employed at the relay node to process the received data. Let $\boldsymbol{u}_R$ be a $d \times 1$ signal vector decoded at the relay node and forwarded to the destination node D. The signal received at D is

$$\boldsymbol{y}_D = \sqrt{P_R}\boldsymbol{G}_{RD}\boldsymbol{\Psi}_R\boldsymbol{u}_R + \sqrt{P_C}\boldsymbol{G}_{CD}\boldsymbol{\Psi}_C\boldsymbol{u}_C + \sum_{i=1}^{L}\sqrt{P_{iD}}\boldsymbol{G}_{iD}\boldsymbol{\Psi}_i\boldsymbol{u}_i + \boldsymbol{n}_D \tag{3.2}$$

where $\boldsymbol{\Psi}_\ell$ is the precoding matrix employed at node ℓ having dimensions $N_t \times d$ and $\boldsymbol{G}_{\ell D}$ are channel matrices of the link connecting nodes ℓ and D, for $\ell \in \{R, C, 1, 2, \ldots, L\}$. The elements of $\boldsymbol{G}_{\ell D}$ are independent and circularly symmetric complex Gaussian distributed with zero mean and unit variance. $\boldsymbol{H}_{\ell R}$ has dimension $N_r \times N_t$. $\boldsymbol{u}_C$ and $\boldsymbol{u}_i$ are $d \times 1$ symbol vectors transmitted over cellular and D2D link with power P_C and P_{iD}, respectively. $\boldsymbol{n}_D$ is $N_r \times 1$ AWGN at the relay.

3.3 Interference Mitigation

The power of the signal transmitted over cellular link is high when compared to that sent over the D2D link, therefore the interference caused due to cellular link is comparatively larger. We consider interference at nodes R and D due to cellular transmission is mitigated using decoding matrices $\boldsymbol{U}_R$ and $\boldsymbol{U}_D$, respectively with dimension $N_r \times d$ [80]. The columns of $\boldsymbol{U}_R$ and $\boldsymbol{U}_D$ are orthonormal basis of the channel matrices $\boldsymbol{H}_{CR}$ and $\boldsymbol{H}_{CD}$, respectively. Using (3.1) and (3.2), the signals at nodes R and D on decoding are represented as

$$\begin{aligned}\hat{\boldsymbol{y}}_R &= \boldsymbol{U}_R^H\boldsymbol{y}_R \\ &= \sqrt{P_S}\boldsymbol{U}_R^H\boldsymbol{H}_{SR}\boldsymbol{\Phi}_S\boldsymbol{x}_S + \sqrt{P_C}\boldsymbol{U}_R^H\boldsymbol{H}_{CR}\boldsymbol{\Phi}_C\boldsymbol{x}_C + \sum_{i=1}^{K}\sqrt{P_{iR}}\boldsymbol{U}_R^H\boldsymbol{H}_{iR}\boldsymbol{\Phi}_i\boldsymbol{x}_i + \boldsymbol{w}_R \end{aligned} \tag{3.3}$$

and

$$\begin{aligned}\hat{\boldsymbol{y}}_D &= \boldsymbol{U}_D^H \boldsymbol{y}_D \\ &= \sqrt{P_R}\boldsymbol{U}_D^H \boldsymbol{G}_{RD}\boldsymbol{\Psi}_R \boldsymbol{u}_R + \sqrt{P_C}\boldsymbol{U}_D^H \boldsymbol{G}_{CD}\boldsymbol{\Psi}_C \boldsymbol{u}_C + \sum_{i=1}^{L}\sqrt{P_{iD}}\boldsymbol{U}_D^H \boldsymbol{G}_{iD}\boldsymbol{\Psi}_i \boldsymbol{u}_i + \boldsymbol{w}_D\,, \quad (3.4)\end{aligned}$$

respectively, where $\boldsymbol{w}_R = \boldsymbol{U}_R^H \boldsymbol{n}_R$ and $\boldsymbol{w}_D = \boldsymbol{U}_D^H \boldsymbol{n}_2$ are $d \times 1$ vectors with PSD N_0. Assuming interference from the CUE is aligned to the null space of the decoding matrices used at nodes R and D. Thus, we have $\boldsymbol{U}_R^H \boldsymbol{H}_{CR}\boldsymbol{\Phi}_C = \boldsymbol{0}$ and $\boldsymbol{U}_D^H \boldsymbol{G}_{CD}\boldsymbol{\Psi}_C = \boldsymbol{0}$. Further, the desired signal is processed through a full rank matrix, that gives $rank(\boldsymbol{U}_R^H \boldsymbol{H}_{SR}\boldsymbol{\Phi}_S) = d$ and $rank(\boldsymbol{U}_D^H \boldsymbol{G}_{RD}\boldsymbol{\Psi}_R) = d$ as in [80]. The precoding and decoding matrices used are assumed to have orthonormal column vectors with $\boldsymbol{\Phi}_i^H \boldsymbol{\Phi}_i = \boldsymbol{I}_{d\times d}$, $\boldsymbol{\Psi}_i^H \boldsymbol{\Psi}_i = \boldsymbol{I}_{d\times d}$ and $\boldsymbol{U}_j^H \boldsymbol{U}_j = I_{d\times d}$, where $\boldsymbol{I}_{d\times d}$ is $d \times d$ identity matrix. This interference alignment technique does not make an attempt to maximize the desired signal power within the desired subspace. Hence, the interference is eliminated while there is no combining or array gain for the desired signal which reduces this technique's optimality at intermediate SNR values. Using (3.3) and (3.4), the instantaneous SINRs at nodes R and D after cancellation of the interference caused by the CUE, are given by

$$\gamma_R = \frac{P_S||\boldsymbol{U}_R^H \boldsymbol{H}_{SR}\boldsymbol{\Phi}_S||^2}{\sum_{i=1}^{K} P_{iR}||\boldsymbol{U}_R^H \boldsymbol{H}_{iR}\boldsymbol{\Phi}_i||^2 + \boldsymbol{n}_0} \quad (3.5a)$$

$$\gamma_D = \frac{P_R||\boldsymbol{U}_D^H \boldsymbol{G}_{RD}\boldsymbol{\Psi}_R||^2}{\sum_{i=1}^{L} P_{iD}||\boldsymbol{U}_D^H \mathbf{G}_{iD}\boldsymbol{\Psi}_i||^2 + \boldsymbol{n}_0}\,, \quad (3.5b)$$

respectively, where $\boldsymbol{n}_0$ is $n_r \times 1$ vector representing the power of noise signal. We consider noise power $\boldsymbol{n}_0$ is very small when compared to interference due to D2D devices at the nodes R and D. Further, we assume that the signal overall D2D communication links is transmitted with the same power P_D. P_D is the power required for reliable communication to the farthest intended user over the link. Using the Cauchy-Schwarz inequality and the fact that $||\boldsymbol{U}_\ell||^2 = 1$, $||\boldsymbol{\Phi}_\ell||^2 = 1$ and $||\boldsymbol{\Psi}_\ell||^2 = 1$, (3.5) can be simplified to

$$\gamma_R \leq \frac{P_S}{P_D}\frac{||\boldsymbol{H}_{SR}||^2}{\sum_{i=1}^{K}||\boldsymbol{H}_{iR}||^2}\,, \quad (3.6a)$$

$$\gamma_D \leq \frac{P_R}{P_D}\frac{||\boldsymbol{G}_{RD}||^2}{\sum_{i=1}^{L}||\boldsymbol{G}_{iD}||^2}\,, \quad (3.6b)$$

respectively. We represent N_tN_r as N for the convenience of writing. In (3.6), numerator is sum of N independent exponentially distributed random variables (RVs) given by Gamma distribution and denominator is sum of K and L independent Gamma distributed RVs [68].

The CDF of γ_q for $q \in \{R, D\}$ is given by

$$F_{\gamma_q}(z) = \frac{\Gamma((\ell_q+1)N)}{\Gamma(N+1)\Gamma(\ell_q N)} \left(\frac{z}{\alpha_q}\right)^N {}_2F_1(N, (\ell_q+1)N; N+1; -z/\alpha_q), \tag{3.7}$$

where $\ell_R = K$, $\ell_D = L$, $\alpha_R = P_S/P_D$ and $\alpha_D = P_R/P_D$. Using [81, eqs. (15.1.1) and (15.3.5)], the Gauss hypergeometric function ${}_2F_1(\cdot)$ in (3.7) can be rewritten written as

$$\begin{aligned} {}_2F_1(N, (\ell_q+1)N; N+1; -z/\alpha_q) &= \left(1+\frac{z}{\alpha_q}\right)^{-N} {}_2F_1\left((\ell_q+1)N, 1; N+1; \frac{z}{z+\alpha_q}\right) \\ &= \left(1+\frac{z}{\alpha_q}\right)^{-N} \frac{\Gamma(N+1)}{\Gamma((\ell_q+1)N)} \sum_{n=0}^{\infty} \frac{\Gamma((\ell_q+1)N+n)}{\Gamma(N+n+1)} \left(\frac{z}{z+\alpha_q}\right)^n. \end{aligned} \tag{3.8}$$

Substituting (3.8) in (3.7), we get

$$F_{\gamma_q}(z) = \frac{1}{\Gamma(\ell_q N)} \sum_{n=0}^{\infty} \frac{\Gamma((\ell_q+1)N+n)}{\Gamma(N+n+1)} \left(\frac{z}{z+\alpha_q}\right)^{N+n}. \tag{3.9}$$

3.4 Performance Analysis

In this section, we present expressions of the outage probability and the SEP for relay-assisted D2D communication underlaying a cellular network.

3.4.1 Outage Probability

The signal received at the destination is in outage if either of the two links connecting nodes S to R or nodes R to D is in outage. Thus the outage probability at node D is

$$\begin{aligned} P_o &= 1 - (1 - P_o^{(R)})(1 - P_o^{(D)}) \\ &= P_o^{(R)} + P_o^{(D)} - P_o^{(R)} P_o^{(D)}, \end{aligned} \tag{3.10}$$

where $P_o^{(R)}$ is the probability that signal transmitted by node S to node R is in outage and $P_o^{(D)}$ is the probability that the signal communicated over link connecting nodes R and D is in outage. The outage probability $P_o^{(q)}$ in (3.10) is same as the CDF $F_{\gamma_q}(z)$ in (3.7) for $z = \gamma_{th}$, where γ_{th} is the threshold SINR for reliable communication.

3.4.2 Symbol Error Probability

The SEP for coherent modulation techniques can be expressed as [82]

$$\begin{aligned} P_e &= a\mathrm{E}[Q(\sqrt{b\gamma})] \\ &= \frac{a}{\sqrt{2\pi}} \int_0^\infty F_\gamma\left(\frac{u^2}{b}\right) \exp\left(-\frac{u^2}{2}\right) du\,, \end{aligned} \tag{3.11}$$

where a and b are constants specific to a modulation technique, the detailed values are specified in Table 6.1 of [82], γ is the instantaneous end-to-end SINR of the link connecting nodes S, R and D. $F_\gamma(\cdot)$ is the CDF of γ. Let $x = u^2/b$, then (3.11) can be rewritten as

$$P_e = \frac{a\sqrt{b}}{2\sqrt{2\pi}} \int_0^\infty \frac{1}{\sqrt{x}} F_\gamma(x) \exp\left(-\frac{bx}{2}\right) dx\,. \tag{3.12}$$

The end-to-end SEP at node D can be determined by substituting the end-to-end CDF $F_\gamma(x)$ in (3.12). Since SR and RD links are independent of each other, we have

$$F_\gamma(x) = F_{\gamma_R}(x) + F_{\gamma_D}(x) - F_{\gamma_R}(x)F_{\gamma_D}(x)\,, \tag{3.13}$$

where $F_{\gamma_q}(x)$ for $q \in \{R, D\}$ is given (3.7). We observe that the end-to-end CDF in (3.13) is same as the outage probability at node D given in (3.10). Using (3.7), (3.12) and (3.13), the end-to-end SEP at node D can be written as

$$\begin{aligned} P_e &= \frac{a\sqrt{b}}{2\sqrt{2\pi}} \left(\int_0^\infty \frac{F_{\gamma_R}(x)}{\sqrt{x}} \exp\left(-\frac{bx}{2}\right) dx + \int_0^\infty \frac{F_{\gamma_D}(x)}{\sqrt{x}} \exp\left(-\frac{bx}{2}\right) dx \right. \\ &\quad \left. - \int_0^\infty \frac{F_{\gamma_R}(x)F_{\gamma_D}(x)}{\sqrt{x}} \exp\left(-\frac{bx}{2}\right) dx \right)\,. \end{aligned} \tag{3.14}$$

Substituting (3.9) in (3.14) and adjusting the terms, the first and second term of (3.14) for $q \in \{R, D\}$ can be rewritten as

$$P_e^{(q)} = \frac{a\sqrt{b}}{2\sqrt{2\pi}} \frac{1}{\Gamma(\ell_q N)} \sum_{n=0}^{\infty} \frac{\Gamma((\ell_q+1)N+n)}{\Gamma(N+n+1)} \int_0^{\infty} \frac{1}{\sqrt{x}} \left(\frac{x}{x+\alpha_q}\right)^{N+n} \exp\left(-\frac{bx}{2}\right) dx\,. \tag{3.15}$$

The integral in (3.15) can be simplified using [71, eq. (3.383.6)], that is

$$\int_0^{\infty} \frac{1}{\sqrt{x}} \left(\frac{x}{x+\alpha_q}\right)^{N+n} \exp\left(-\frac{bx}{2}\right) dx = 2^{N+n}\sqrt{\frac{2}{b}}\Gamma(N+n+\frac{1}{2}) \exp\left(\frac{\alpha_q b}{4}\right) D_{1-2(N+n+1/2)}(\sqrt{\alpha_q b})\,. \tag{3.16}$$

Substituting (3.16) in (3.15), we get

$$P_e^{(q)} = \frac{2^{N+n-1}a}{\sqrt{\pi}} \sum_{n=0}^{\infty} \frac{\Gamma((\ell_q+1)N+n)\Gamma(N+n+1/2)}{\Gamma(\ell_q N)\Gamma(N+n+1)} \exp\left(\frac{\alpha_q b}{4}\right) D_{1-2(N+n+1/2)}(\sqrt{\alpha_q b})\,, \tag{3.17}$$

where $D_v(\cdot)$ is parabolic cylinder function.

The third term of (3.14) can be similarly simplified. However, it does not contribute much to the overall value of SEP therefore it can be ignored in order to obtain the simplified expression of P_e.

3.5 Numerical Results and Discussion

In this section, numerical results for the outage probability and SEP at the destination of the relay-assisted D2D underlying cellular system are plotted. It is observed that the numerical results are perfectly matching with the simulation results obtained using Monte Carlo method. We have generated 10^6 samples to plot the simulation results. We observe the impact on performance due to the increase in transmit and receive antennas, the number of interferes at the relay and destination node, transmit power at node S and node R, modulation scheme, and modulation order.

Numerical results for the outage probability in (3.10) are plotted with varying SIR thresholds in Figs. 3.2 and 3.3. In 3.2, we observe that with an increase in the number of transmit and receive antennas, the outage probability reduces. Further, it is observed that outage probability degrades with an increase in the number of D2D devices interfering at the relay and the destination node. The simulation plots justifies the analytical results obtained for the outage probability. The outage probability is plotted on varying α_1 and α_2 in Fig. 3. From the figure, it is observed that with an

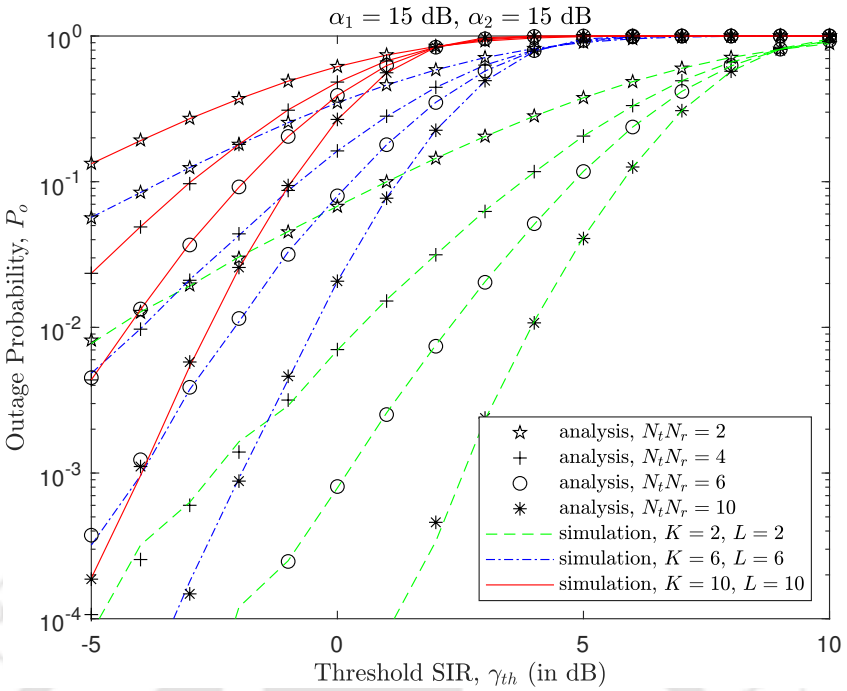

FIGURE 3.2: Plot of outage probability P_o versus threshold SIR γ_{th}.

increase in transmit power at the D2D source or relay with respect to the power transmitted by the other D2D devices the outage probability reduces.

The SEP versus α_1 is plotted in Fig. 3.4 for M-ary phase shift keying (MPSK) modulated data using (3.12), where $a = 2$ and $b = 2(\sin(\pi/M))^2$. We consider α_2 is same as α_1 for the plot. The results are shown for varying modulation order $M \in \{2, 4, 8, 16\}$, $K \in \{1, 10\}$, and $L \in \{1, 10\}$. The reduction in SEP performance with increase in modulation order and the number of interferes can be seen from the plot. Further, in Fig. 3.5 the SEP is plotted with α, where α is fraction of total power P_t assigned to node S and node R. Here, $P_S = (1 - \alpha)P_t$ and $P_R = \alpha P_t$. It is observed from the plot that performance is better when power communicated at node S and node R are almost equally assigned. However, the optimum performance is obtained for $\alpha > 0.5$, that is, power at relay node to be slightly greater than that at node S.

3.6 Conclusion

In this chapter, we analyze of the outage probability and SEP for a relay-assisted D2D communication system underlying a cellular network. We consider that the interference due to the cellular link is removed using an interference mitigation technique. Numerical results are plotted to observe

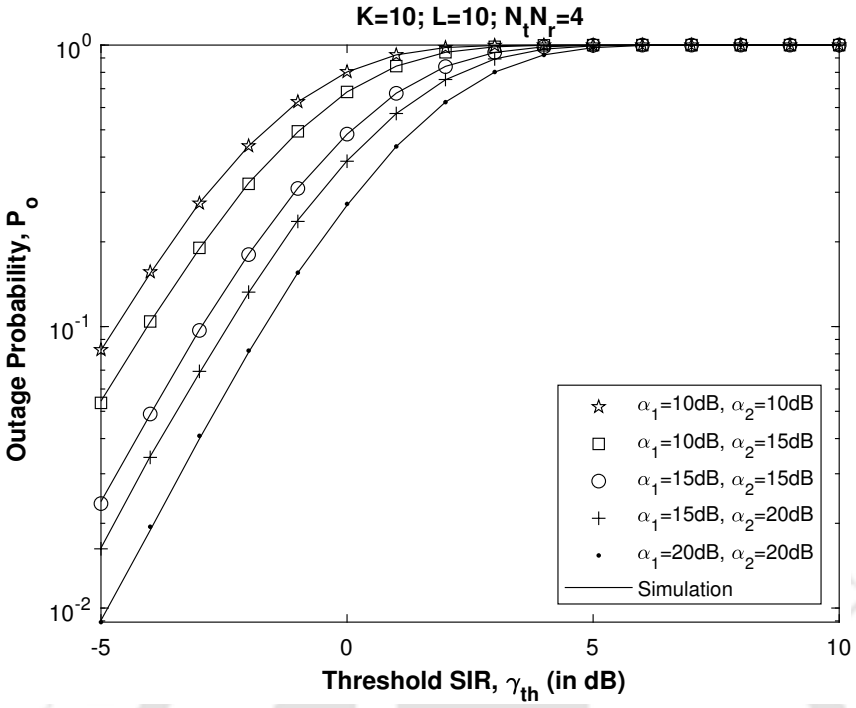

FIGURE 3.3: Plot of outage probability P_o versus SIR thresholds γ_{th} for $k = 10$, $L = 10$, $N = 4$ and varying α_1 and α_2.

the effects of different parameters on the outage and SEP performance measures. It is observed that the outage probability reduces with an increase in the number of transmit/receive antennas. Further, the outage performance improves with increase in power at the D2D source and relay node. The SEP performance of the system degrades with an increase in the modulation order and increment in number of interferes. The relay-assisted D2D system performs best when the data at relay node is transmitted with slightly more power than that at the source node. The end-to-end performance is also dependent on the placement of relay node with respect to the source and destination node. This can be explored as part of future work.

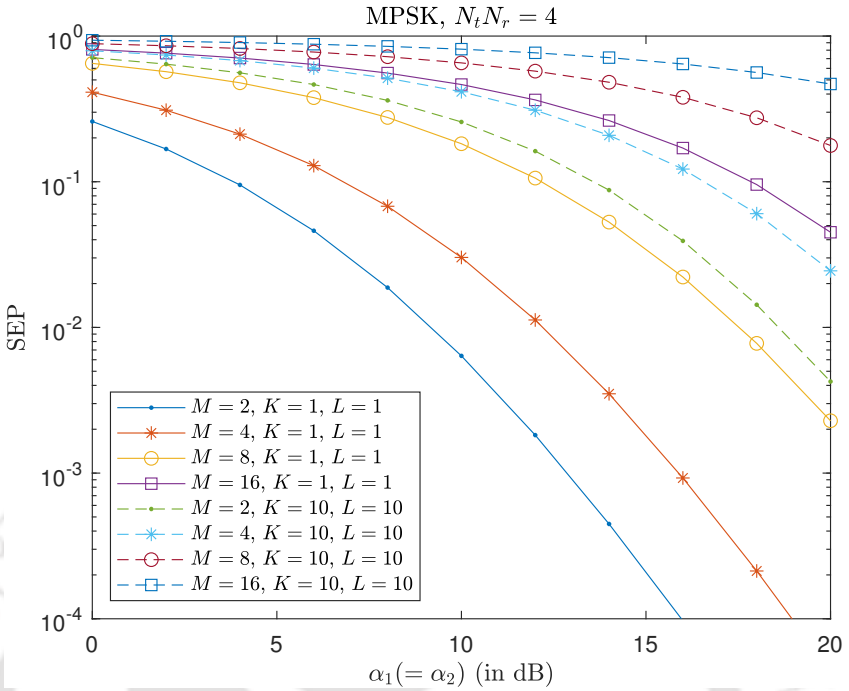

FIGURE 3.4: Plot of SEP versus $\alpha_1(=\alpha_2)(in$ dB) for $K \in \{1, 10\}$, $L \in \{1, 10\}$, $N_tN_r = 4$ and MPSK modulation with varying M.

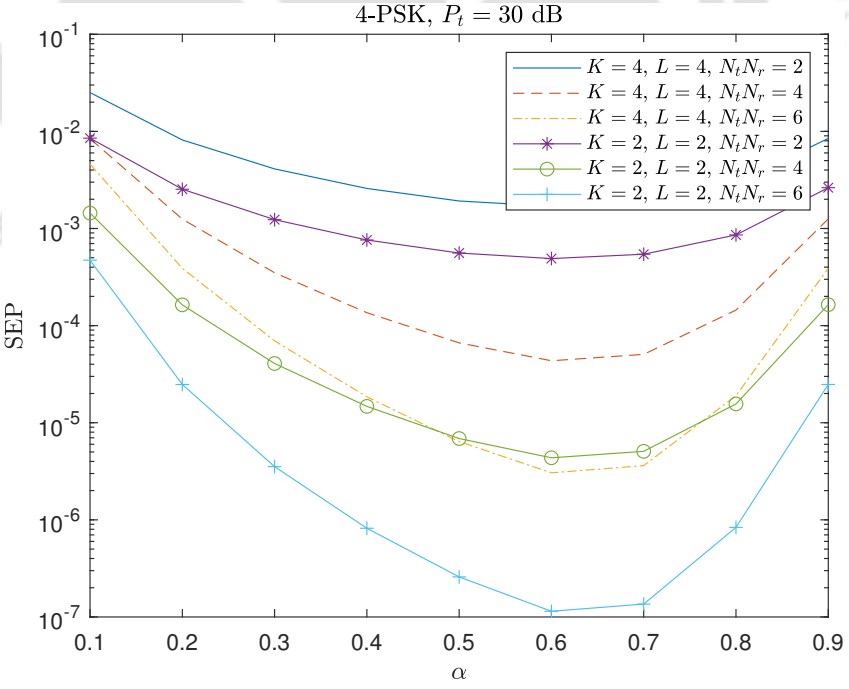

FIGURE 3.5: Plot of SEP versus α, where α is fraction of total power P_t assigned to node S and node R. $P_S = (1-\alpha)P_t$, $P_R = \alpha P_t$, $K \in \{2, 4\}$, $L \in \{2, 4\}$, $N_tN_r = \{2, 4, 6\}$, and $M = 4$.

Chapter 4

Performance Analysis of Underlay DF Relay System under Beaulieu-Xie Fading

4.1 Introduction

D2D underlaying cellular communication reuses the resources within a cell. This increases the cell capacity by accommodating more users in a cell. At high frequencies, the signal is heavily attenuated by obstacles and can reach shorter distances. Thus, relaying can assist in extending the coverage range and improving reliability at the receiver. DF is one of the popular techniques used for relaying in which the signal is decoded and then forwarded to the destination. In the literature, various channel models that characterize channels with scattered and LOS components are presented. In [21], the BX fading model that characterizes channels with multiple specular components when compared to the Ricean and generalized Ricean channel model used for LOS communication is presented. The BX model has applications in high-frequency wireless systems operating in millimeter-wave and terahertz bands having small cell sizes. The model is also applicable for high-speed vehicular communication. The BX distribution is derived from the non-central chi distribution. Also, it exhibits a seamless relationship to other fading models, such as the Ricean, generalized Ricean, Nakagami-m, Rayleigh fading models, and κ-μ distributions.

D2D communications underlaying cellular networks are widely explored in literature. Channel allocation and power control techniques for improved spectral efficiency and power efficiency of an underlay D2D system are presented in [64]. A centralized power control technique for an underlay D2D system is presented in [83] for improved coverage probability while reducing interference. In [61], algorithms are demonstrated for joint power control at the cellular and D2D source node in the case of an underlay D2D communication system to reduce the outage probability based on SINR.

The authors proposed the BX fading model in [21], where they discussed the transformation of BX distribution to generalized Ricean, non-central chi, and $\kappa - \mu$ distribution. The performance metrics like the level crossing rate and the average fade duration for the BX fading model are analyzed in [84]. The lower and the upper bound of the outage probability and the bit error rate (BER) on employing selection combining and equal-gain combining at the receiver are obtained in [85] and [86], respectively. The outage probability of an amplify-and-forward (AF)) relay system with a BX faded RF link and a free-space optical (FSO) link is analyzed in [87]. The PDF, CDF, and moment generating function (MGF) of the envelope for the cascaded double BX fading channel are deduced in [88]. These parameters are then used to obtain different performance metrics in this chapter.

In our previous work 3 [89], we analyzed the performance of a DF relay system underlaying a cellular network in the presence of interfering sources; the links are considered to be Rayleigh faded. In this work, we have examined the performance when links are BX faded which is more practical in high-frequency wireless applications. To the best of our knowledge, no work is reported in the literature on analyzing the effect of interference on the performance of a system with BX faded RF links. Each link of the system can be considered to be faded differently allowing us to analyze the system performance under varying channel conditions. In our system, an interference link affects the signal received at the relay and the destination node in a DF relay-based underlay D2D communication system. The expressions for the end-to-end average symbol error rate, outage probability, and outage capacity of the system are deduced. Further, we observe the effect of distance and power allocation on the performance of the system.

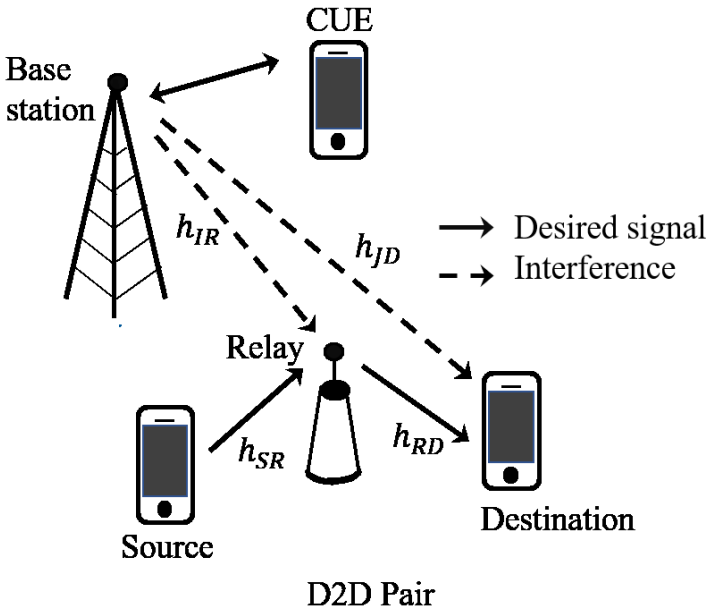

FIGURE 4.1: System model

4.2 System Model and Channel Model

4.2.1 System model

We consider an underlay D2D cellular system as shown in Fig. 4.1. The D2D pair constitutes a source S, a relay R, and a destination D. The resources used for cellular communication are reused for transmission at S and R in the D2D pair. Consider R and D observe co-channel interference due to the reuse of resources assigned for uplink/downlink transmission in cellular communication at node I in time slot 1 and node J in time slot 2, respectively. The nodes S, R, D, I, and J are assumed to be in the same cell. The link connecting nodes i and j for $i \in \{S, R, I, J\}$ and $j \in \{R, D\}$ are represented as ij. Assume the direct link between S and D is absent and each node is equipped with a single antenna.

The signal received at the relay y_R and the destination y_D in the first and the second time slots are

$$\begin{aligned} y_R &= \sqrt{P_S d_{SR}^{-\alpha}} h_{SR} x_S + \sqrt{P_I d_{JR}^{-\alpha}} h_{IR} x_I + n_R \quad \text{and} \\ y_D &= \sqrt{P_R d_{RD}^{-\alpha}} h_{RD} x_R + \sqrt{P_J d_{JD}^{-\alpha}} h_{JD} x_J + n_D \,, \end{aligned} \tag{4.1}$$

respectively. P_i is power transmitted at node i, d_{ij} is the distance between nodes i and j, h_{ij} is the channel gain of the link ij, x_i is the symbol transmitted at node i, and n_j is additive white Gaussian noise (AWGN) added at node j, for $i \in \{S, R, I, J\}$ and $j \in \{R, D\}$. α is the path loss exponent. All links are assumed to have the same path loss exponent for computational ease. Both the signal and the interference links are considered to be BX faded. Using (4.1), the instantaneous SINR at nodes R and D are given by

$$\begin{aligned} \zeta_{SR} &= \frac{P_S d_{SR}^{-\alpha} |h_{SR}|^2}{P_I d_{IR}^{-\alpha} |h_{IR}|^2 + N_0} \\ \zeta_{RD} &= \frac{P_R d_{RD}^{-\alpha} |h_{RD}|^2}{P_J d_{JD}^{-\alpha} |h_{JD}|^2 + N_0}, \end{aligned} \tag{4.2}$$

respectively, where N_0 is noise power spectral density. The instantaneous SINRs in (4.2) can be approximated for $(P_I/N_0) d_{IR}^{-\alpha} |h_{IR}|^2 >> 1$ and $(P_J/N_0) d_{JD}^{-\alpha} |h_{JD}|^2 >> 1$ as

$$\begin{aligned} \zeta_{SR} &\approx \frac{(P_S/N_0) d_{SR}^{-\alpha} |h_{SR}|^2}{(P_I/N_0) d_{IR}^{-\alpha} |h_{IR}|^2} \\ \zeta_{RD} &\approx \frac{(P_R/N_0) d_{RD}^{-\alpha} |h_{RD}|^2}{(P_J/N_0) d_{JD}^{-\alpha} |h_{JD}|^2}. \end{aligned} \tag{4.3}$$

4.2.2 Channel model

The PDF of the BX fading model is given by

$$f_X(x) = \frac{2m x^m}{\Omega \lambda^{m-1}} \exp\left(-\frac{m(x^2+\lambda^2)}{\Omega}\right) I_{m-1}\left(\frac{2m}{\Omega}\lambda x\right) u(x), \tag{4.4}$$

where $u(\cdot)$ is the unit step function and $I_n(\cdot)$ is modified Bessel function of the first kind and nth order. The parameter m controls the shape, Ω the spread, and λ influences the location and height of the mode of the PDF. Parameter m is a measure of the severity of fading and is also known as the fading figure. Similar to the K factor in the Rician distribution, the parameter K for BX faded channel is defined as $K = \lambda^2/\Omega$, where λ^2 is the power contained in LOS components and Ω represents the power of non-LOS components [21].

The PDF of instantaneous SNR of ijth link γ_{ij} given by $(P_i/N_0)d_{ij}^{-\alpha}|h_{ij}|^2$ in (4.3) can be represented in terms of parameters m_i and K_i of link ij. The PDF distribution is given by [90]

$$\begin{aligned} f_{\gamma_{ij}}(\gamma) &= \frac{m_i K_i}{\gamma}\left(\frac{(1+K_i)\gamma}{K_i\bar{\gamma}_{ij}}\right)^{\frac{m_i+1}{2}} \exp\left(-m_i\left(K_i+\frac{(1+K_i)\gamma}{\bar{\gamma}_{ij}}\right)\right) \\ &\quad \times I_{m_i-1}\left(2m_i\sqrt{\frac{K_i(1+K_i)\gamma}{\bar{\gamma}_{ij}}}\right), \end{aligned} \tag{4.5}$$

where $\bar{\gamma}_{ij}$ is the average SNR of link ij. Using the series form representation of the Bessel function, the PDF in (4.5) can be rewritten as

$$f_{\gamma_{ij}}(\gamma) = \left(\frac{m_i(1+K_i)}{\bar{\gamma}_{ij}}\right)^{\ell+m_i} \exp\left(-m_i\left(K_i+\frac{(1+K_i)\gamma}{\bar{\gamma}_{ij}}\right)\right)\sum_{\ell=0}^{\infty} m_i^{\ell}\frac{K_i^{\ell}\gamma^{\ell+m_i-1}}{\ell!\Gamma(\ell+m_i)}, \tag{4.6}$$

where $\Gamma(\cdot)$ is Gamma operation.

4.3 Performance Analysis

Let X represent the numerator and Y denote the denominator term of the instantaneous SINR in (4.3). For BX faded channel, the distribution of X and Y is given by (4.5). Using variable transformation, the PDF of $Z = X/Y$ is obtained using

$$f_Z(z) = \int_{-\infty}^{\infty} |y| f_{XY}(yz, y)dy, \tag{4.7}$$

where $f_{XY}(x, y)$ is the joint distribution of random variables X and Y. The signal and the interference link are independent, therefore the joint distribution in (4.7) can be rewritten as $f_{XY}(yz, y) = f_X(yz)f_Y(y)$. Using (4.6) and (4.7), the PDF of the instantaneous SINR ζ_{SR} in (4.3) can be written as

$$\begin{aligned} f_{\zeta_{SR}}(z) &= \exp\left(-\left(m_S K_S + m_I K_I\right)\right)\sum_{i=0}^{\infty}\sum_{j=0}^{\infty}\left(m_S K_S\right)^i\left(m_I K_I\right)^j \frac{z^{i+m_S-1}A_S^{i+m_S}A_I^{j+m_I}}{i!j!\Gamma(i+m_S)\Gamma(j+m_I)} \\ &\quad \times \int_0^{\infty} y^{(i+j+m_S+m_I-1)}\exp\left(-y(A_S z + A_I)\right)dy, \end{aligned} \tag{4.8}$$

where $A_n = m_n(1+K_n)/\bar{\gamma}_n$, $n \in \{S, I\}$. On solving the integral in (4.8), we get

$$f_{\zeta_{SR}}(z) = \exp\left(-\left(m_S K_S + m_I K_I\right)\right) \sum_{i=0}^{\infty}\sum_{j=0}^{\infty} \left(m_S K_S\right)^i \left(m_I K_I\right)^j \frac{z^{i+m_S-1}}{i!j!} \frac{\Gamma(i+j+m_S+m_I)}{\Gamma(i+m_S)\Gamma(j+m_I)} \times \frac{A_S^{i+m_S} A_I^{j+m_I}}{(A_S z + A_I)^{(i+j+m_S+m_I)}}\,. \tag{4.9}$$

Using (4.9), the CDF of ζ_{SR} is obtained as

$$F_{\zeta_{SR}}(z) = \exp\left(-\left(m_S K_S + m_I K_I\right)\right) \sum_{i=0}^{\infty}\sum_{j=0}^{\infty} \frac{\left(m_S K_S\right)^i}{(i+m_S)} \left(m_I K_I\right)^j \frac{\Gamma(i+j+m_S+m_I)}{\Gamma(i+m_S)\Gamma(j+m_I)} \times \left(\frac{A_S}{A_I}\right)^{i+m_S} \frac{z^{(i+m_S)}}{i!j!}\, {}_2F_1\left(i+m_S, i+j+m_S+m_I; 1+i+m_S; -\frac{A_S}{A_I} z\right), \tag{4.10}$$

where $A_n = m_n(1+K_n)/\bar{\gamma}_n$, $n \in \{R, J\}$. ${}_2F_1(\cdot;\cdot;\cdot)$ is the Gaussian hypergeometric function. Similarly, the CDF of the instantaneous SINR ζ_{RD} in (4.3) can be written as

$$F_{\zeta_{RD}}(z) = \exp\left(-\left(m_R K_R + m_J K_J\right)\right) \sum_{i=0}^{\infty}\sum_{j=0}^{\infty} \frac{\left(m_R K_R\right)^i}{(i+m_R)} \left(m_J K_J\right)^j \frac{\Gamma(i+j+m_R+m_J)}{\Gamma(i+m_R)\Gamma(j+m_J)} \times \left(\frac{A_R}{A_J}\right)^{i+m_R} \frac{z^{(i+m_R)}}{i!j!}\, {}_2F_1\left(i+m_R, i+j+m_R+m_J; 1+i+m_R; -\frac{A_R}{A_J} z\right). \tag{4.11}$$

4.3.1 Outage Probability

In a DF relay system, the signal received at the node D is in the outage if one of the two links SR and RD is in the outage. Since the links SR and RD are independent of each other, the outage probability of the system is given by

$$\begin{aligned} F_{\zeta}(\zeta_{th}) &= \Pr(\zeta < \zeta_{th}) \\ &= 1 - \Pr(\zeta_{SR} > \zeta_{th}) \Pr(\zeta_{RD} > \zeta_{th})\,, \end{aligned} \tag{4.12}$$

where ζ_{th} is the predefined threshold. Rewriting (4.12) in terms of the CDF function, we get

$$\begin{aligned} F_{\zeta}(\zeta_{th}) &= 1 - (1 - F_{\zeta_{SR}}(\zeta_{th}))(1 - F_{\zeta_{RD}}(\zeta_{th})) \\ &= F_{\zeta_{SR}}(\zeta_{th}) + F_{\zeta_{RD}}(\zeta_{th}) - F_{\zeta_{SR}}(\zeta_{th}) F_{\zeta_{RD}}(\zeta_{th})\,. \end{aligned} \tag{4.13}$$

The end-to-end outage probability can be obtained by substituting (4.10) and (4.11) in (4.13).

4.3.2 Outage capacity

Outage capacity is defined as the probability that the capacity falls below a certain threshold, η_{th}. We have

$$C_{out} = F_{\zeta}(2^{\eta_{th}/W} - 1)\,, \tag{4.14}$$

where $F_{\zeta}(\cdot)$ is the CDF of the end-to-end instantaneous SINR expressed in (4.13) and W is the received signal bandwidth.

4.3.3 Average Symbol Error Probability

The generalized expression for the average SEP of coherent modulation techniques is

$$P_e = aE[Q(\sqrt{b\zeta})]\,. \tag{4.15}$$

The expression in (4.15) can be simplified to

$$P_e = \frac{a\sqrt{b}}{2\sqrt{2\pi}} \int_0^{\infty} \frac{1}{\sqrt{x}} F_{\zeta}(x) \exp\left(-\frac{bx}{2}\right) dx\,, \tag{4.16}$$

where $F_{\zeta}(x)$ is defined in (4.13). On substituting (4.13) in (4.16), the end-to-end average SEP can be written as

$$\begin{aligned} P_e &= \frac{a\sqrt{b}}{2\sqrt{2\pi}} \left(\int_0^{\infty} \frac{1}{\sqrt{x}} F_{\zeta_{SR}}(x) \exp\left(-\frac{bx}{2}\right) dx + \int_0^{\infty} \frac{1}{\sqrt{x}} F_{\zeta_{RD}}(x) \exp\left(-\frac{bx}{2}\right) dx \right. \\ &\quad \left. - \int_0^{\infty} \frac{1}{\sqrt{x}} F_{\zeta_{SR}}(x) F_{\zeta_{RD}}(x) \exp\left(-\frac{bx}{2}\right) dx \right) \\ &= \frac{a\sqrt{b}}{2\sqrt{2\pi}} (T_1 + T_2 - T_3)\,, \end{aligned} \tag{4.17}$$

where T_1, T_2, and T_3 are the three integral terms in (4.17). On substituting (4.23) in (4.17), the term T_1 can be simplified to

$$\begin{aligned}
T_1 &= \exp\left(-m_S K_S\right)\exp\left(-m_I K_I\right)\sum_{i=0}^{\infty}\sum_{j=0}^{\infty}\frac{\left(m_S K_S\right)^i\left(m_I K_I\right)^j\Gamma(i+j+m_S+m_I)}{i!j!\Gamma(i+m_S+1)\Gamma(j+m_I)}\left(\frac{A_S}{A_I}\right)^{i+m_S}\\
&\quad\times\int_0^{\infty} z^{(i+m_S-0.5)}\exp\left(-\frac{bz}{2}\right)\,{}_2F_1\left(i+m_S,i+j+m_S+m_I,1+i+m_S,-\frac{A_S z}{A_I}\right)dz\\
&= \exp\left(-m_S K_S\right)\exp\left(-m_I K_I\right)\sum_{i=0}^{\infty}\sum_{j=0}^{\infty}\frac{\left(m_S K_S\right)^i\left(m_I K_I\right)^j}{i!j!}\left(\sqrt{\frac{2\pi}{b}}\right.\\
&\quad-2\left(\frac{A_I}{A_S}\right)^{1/2}\frac{\Gamma(i+m_S+1/2)\Gamma(j+m_I-1/2)}{\Gamma(i+m_S)\Gamma(j+m_I)}\,{}_pF_q\left(\frac{1}{2},i+m_S+\frac{1}{2};\frac{3}{2},\frac{3}{2}-j-m_I;\frac{b}{2}\frac{A_I}{A_S}\right)\\
&\quad-\left(\frac{b}{2}\right)^{j+m_I-1/2}\left(\frac{A_I}{A_S}\right)^{j+m_I}\frac{\Gamma(1/2-j-m_I)\Gamma(i+j+m_S+m_I)}{\Gamma(i+m_S)\Gamma(j+m_I+1)}\\
&\quad\left.\times\,{}_pF_q\left(j+m_I,i+j+m_S+m_I;j+m_I+\frac{1}{2},j+m_I+1;\frac{b}{2}\frac{A_I}{A_S}\right)\right). \qquad (4.18)
\end{aligned}$$

The term T_2 can be similarly evaluated and is expressed as

$$\begin{aligned}
T_2 &= \exp\left(-m_R K_R\right)\exp\left(-m_J K_J\right)\sum_{i=0}^{\infty}\sum_{j=0}^{\infty}\frac{\left(m_R K_R\right)^i\left(m_J K_J\right)^j}{i!j!}\left(\sqrt{\frac{2\pi}{b}}\right.\\
&\quad-2\left(\frac{A_J}{A_R}\right)^{1/2}\frac{\Gamma(i+m_R+1/2)\Gamma(j+m_J-1/2)}{\Gamma(i+m_R)\Gamma(j+m_J)}\,{}_pF_q\left(\frac{1}{2},i+m_R+\frac{1}{2};\frac{3}{2},\frac{3}{2}-j-m_J;\frac{b}{2}\frac{A_J}{A_R}\right)\\
&\quad-\left(\frac{b}{2}\right)^{j+m_J-1/2}\left(\frac{A_J}{A_R}\right)^{j+m_J}\frac{\Gamma(1/2-j-m_J)\Gamma(i+j+m_R+m_J)}{\Gamma(i+m_R)\Gamma(j+m_J+1)}\\
&\quad\left.\times\,{}_pF_q\left(j+m_J,i+j+m_R+m_J;j+m_J+\frac{1}{2},j+m_J+1;\frac{b}{2}\frac{A_J}{A_R}\right)\right). \qquad (4.19)
\end{aligned}$$

Further, the term T_3 can be simplified using [91, eq. (4.3.14)] to

$$
\begin{aligned}
T_3 &= \exp\left(-m_S K_S\right)\exp\left(-m_I K_I\right)\exp\left(-m_R K_R\right)\exp\left(-m_J K_J\right)\sum_{i=0}^{\infty}\sum_{j=0}^{\infty}\sum_{k=0}^{\infty}\sum_{\ell=0}^{\infty}\frac{\left(m_S K_S\right)^i\left(m_I K_I\right)^j}{i!j!}\\
&\times\frac{\left(m_R K_R\right)^k\left(m_J K_J\right)^\ell}{k!\ell!}\frac{\Gamma(i+j+m_S+m_I)}{\Gamma(i+m_S+1)\Gamma(j+m_I)}\frac{\Gamma(k+\ell+m_R+m_J)}{\Gamma(k+m_R+1)\Gamma(\ell+m_J)}\left(\frac{A_S}{A_I}\right)^{i+m_S}\left(\frac{A_R}{A_J}\right)^{k+m_R}\\
&\times\int_0^{\infty} z^{(i+k+m_S+m_R-0.5)}\exp\left(-\frac{bz}{2}\right)\,{}_2F_1\left(i+m_S, i+j+m_S+m_I, 1+i+m_S, -\frac{A_S z}{A_I}\right)\\
&\times\,{}_2F_1\left(k+m_R, k+\ell+m_R+m_J, 1+k+m_R, -\frac{A_R z}{A_J}\right)dz\\
&=\exp\left(-m_S K_S\right)\exp\left(-m_I K_I\right)\exp\left(-m_R K_R\right)\exp\left(-m_J K_J\right)\sum_{i=0}^{\infty}\sum_{j=0}^{\infty}\sum_{k=0}^{\infty}\sum_{\ell=0}^{\infty}\frac{\left(m_S K_S\right)^i\left(m_I K_I\right)^j}{i!j!}\\
&\times\frac{\left(m_R K_R\right)^k\left(m_J K_J\right)^\ell}{k!\ell!}\frac{\Gamma(i+j+m_S+m_I)}{\Gamma(i+m_S+1)\Gamma(j+m_I)}\frac{\Gamma(k+\ell+m_R+m_J)}{\Gamma(k+m_R+1)\Gamma(\ell+m_J)}\left(\frac{A_S}{A_I}\right)^{i+m_S}\left(\frac{A_R}{A_J}\right)^{k+m_R}\\
&\times\int_0^{\infty}\sum_{n=0}^{\infty}\frac{(i+m_S)_n(i+j+m_S+m_I)_n}{n!(1+i+m_S)_n}z^{(i+k+m_S+m_R-0.5)}\exp\left(-\frac{bz}{2}\right)\left(-\frac{A_S z}{A_I}\right)^n dz\\
&\times\,{}_4F_3\left(k+m_R, k+\ell+m_R+m_J, -(i+m_S+n), -n; 1+k+m_R, 1-i-m_S-n, 1-i-j-m_S-m_I-n; \frac{A_I A_R}{A_S A_J}\right)\\
&=\exp\left(-m_S K_S\right)\exp\left(-m_I K_I\right)\exp\left(-m_R K_R\right)\exp\left(-m_J K_J\right)\sum_{i=0}^{\infty}\sum_{j=0}^{\infty}\sum_{k=0}^{\infty}\sum_{\ell=0}^{\infty}\frac{\left(m_S K_S\right)^i\left(m_I K_I\right)^j}{i!j!}\\
&\times\frac{\left(m_R K_R\right)^k\left(m_J K_J\right)^\ell}{k!\ell!}\frac{\Gamma(i+j+m_S+m_I)}{\Gamma(i+m_S+1)\Gamma(j+m_I)}\frac{\Gamma(k+\ell+m_R+m_J)}{\Gamma(k+m_R+1)\Gamma(\ell+m_J)}\left(\frac{A_S}{A_I}\right)^{i+m_S}\left(\frac{A_R}{A_J}\right)^{k+m_R}\\
&\times\sum_{n=0}^{\infty}\frac{(i+m_S)_n(i+j+m_S+m_I)_n}{n!(1+i+m_S)_n}\left(-\frac{A_S}{A_I}\right)^n\left(\frac{b}{2}\right)^{-(0.5+i+k+n+m_S+m_R)}\Gamma(0.5+i+k+n+m_S+m_R)\\
&\times\,{}_4F_3\left(k+m_R, k+\ell+m_R+m_J, -(i+m_S+n), -n; 1+k+m_R, 1-i-m_S-n, 1-i-j-m_S-m_I-n; \frac{A_I A_R}{A_S A_J}\right).
\end{aligned}
\tag{4.20}
$$

4.4 Asymptotic Approximations

4.4.1 Outage probability

At high SNRs, the CDF expressions in (4.10) and (4.11) can be approximated as

$$
\begin{aligned}
\lim_{\bar{\gamma}_{SR}\to\infty} F_{\zeta_{SR}}(z) &= F^{\infty}_{\zeta_{SR}}(z)\\
&= \exp\left(-\left(m_S K_S + m_I K_I\right)\right)\sum_{i=0}^{\infty}\sum_{j=0}^{\infty}\frac{\left(m_S K_S\right)^i\left(m_I K_I\right)^j}{i!j!}\\
&\quad\times\frac{\Gamma(i+j+m_S+m_I)}{\Gamma(i+m_S+1)\Gamma(j+m_I)}\left(\frac{A_S}{A_I}\right)^{i+m_S} z^{(i+m_S)}
\end{aligned}
\tag{4.21}
$$

and

$$\begin{aligned}\lim_{\bar{\gamma}_{RD}\to\infty} F_{\zeta_{RD}}(z) &= F^{\infty}_{\zeta_{RD}}(z)\\ &= \exp(-(m_R K_R + m_J K_J))\sum_{i=0}^{\infty}\sum_{j=0}^{\infty}\frac{(m_R K_R)^i (m_J K_J)^j}{i!j!}\\ &\quad\times\frac{\Gamma(i+j+m_R+m_J)}{\Gamma(i+m_R+1)\Gamma(j+m_J)}\left(\frac{A_R}{A_J}\right)^{i+m_R} z^{(i+m_R)}, \end{aligned} \tag{4.22}$$

respectively. Substituting A_n for $n \in \{S, R, I, J\}$ in (4.23) and (4.24), respectively and replacing $\bar{\gamma}_S/\bar{\gamma}_I$ and $\bar{\gamma}_R/\bar{\gamma}_J$ by $\bar{\zeta}_{SR}$ and $\bar{\zeta}_{RD}$, respectively, we get

$$\begin{aligned}F^{\infty}_{\zeta_{SR}}(z) &= \exp\left(-(m_S K_S + m_I K_I)\right)\sum_{i=0}^{\infty}\sum_{j=0}^{\infty}\frac{K_S^i K_I^j}{i!j!}\left(\frac{1+K_S}{1+K_I}\right)^{i+m_S}\\ &\quad\times\frac{\Gamma(i+j+m_S+m_I)}{\Gamma(i+m_S+1)\Gamma(j+m_I)}\frac{m_S^{(2i+m_S)}}{m_I^{(i-j+m_S)}}\left(\frac{z}{\bar{\zeta}_{SR}}\right)^{(i+m_S)}\end{aligned} \tag{4.23}$$

and

$$\begin{aligned}F^{\infty}_{\zeta_{RD}}(z) &= \exp\left(-(m_R K_R + m_J K_J)\right)\sum_{i=0}^{\infty}\sum_{j=0}^{\infty}\frac{K_R^i K_J^j}{i!j!}\left(\frac{1+K_R}{1+K_J}\right)^{i+m_R}\\ &\quad\times\frac{\Gamma(i+j+m_R+m_J)}{\Gamma(i+m_R+1)\Gamma(j+m_J)}\frac{m_R^{(2i+m_R)}}{m_J^{(i-j+m_R)}}\left(\frac{z}{\bar{\zeta}_{RD}}\right)^{(i+m_R)}.\end{aligned} \tag{4.24}$$

Here $\bar{\zeta}_{SR}$ and $\bar{\zeta}_{RD}$ are average SINR at nodes R and D, respectively. The asymptotic approximation for the outage probability can be obtained by substituting (4.23) and (4.24) in (4.13).

4.4.2 Average symbol error probability

The contribution of the term involving the product of $F_{\zeta_{SR}}(x)$ and $F_{\zeta_{RD}}(x)$ in (4.17) is little, thus it can be ignored. Further, using the asymptotic approximations of CDFs $F_{\zeta_{SR}}(x)$ and $F_{\zeta_{RD}}(x)$ in (4.23) and (4.24), respectively, the SEP is given by

$$P_e \approx \frac{a\sqrt{b}}{2\sqrt{2\pi}}(\tilde{T}_1 + \tilde{T}_2). \tag{4.25}$$

Here, $\tilde{T}_1$ and $\tilde{T}_2$ are simplified to

$$\begin{aligned}\tilde{T}_1 &= \exp\left(-(m_S K_S + m_I K_I)\right) \sum_{i=0}^{\infty}\sum_{j=0}^{\infty} \frac{(m_S K_S)^i (m_I K_I)^j \Gamma(i+j+m_S+m_I)}{i!j!\Gamma(i+m_S+1)\Gamma(j+m_I)} \\ &\quad \times \left(\frac{A_S}{A_I}\right)^{i+m_S} \int_0^{\infty} z^{(i+m_S-0.5)} \exp\left(-\frac{bz}{2}\right) dz \\ &= \exp\left(-(m_S K_S + m_I K_I)\right) \sum_{i=0}^{\infty}\sum_{j=0}^{\infty} \frac{(m_S K_S)^i (m_I K_I)^j}{i!j!} \\ &\quad \times \frac{\Gamma(i+j+m_S+m_I)\Gamma(i+m_S+0.5)}{\Gamma(i+m_S+1)\Gamma(j+m_I)} \left(\frac{A_S}{A_I}\right)^{i+m_S} \left(\frac{2}{b}\right)^{i+m_S+0.5} \end{aligned} \tag{4.26}$$

and

$$\begin{aligned}\tilde{T}_2 &= \exp\left(-m_R K_R\right) \exp\left(-m_J K_J\right) \sum_{i=0}^{\infty}\sum_{j=0}^{\infty} \frac{(m_R K_R)^i (m_J K_J)^j}{i!j!} \\ &\quad \times \frac{\Gamma(i+j+m_R+m_J)\Gamma(i+m_R+0.5)}{\Gamma(i+m_R+1)\Gamma(j+m_J)} \left(\frac{A_R}{A_J}\right)^{i+m_R} \left(\frac{2}{b}\right)^{i+m_R+0.5}, \end{aligned} \tag{4.27}$$

respectively.

4.5 Numerical Results and Discussion

In this section, we have plotted the analytical results obtained in sections III and IV. The analytical results are validated with the simulation results. The simulation results are obtained using the Monte Carlo method on assuming perfect channel state information at the receiver. We consider the transmit power P_S and P_R at S and R to be -10 dBm and the power transmitted at the cellular user equipment (CUE), that is, $P_I = P_J = 20$ dBm. Further, the distance of nodes R and D from the CUE are assumed as $d_{JR} = d_{JD} = 500$ meters. The distances $d_{SR} = d_{RD} = 10$ meters. The signal and interference links are assumed to have the same path loss exponent $\alpha = 3$. The noise power spectral density N_0 is assumed to be -143.97 dBm. The parameter K is 0 dB for no specular component.

The outage probability is plotted in Figs. 4.2-4.4 using (4.10), (4.11), and (4.13). The number of summation terms considered in (4.10) and (4.11) for i and j is 20. The terms needed for improved accuracy vary with the numeric value of the parameters m and K. Even the smaller number of terms provide reasonably good accuracy for lower values of parameters m and K. The terms

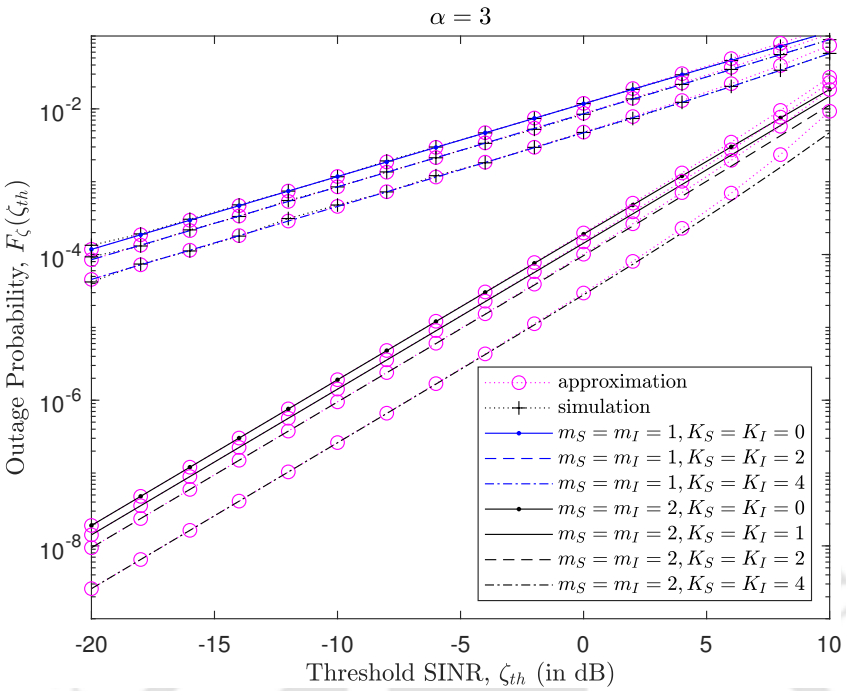

FIGURE 4.2: Plot of outage probability versus threshold SINR for varying mean SNR and channel parameters.

considered increase with increment in the value of parameters. For $K = 4$ dB and $m = 4$, 20 summation terms give reliable results. This is also justified in the plot comparing analytical and simulation results. Therefore, we have considered 20 summation terms for the numerical plots.

The plot of end-to-end outage probability versus threshold SINR is shown in Fig. 4.2. We consider the parameters of all the BX faded links to be the same, that is $K_S = K_R = K_I = K_J$ and $m_S = m_R = m_I = m_J$. The plots for Rayleigh faded ($m = 1$ and $K = 0$) and Rician faded ($m = 1$) links are also shown in the figure. It is observed that the probability of a signal in an outage reduces with an increase in channel parameters m or/and K since fading decreases with an increment in m or/and K. The growth in performance is more for the increase in m corresponding to the severity of fading. The numerical outcomes are validated using simulation results in the plot. The high SNR approximation for the outage probability obtained in Section IV is also plotted. It is found to be a close approximation of the outage probability.

In Fig. 4.3, we have shown the effect of power assignment at the source and the relay node on the outage performance. P_T is considered to be the normalized total power. A fraction η of P_T is used at the source node and the remaining fraction $(1 - \eta)$ is utilized at the relay node for data transmission. The plots are shown for varying K, that is, *i)* $K_S = 4$dB and $K_R = 1$dB and *ii)*

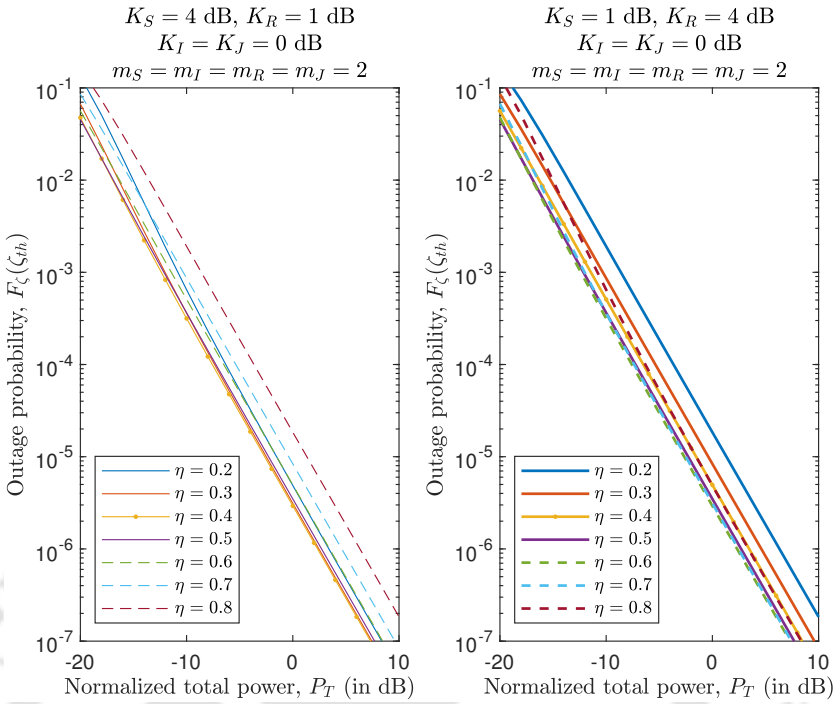

FIGURE 4.3: Plot of outage probability versus normalized total power P_T where $P_{SR} = \eta P_T$ and $P_{RD} = (1-\eta)P_T$, $\eta \in (0,1)$.

$K_S = 1$dB and $K_R = 4$dB. In i), the SR link has a higher directional component when compared to the RD link, and in ii) RD link has a more prominent directional component than the SR link. As seen in the figure, the optimal $\eta \approx 0.4$ for i) and $\eta \approx 0.6$ for ii). The power assigned at a node for optimal performance is higher for the node transmitting over the link with a lesser directional component. When both SR and RD links are equally faded, the optimal value of η is 0.5, which means equal power allocation at nodes S and R.

The effect of relay location on the end-to-end outage performance of the system is shown in Fig. 4.4. Here d_{SD} is considered 20 meters. Further, it is assumed that S, R, and D are co-linear, that is $d_{SD} = d_{SR} + d_{RD}$. Considering the links are similarly faded, the optimal location of the relay node is halfway between the source and destination (≈ 10 meters). However, if the links fade differently, the optimum relay location shifts from the center towards the node with weaker link quality. The performance improves if the signal travels a smaller distance over the poorer link. The deviation from halfway is more prominent with increment in m.

The outage capacity of the system obtained using (4.14) is plotted against the normalized outage threshold in Fig. 4.5 for the varying value of parameters m ($m_S = m_R = m_I = m_J = m$) and K

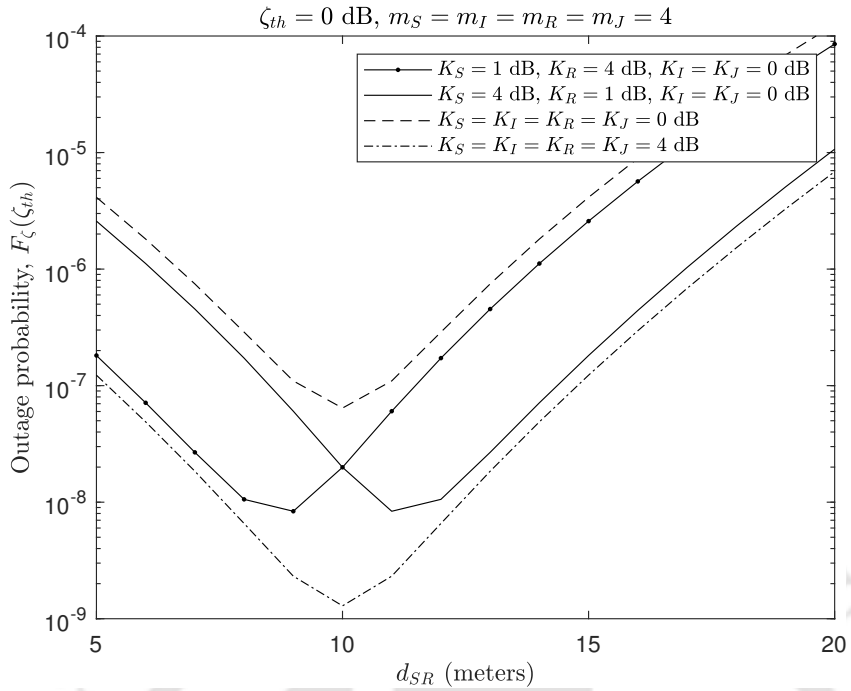

FIGURE 4.4: Plot of outage probability versus d_{SR} for $d_{SD} = 10$ meters and $d_{SD} = d_{SR} + d_{RD}$.

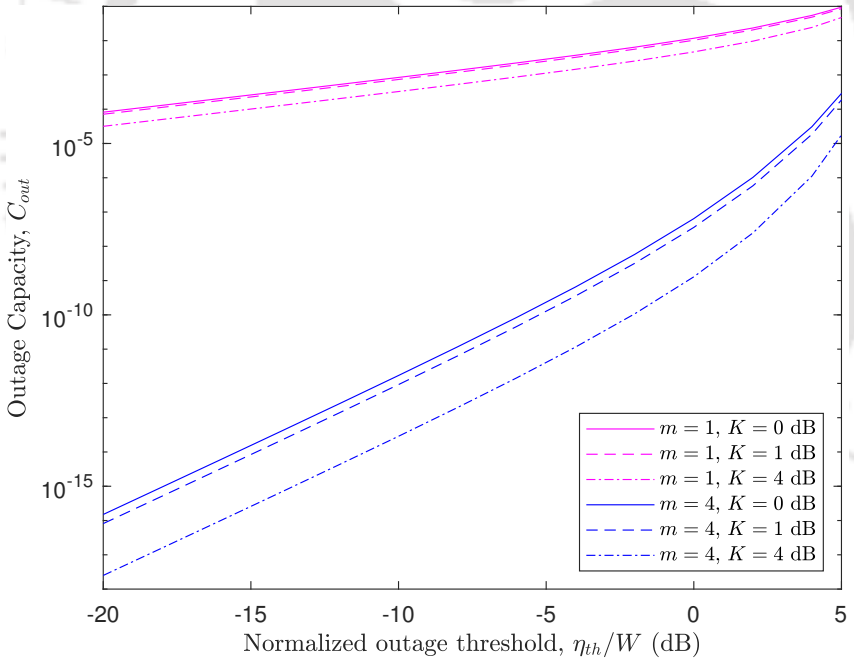

FIGURE 4.5: Plot of outage capacity versus normalized outage threshold for varying channel parameters.

($K_S = K_R = K_I = K_J = K$). The outage capacity reduces with growth in parameters m and K. The reduction is more for an increase in m.

Using (4.17), the average SEP P_e versus average SNR $\bar{\gamma}$ ($\bar{\gamma} = \bar{\gamma}_{SR} = \bar{\gamma}_{RD}$) is plotted in Fig. 4.6 for varying modulation order M and channel parameters. The data at the source and relay are

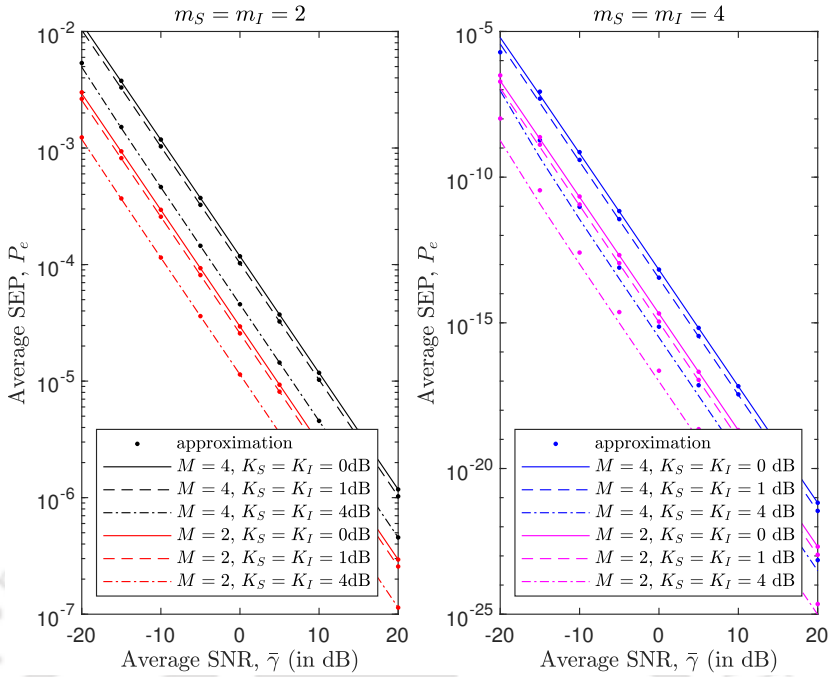

FIGURE 4.6: Plot of SEP versus mean SNR $\bar{\gamma}_{SR} = \bar{\gamma}_{RD} = \bar{\gamma}$ for varying M

considered to be MPSK modulated. The average power transmitted at the CUE is considered as 10dBm, thus $\bar{\gamma}_{IR} = \bar{\gamma}_{JD} = 10$dBm. As expected, the average SEP rises with an increase in the modulation order. For the same M, the SEP reduces with an increment in channel parameters. The approximate expression for the SEP in (4.25) is also plotted and is found to be a close approximation. The plots can be obtained for other coherent modulation techniques by substituting a and b in (4.15) [82, Table 6.1].

The effect of relay location on the end-to-end outage performance of the system is shown in Fig. 4.4. Here d_{SD} is considered 20 meters. Further, it is assumed that S, R, and D are co-linear, that is $d_{SD} = d_{SR} + d_{RD}$. We observe the optimal location of the relay node is halfway between the source and destination, that is 10 meters if the links are similarly faded. However, if the links are differently faded the optimum relay location shift from the center towards the node with weaker link quality. This is because the performance improves if the signal travels a smaller distance over the poorer link. The deviation from halfway is more prominent when m increases.

4.6 Conclusion

In this chapter, we deduced the expressions for the outage probability, the outage capacity, and the average SEP of a DF relay-assisted D2D communication system underlying a cellular network. We consider that the RF links are modeled by BX fading. Numerical results are plotted to observe the effects of channel parameters on the end-to-end performance of the system. It is observed that the probability of signal in outage decreases with a reduction in fading, that is, an increase in parameters m and K. For the same m, the performance improves with an increase in parameter K. However, the performance improvement is significantly more with an increase in m. This follows for the outage capacity which also reduces with an increase in channel parameters m and K. The outage probability is also plotted with varying fractions of the normalized total power assigned at the source and the relay node. The optimum power assignment is higher for nodes with poor link quality to ensure reliable end-to-end communication. Further, the effect of relay location on the outage performance is also explored. The optimal relay location is halfway between the source and destination node when both SR and RD links are identically faded. In case, the channel parameters of the links are different, the optimal relay location drifts from halfway to the node with weaker link quality. The approximate expression for the outage probability and the average SEP are also obtained and are found to be a close approximation.

Chapter 5

Performance Analysis of D2D-based V2V Communication System

5.1 Introduction

Intelligent transportation technologies are continuously evolving with the advancement in wireless technology. The evolution in wireless technology has further enabled vehicular communication with immense growth in data rate and reduced latency. Due to the localized nature of V2V, it is promising to adapt to the sudden changes in surroundings. This can avoid fatal roadway accidents by providing early warnings. It can also provide additional features including information on smart parking and traffic congestion. D2D communication technology can be an enabler for V2V applications as later also have a localized nature which fits the core idea of D2D communications [22, 92]. The devices located in the coverage range of each other can communicate directly without or with partial involvement of the BS. This offers an inherent advantage in terms of lower latency and higher reliability [22]. A low latency transmission is required in V2V applications to send ultra-fast warning messages with a concise time frame [23, 25]. Emerging technologies are considering high-frequency bands between 30 GHz and 300 GHz that offer extremely high data rate up and latency less than 1 ms [25, 26].

In this chapter, an underlay D2D-based V2V system is considered where each user is equipped with multiple antennas. The system performance is analyzed in presence of the intra-cell mutual interference between two V2V pairs moving in opposite directions on a divided highway and using the same uplink resources. Two cases are considered for the analysis: i) direct V2V communication and ii) relayed V2V communication in absence of direct link.

5.2 System Model

We consider the system shown in Fig. 5.1 where a V2V source S communicates a signal to the V2V destination D via a direct or relayed link. A relay R mounted on the vehicle helps to extend the coverage. During transmission, vehicles may have a coverage range longer than half of the highway width, this results in interference as vehicles on the other half of the highway move in the opposite direction. Interfering nodes in the case of direct and relayed transmission are denoted by I and J, respectively. The links connecting nodes p and q be denoted as pq, where $p \in \{S, R, I, J\}$ and $q \in \{R, D\}$. To avoid rapid communication interruptions and handoffs, vehicles moving in the same direction communicate with each other. Thus, we assume nodes S, R, and D are moving in the same direction. We assume the highway is crowded (rush hour) or vehicles move at almost the same velocity. In both scenarios, the relative velocity is almost constant resulting in a small doppler shift that can be ignored. Further, the effect of Doppler shift on the interference link is considered negligible. All the vehicular nodes are assumed to be equipped with N_t transmit and N_r receive antennas. A full duplex DF relay is considered to forward the signal, thus the self-interference experienced at the relay node is included in the analysis. The channel coefficients are assumed to follow an independent complex Gaussian distribution.

Consider V2V source S and interfering vehicle I transmits symbol vector $\boldsymbol{x}_S$ and $\boldsymbol{x}_I$, respectively having dimension $N_t \times 1$. The signal received at V2V destination D in case of direct transmission is given by

$$\boldsymbol{y}_D = \sqrt{P_S} d_{SD}^{-\beta} \boldsymbol{H}_{SD} \boldsymbol{x}_S + \sqrt{P_I} d_{ID}^{-\beta} \boldsymbol{H}_{ID} \boldsymbol{x}_I + \boldsymbol{\eta}_D \,, \tag{5.1}$$

where $\boldsymbol{H}_{SD}$ and $\boldsymbol{H}_{ID}$ are $N_r \times N_t$ channel matrices corresponding to SD and interference link ID, respectively. d_{SD} and d_{RD} are the distances between links SD and ID, respectively. β is the path loss exponent. P_S and P_I are the power transmitted at the source and interfering vehicle and

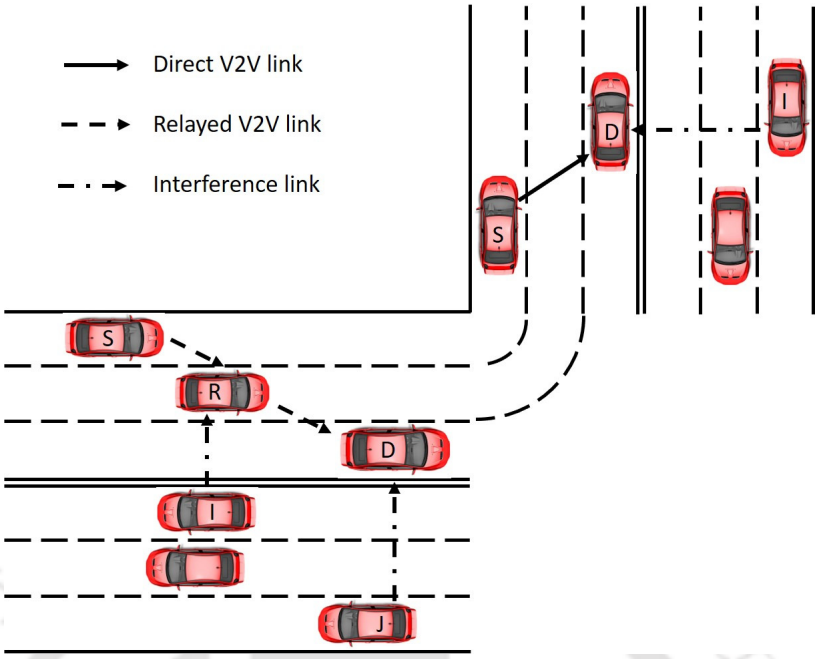

FIGURE 5.1: System model of D2D-based underlay V2V network with a direct and relayed link.

$\boldsymbol{\eta}_D$ is additive white Gaussian noise (AWGN) at D having dimension $N_r \times 1$. The $(i,j)^{th}$ elements of the channel matrices represent complex gain from transmit antenna j to receive antenna i. The elements are independent and circularly symmetric complex Gaussian with zero mean and variance N_0.

In the case of V2V communication through a relaying vehicle, the signal received at nodes R and D are

$$\begin{aligned} \boldsymbol{y}_R &= \sqrt{P_S} d_{SR}^{-\beta} \boldsymbol{H}_{SR} \boldsymbol{x}_S + \sqrt{P_I} \boldsymbol{H}_{IR} \boldsymbol{x}_I + \sqrt{P_R} \boldsymbol{H}_{RR} \boldsymbol{x}_R + \boldsymbol{\eta}_R, \quad \text{and} \\ \boldsymbol{y}_D &= \sqrt{P_R} d_{RD}^{-\beta} \boldsymbol{H}_{RD} \boldsymbol{x}_R + \sqrt{P_J} d_{JD}^{-\beta} \boldsymbol{H}_{JD} \boldsymbol{x}_J + \boldsymbol{\eta}_D, \end{aligned} \tag{5.2}$$

respectively. Here $\boldsymbol{H}_{SR}$, $\boldsymbol{H}_{RD}$, $\boldsymbol{H}_{RR}$, $\boldsymbol{H}_{IR}$ and $\boldsymbol{H}_{JD}$ are $N_r \times N_t$ channel matrices corresponding to links SR, RD, RSI, IR, and JD, respectively. The $(i,j)^{th}$ elements of the channel matrices represent complex gain from transmit antenna j to receive antenna i for the corresponding link. The matrix elements are independent and circularly symmetric complex Gaussian distributed with zero mean and variance N_0. $\boldsymbol{\eta}_R$ and $\boldsymbol{\eta}_D$ are $N_r \times 1$ for AWGN at R and D, respectively.

Using (5.1), the SINR of the direct link is given by

$$\Gamma_{SD} = \frac{\sigma_{SD} ||\boldsymbol{H}_{SD}||^2}{\sigma_{ID} ||\boldsymbol{H}_{ID}||^2 + 1}, \tag{5.3}$$

where σ_{SD} ($= P_S d_{SD}^{-\beta}/N_0$) and σ_{ID} ($= P_I d_{ID}^{-\beta}/N_0$) are the desired signal-to-noise power ratio (SNR) and interference-to-noise power ratio (INR) at node D. Similarly, the SINR for SR and RD link in case of relayed transmission can be obtained using (5.2) as

$$\Gamma_{SR} = \frac{\sigma_{SR}||\boldsymbol{H}_{SR}||^2}{\sigma_{IR}||\boldsymbol{H}_{IR}||^2 + \sigma_{RR}||\boldsymbol{H}_{RR}||^2 + 1}, \quad \text{and} \tag{5.4a}$$

$$\Gamma_{RD} = \frac{\sigma_{RD}||\boldsymbol{H}_{RD}||^2}{\sigma_{JD}||\boldsymbol{H}_{JD}||^2 + 1}. \tag{5.4b}$$

where σ_{SR} ($= P_S d_{SR}^{-\beta}/N_0$), σ_{IR} ($= P_I d_{IR}^{-\beta}/N_0$), σ_{RR} ($= \alpha P_R/N_0$), σ_{RD} ($= P_R d_{RD}^{-\beta}/N_0$), and σ_{JD} ($= P_J d_{JD}^{-\beta}/N_0$) are the desired SNR at R, INR at R, RSI to noise power ratio, desired SNR at D and INR at D.

5.3 Outage Probability

In this section, the closed-form expressions for the end-to-end outage probabilities of direct and relay-assisted D2D-based V2V communication systems are deduced. The signal received is said to be in an outage if the SINR at the destination is smaller than the predefined threshold γ_{th}.

5.3.1 Direct transmission

Consider SINR on direct transmission in (5.3) and assume $X = \sigma_{SD}||\boldsymbol{H}_{SD}||^2$ and $Y = \sigma_{ID}||\boldsymbol{H}_{ID}||^2 + 1$. The channel coefficients are assumed to be Rayleigh faded, therefore $||\boldsymbol{H}_{SD}||^2$ and $||\boldsymbol{H}_{ID}||^2$ follows a gamma distribution [68]. The channels are assumed to be i.i.d. The PDFs of X and Y are given as

$$f_X(x) = \frac{x^{N-1}}{\Gamma(N)\sigma_{SD}^N} \exp\left(-\frac{x}{\sigma_{SD}}\right) u(x) \tag{5.5}$$

and

$$f_Y(y) = \frac{(y-1)^{N-1}}{\Gamma(N)\sigma_{ID}^N} \exp\left(-\frac{(y-1)}{\sigma_{ID}}\right) u(y-1), \tag{5.6}$$

respectively, where $N = N_r \times N_t$ and $u(\cdot)$ unit step function. Using the PDFs of X and Y, the PDF of SINR $Z = X/Y$, can be calculated using

$$f_Z(z) = \int_{-\infty}^{\infty} |y| f_X(yz) f_Y(y) dy. \tag{5.7}$$

Substituting the PDFs (5.5) and (5.6) in (5.7), we have

$$f_Z(z) = \frac{z^{(N-1)} \exp\left(1/\sigma_{ID}\right)}{(\Gamma(N))^2(\sigma_{SD}\sigma_{ID})^N} \int_1^\infty y^N (y-1)^{(N-1)} \exp\left(-y\left(\frac{z}{\sigma_{SD}} + \frac{1}{\sigma_{ID}}\right)\right) dy\,. \tag{5.8}$$

On making a variable change, (5.8) can be rewritten as

$$f_Z(z) = \frac{z^{(N-1)} \exp\left(1/\sigma_{ID}\right)}{(\Gamma(N))^2(\sigma_{SD}\sigma_{ID})^N} \int_0^\infty \tau^{(N-1)} (\tau+1)^N \exp\left(-\tau\left(\frac{z}{\sigma_{SD}} + \frac{1}{\sigma_{ID}}\right)\right) d\tau\,. \tag{5.9}$$

On employing the binomial expansion of $(\tau+1)^N$, (5.9) can be rewritten as

$$f_Z(z) = \frac{z^{(N-1)} \exp\left(-z/\sigma_{SD}\right)}{(\Gamma(N))^2(\sigma_{SD}\sigma_{ID})^N} \sum_{k=0}^{N} \binom{N}{k} \int_0^\infty \tau^{(N+k-1)} \exp\left(-\tau\left(\frac{z}{\sigma_{SD}} + \frac{1}{\sigma_{ID}}\right)\right) d\tau\,, \tag{5.10}$$

where $\binom{N}{k}$ is binomial coefficient. The integral in (5.10) can be solved using [18, eq. 3.351.3], thus we have

$$f_Z(z) = \frac{z^{(N-1)} \exp\left(-z/\sigma_{SD}\right)}{\left(\Gamma(N)\right)^2 \left(\sigma_{ID}\sigma_{SD}\right)^N} \sum_{k=0}^{N} \binom{N}{k} \Gamma(N+k) \left(\frac{z}{\sigma_{SD}} + \frac{1}{\sigma_{ID}}\right)^{-(N+k)}\,, \tag{5.11}$$

where $\Gamma(\cdot)$ is gamma function. Using the PDF in (5.11), the CDF of Z can be evaluated as

$$F_Z(z) = \frac{1}{\left(\Gamma(N)\right)^2 \left(\sigma_{ID}\sigma_{SD}\right)^N} \sum_{k=0}^{N} \binom{N}{k} \Gamma(N+k) \int_0^z z^{(N-1)} \left(\frac{z}{\sigma_{SD}} + \frac{1}{\sigma_{ID}}\right)^{-(N+k)} \exp\left(-\frac{z}{\sigma_{SD}}\right) dz\,. \tag{5.12}$$

The outage probability at the destination, $P_o^{dir}(\gamma_{th})$ is same as the CDF calculated in (5.12) for $z = \gamma_{th}$. Substituting the Taylor series expansion of exponential function in (5.12), that is $\exp(-z/\sigma_{SD}) = \sum_{\ell=0}^{\infty}((-1)^\ell z^\ell)/(\sigma_{SD}^\ell \ell!)$ and solving the integral, we get

$$\begin{aligned} P_o^{dir}(\gamma_{th}) \;=\; & \frac{1}{(\Gamma(N))^2 \sigma_{SD}^N} \sum_{k=0}^{N} \sum_{\ell=0}^{\infty} (-1)^\ell \binom{N}{k} \frac{\Gamma(N+k)\sigma_{ID}^k}{\ell!(N+\ell)\sigma_{SD}^\ell} \gamma_{th}^{(N+\ell)} \\ & \times {}_2F_1\left(N+k, N+\ell; N+\ell+1; -\frac{\sigma_{ID}\gamma_{th}}{\sigma_{SD}}\right), \end{aligned} \tag{5.13}$$

where ${}_2F_1(\cdot,\cdot;\cdot;\cdot)$ represents Gauss hypergeometric function.

5.3.2 DF Relaying

In the case of relayed transmission, the SINR at R is given in (5.4a). Let $X = \sigma_{SR}||\boldsymbol{H}_{SR}||^2$ and $Y = \sigma_{IR}||\boldsymbol{H}_{IR}||^2 + \sigma_{RR}||\boldsymbol{H}_{RR}||^2 + 1 = U + V + 1$. The channel coefficients are assumed to be Rayleigh distributed, thus, $||\boldsymbol{H}_{SR}||^2$, $||\boldsymbol{H}_{IR}||^2$ and $||\boldsymbol{H}_{RR}||^2$ follows a gamma distribution. The channels are also assumed to be iid. The PDF of X is

$$f_X(x) = \frac{x^{N-1}}{\Gamma(N)\sigma_{SR}^N} \exp\left(-\frac{x}{\sigma_{SR}}\right), \quad \text{for } x \geq 0\,. \tag{5.14}$$

Now to find the PDF of Y, the PDF of $W = U + V$ is derived using

$$f_W(w) = \int_{-\infty}^{\infty} f_U(w-v) f_V(v) dv\,, \tag{5.15}$$

where the PDFs of U and V are given as

$$\begin{aligned} f_U(u) &= \frac{u^{N-1}}{\Gamma(N)\sigma_{IR}^N} \exp\left(-\frac{u}{\sigma_{IR}}\right), \quad \text{for } u \geq 0 \quad \text{and} \\ f_V(v) &= \frac{v^{N-1}}{\Gamma(N)\sigma_{RR}^N} \exp\left(-\frac{v}{\sigma_{RR}}\right), \quad \text{for } v \geq 0\,, \end{aligned} \tag{5.16}$$

respectively. On substituting (5.16) in (5.15) and using $Y = W + 1$, the distribution of Y can be written as

$$f_Y(y) = \frac{\exp(-(y-1)/\sigma_{IR})}{(\Gamma(N))^2(\sigma_{IR}\sigma_{RR})^N} \int_0^{(y-1)} (y-v-1)^{(N-1)} v^{(N-1)} \exp\left(-v\left(\frac{1}{\sigma_{RR}} - \frac{1}{\sigma_{IR}}\right)\right) dv\,. \tag{5.17}$$

The PDF of $Z = X/Y$ can be deduced on substituting (5.14) and (5.17) in (5.7), we get

$$\begin{aligned} f_Z(z) &= \frac{z^{N-1}\exp(1/\sigma_{IR})}{(\Gamma(N))^3(\sigma_{SR}\sigma_{IR}\sigma_{RR})^N} \int_1^{\infty} y^N \exp\left(-y\left(\frac{z}{\sigma_{SR}} + \frac{1}{\sigma_{IR}}\right)\right) \int_0^{(y-1)} (y-v-1)^{(N-1)} \\ &\quad \times v^{(N-1)} \exp\left(-v\left(\frac{1}{\sigma_{RR}} - \frac{1}{\sigma_{IR}}\right)\right) dvdy\,. \end{aligned} \tag{5.18}$$

The integral over v in (5.18) can be simplified using [70, eqs. 3.383.1], which on substituting [70, 8.384.1] and [81, eq. 13.1.2] results in

$$f_Z(z) = \frac{z^{N-1}\exp(1/\sigma_{IR})}{(\Gamma(N))^2(\sigma_{SR}\sigma_{IR}\sigma_{RR})^N}\sum_{k=0}^{\infty}\frac{\Gamma(N+k)}{k!\Gamma(2N+k)}\left(\frac{1}{\sigma_{IR}}-\frac{1}{\sigma_{RR}}\right)^k\int_1^{\infty}y^N(y-1)^{(2N+k-1)} \times\exp\left(-y\left(\frac{z}{\sigma_{SR}}+\frac{1}{\sigma_{IR}}\right)\right)dy\,. \tag{5.19}$$

Solving the integral in (5.19) using [70, eq. 3.383.4] and simplifying the expression on employing [70, eqs. 9.232 and 9.220.4], the PDF of Γ_{SR} in (5.4a) is obtained as

$$f_Z(z) = \frac{z^{N-1}}{(\Gamma(N))^2(\sigma_{SR}\sigma_{IR}\sigma_{RR})^N}\sum_{k=0}^{\infty}\frac{\Gamma(N+k)}{k!}\left(\frac{1}{\sigma_{IR}}-\frac{1}{\sigma_{RR}}\right)^k\exp\left(-\frac{z}{\sigma_{SR}}\right) \times\psi\left(2N+k,3N+k+1;\frac{z}{\sigma_{SR}}+\frac{1}{\sigma_{IR}}\right). \tag{5.20}$$

The PDF in (5.20) can be rewritten using the series form expansion of $\psi(\cdot)$ in [101]. Thus we get

$$f_Z(z) = \frac{z^{N-1}}{(\Gamma(N))^2(\sigma_{SR}\sigma_{IR}\sigma_{RR})^N}\sum_{k=0}^{\infty}\sum_{\ell=0}^{N}\frac{\Gamma(N+k)}{k!}\frac{\Gamma(2N+k+\ell)}{\Gamma(2N+k)}\binom{N}{N-\ell}\left(\frac{1}{\sigma_{IR}}-\frac{1}{\sigma_{RR}}\right)^k \times\left(\frac{z}{\sigma_{SR}}+\frac{1}{\sigma_{IR}}\right)^{-(2N+k+\ell)}\exp\left(-\frac{z}{\sigma_{SR}}\right). \tag{5.21}$$

The CDF of Γ_{SR} can be deduced by expressing the exponential function in terms of its Taylor series expansion and integrating it over the interval $[0,z]$, that is

$$F_Z(z) = \frac{1}{(\Gamma(N))^2(\sigma_{SR}\sigma_{IR}\sigma_{RR})^N}\sum_{k=0}^{\infty}\sum_{\ell=0}^{N}\sum_{m=0}^{\infty}\frac{(-1)^m}{k!m!\sigma_{SR}^m}\frac{\Gamma(N+k)\Gamma(2N+k+\ell)}{\Gamma(2N+k)} \times\binom{N}{N-\ell}\left(\frac{1}{\sigma_{IR}}-\frac{1}{\sigma_{RR}}\right)^k\int_0^z z^{N+m-1}\left(\frac{z}{\sigma_{SR}}+\frac{1}{\sigma_{IR}}\right)^{-(2N+k+\ell)}dz\,. \tag{5.22}$$

The outage probability of SR link, $P_o^{SR}(\gamma_{th})$ is same as the CDF of Γ_{SR} in (5.22) for $z=\gamma_{th}$. The integral in (5.22) can be solved using [70, eq. 3.383.4], we have

$$P_o^{SR}(\gamma_{th}) = \frac{\sigma_{IR}^N}{(\Gamma(N))^2(\sigma_{SR}\sigma_{RR})^N}\sum_{k=0}^{\infty}\sum_{\ell=0}^{N}\sum_{m=0}^{\infty}\frac{(-1)^m\sigma_{IR}^{(k+\ell)}}{k!m!\sigma_{SR}^m}\frac{\Gamma(N+k)\Gamma(2N+k+\ell)}{\Gamma(2N+k)(N+m)}\binom{N}{N-\ell} \times\left(\frac{1}{\sigma_{IR}}-\frac{1}{\sigma_{RR}}\right)^k\gamma_{th}^{(N+m)}\,{}_2F_1\left(2N+k+\ell,N+m;1+N+m;-\frac{\sigma_{IR}}{\sigma_{SR}}\gamma_{th}\right). \tag{5.23}$$

The outage probability of RD link has the same form as (5.16). Thus

$$P_o^{RD}(\gamma_{th}) = \frac{1}{(\Gamma(N))^2\sigma_{RD}^N}\sum_{k=0}^{N}\sum_{\ell=0}^{\infty}(-1)^\ell\binom{N}{k}\frac{\Gamma(N+k)\sigma_{JD}^k}{\ell!(N+\ell)\sigma_{RD}^\ell}\gamma_{th}^{(N+\ell)} \times {}_2F_1\left(N+k, N+\ell; N+\ell+1; -\frac{\sigma_{JD}\gamma_{th}}{\sigma_{RD}}\right). \quad (5.24)$$

The signal received at the destination is in an outage if one of the two links SR and RD is in an outage or both SR and RD links are in an outage. Therefore the outage probability at the destination is

$$P_o^{rel}(\gamma_{th}) = P_o^{SR}(\gamma_{th}) + P_o^{RD}(\gamma_{th}) - P_o^{SR}(\gamma_{th})P_o^{RD}(\gamma_{th}), \quad (5.25)$$

where analytical expression of $P_o^{SR}(\gamma_{th})$ and $P_o^{RD}(\gamma_{th})$ are given in (5.23) and (5.24), respectively.

5.4 Asymptotic Outage Probability and Diversity Order

Using (5.13), the asymptotic expression for the outage probability of the direct link can be obtained for $\sigma_{SD} \to \infty$ as

$$\lim_{\sigma_{SD}\to\infty} P_o^{dir}(\gamma_{th}) = \frac{\gamma_{th}^N}{\Gamma(N)\sigma_{SD}^N}\sum_{k=0}^{N}\frac{\Gamma(N+k)}{k!(N-k)!}\sigma_{ID}^k. \quad (5.26)$$

Since $P_o^{dir} \propto \sigma_{SD}^{-N}$ in (5.26), the diversity order of the SD link is N.

In the case of relayed transmission, the high SINR approximation for the outage probability of SR link deduced using (5.23) can be given by

$$\lim_{\sigma_{SR}\to\infty} P_o^{SR}(\gamma_{th}) = \frac{\gamma_{th}^N}{\Gamma(N)\sigma_{SR}^N\sigma_{RR}^N}\sum_{k=0}^{\infty}\sum_{\ell=0}^{N}\frac{\sigma_{IR}^{(N+k+\ell)}}{k!\ell!(N-\ell)!}\frac{\Gamma(N+k)\Gamma(2N+k+\ell)}{\Gamma(2N+k)}\left(\frac{1}{\sigma_{IR}}-\frac{1}{\sigma_{RR}}\right)^k. \quad (5.27)$$

Similar to (5.26), the asymptotic expression for the outage probability of RD link is

$$\lim_{\sigma_{RD}\to\infty} P_o^{RD}(\gamma_{th}) = \frac{\gamma_{th}^N}{\Gamma(N)\sigma_{RD}^N}\sum_{k=0}^{N}\frac{\Gamma(N+k)}{k!(N-k)!}\sigma_{JD}^k. \quad (5.28)$$

On substituting (5.27) and (5.28) in (5.25), the high SINR approximation of the outage probability on relaying can be obtained. Since $P_o^{SR}(\gamma_{th})$ and $P_o^{RD}(\gamma_{th})$ for high SINRs in (5.27) and (5.28) are proportional to σ_{SR}^N and σ_{RD}^N, respectively, the diversity order on relaying is N.

Parameter	**Value**
Transmit power, P_S, P_R, P_I, P_J	27 dBm
Noise power, N_0	-143.97 dBm
Number of highway lanes	4-12 meters
Lane width	2.7-4.6 m as per [102]
Desired link length	4-24 meters
Interfering link length	8-44 meters
Path loss exponent	$2-6$

5.5 Numerical Results and Discussion

In this section, the analytical results deduced in Sections III and IV are plotted along with the simulation results obtained using the Monte Carlo method on assuming perfect CSI at the receiver. The transmit power at the V2V nodes is considered as 27 dBm, that is $P_{SR} = P_{RD} = P_{IR} = P_{JD} =$ 27 dBm. The distances d_{SD}, d_{SR}, and d_{RD} links are considered to be i) 10m, 5m, 5m and ii) 10m, 6m, 5m respectively. Further, the length of the interference links d_{IR} and d_{JD} are assumed to be 80m. Let the signal and interference links have the same path loss exponent $\alpha = 3$. The noise power spectral density is considered to be -143.97 dBm. The range of the parameters is tabulated below

The analytical expression for the outage probabilities deduced in section III for Rayleigh faded links are plotted in Figs. 5.2 for varying values of $N = N_t \times N_r$. It is observed that the probability of signal received at node D in an outage for the same threshold value is small for the higher number of antennas. This is attributed to the fact that diversity order improves with increase in N. The slope of plots increases with N indicating increment in diversity order with N. Further, it is observed that the performance improves on relaying for the same linear distance between the source and destination node, that is $d_{SR} + d_{RD} = d_{SD}$. The relay node may not be advantageous when the $d_{SR} + d_{RD} >> d_{SD}$. The analytical results are validated using the simulation plots.

In Fig. 5.3, the closed form and the asymptotic approximation for the outage probability obtained in sections III and IV are plotted. The analytical results for outage probability are plotted with

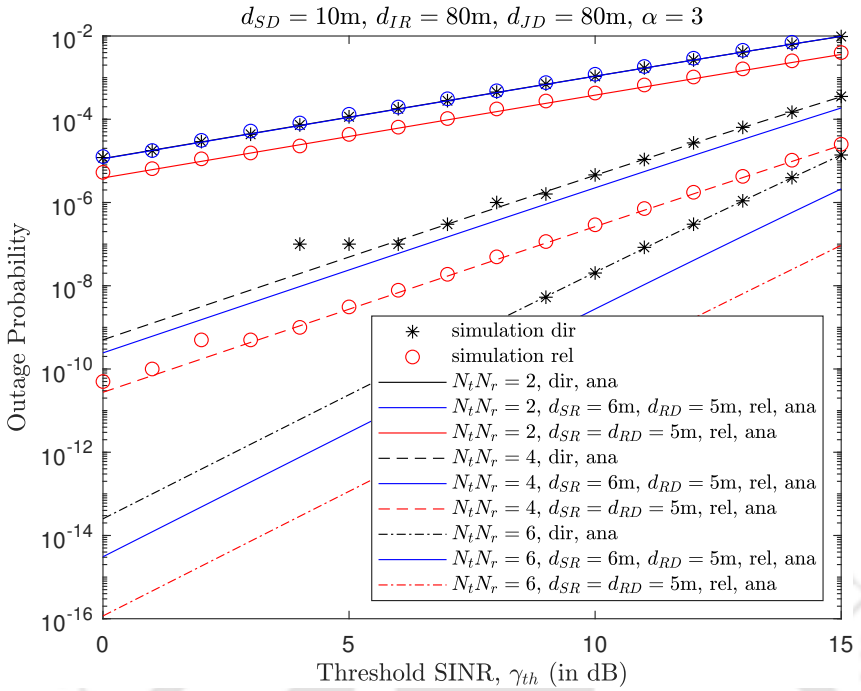

FIGURE 5.2: Plot of outage probability versus SINR threshold for direct transmission (dir) and on DF relaying (rel)

varying transmit power for $\bar{\gamma}_{th} = 0$ (dB). It is observed that the asymptotic results closely approximate the closed-form expressions at high SINRs. Further, the diversity order obtained in section IV is also justified through the plots.

5.6 Conclusions

In this chapter, we deduced the closed-form expressions of the outage probability for a multi-antenna V2V underlying cellular network. The analysis is presented for V2V communication over i) direct link and ii) relayed transmission using a relay node mounted on a vehicle. The links are assumed to be Rayleigh faded. It is observed that a relay-based V2V system outperforms direct transmission for the same linear distance between source and destination. Further, the asymptotic expressions for the outage probability are obtained and agree with the simulation and analytical results at high SINRs. The outage performance improves with an increase in the number of transmit and receive antennas. The systems' diversity order is a product of the number of transmit and receive antennas.

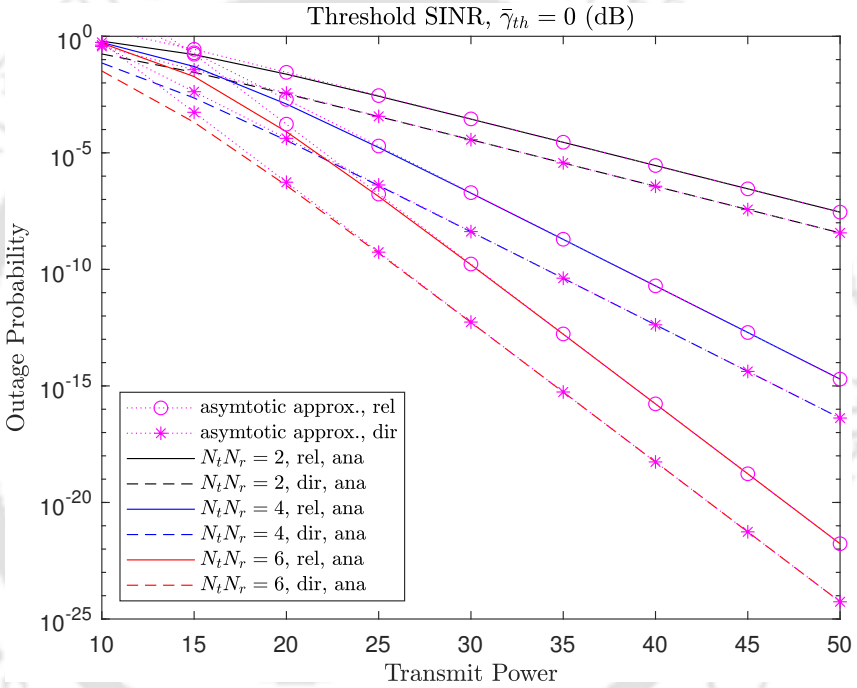

FIGURE 5.3: Plot of outage probability versus transmit power considering equal transmit power at each network node.

Chapter 6
Conclusions and Future Work

In this thesis, interference management, one of the core and challenging issues of D2D underlying cellular network is considered. The performance analysis and interference management of different system models with underlying D2D have been investigated. In this chapter, we conclude the thesis by summarizing the work done highlighting the main contributions, and suggesting some directions for possible future work.

6.1 Summary of Contributions

Chapter 2 of the thesis focuses on analyzing performance of underlay D2D communication system where the resources assigned for cellular DL or UL transmissions are shared with D2D users. IC method is considered which allocates orthogonal precoding vectors in case of underlay D2D transmissions over the channel assigned for cellular communication. The expressions for the outage probability, ergodic capacity, outage capacity at the cellular and D2D receiver are deduced. Numerical results are plotted to observe the effect of the different parameters on the performance.

The performance analysis of a relay assisted D2D communication underlaying cellular network is performed in Chapter 3. The interference due to cellular transmission at the relay and destination node of the relay-assisted D2D link are mitigated using interference alignment technique. The exact expressions of the end-to-end outage probability and average SEP are deduced. Numerical results

are plotted to observe the impact of number of transmit/receive antennas, power transmitted at the source and relay nodes, modulation order, and interference due to other D2D devices.

In Chapter 4, the expression for performance analysis of a DF relay based D2D communication system is analyzed. The RF links connecting the nodes are considered to BX faded. The expressions for the end-to-end average SEP, outage probability, and outage capacity are derived. Further, plots to present the effect of RF link parameters on the optimal relay location.

The performance of a direct and relayed D2D-based V2V underlay communications system is analyzed in Chapter 5. Orthogonal precoding is consider to handle the interference at receiving nodes. A closed form expression for the end-to-end outage probability is derived for direct and relayed transmission.

6.2 Future Work

The topics presented in this thesis have a potential for further explorations and following are some of the possible future research directions

- The orthogonal precoding technique is considered to mitigate interference due to other D2D links operating in the vicinity and are located in the same cell. This can be extended to cell-free MIMO scenario.
- In interference alignment technique considered for relayed-assisted D2D underlay cellular network, the interference due to cellular link is aligned due to its higher power. In the future, a decoding matrix can be designed to handle interference due to other D2D links.
- The contribution of interference is analyzed in Chapter 4 for an underlay D2D SISO system with BX faded channel. The analysis for the outage probability, capacity and SEP, can be extended to MIMO system with multiple D2D links.
- In all the works, the devices are considered to be stationary for the analysis. This can be extended to the system when the UE terminals are moving.
- A single cell scenario is considered for the analysis, this can be extended to multi-cell and cell-free scenario.

- In the performance analysis of D2D based V2V applications, the effect of mobility and Doppler shift are ignored assuming vehicles are moving on a crowded highway during rush hours. In the future work, the mobility and Doppler shift can be taken into consideration for the analysis.

Bibliography

[1] H. Baur, "Heterogeneous networks—meeting mobile broadband expectations with maximum efficiency," *e & i Elektrotechnik und Informationstechnik*, vol. 129, no. 6, pp. 491–421, 2012.

[2] *5G radio access-research and vision-Ericsson*, 06 2013.

[3] J. G. Andrews, S. Buzzi, W. Choi, S. V. Hanly, A. Lozano, A. C. K. Soong, and J. C. Zhang, "What will 5G be?" *IEEE Journal on Selected Areas in Communications*, vol. 32, no. 6, pp. 1065–1082, 2014.

[4] Z. Pi and F. Khan, "An introduction to millimeter-wave mobile broadband systems," *IEEE Communications Magazine*, vol. 49, no. 6, pp. 101–107, 2011.

[5] A. Asadi, Q. Wang, and V. Mancuso, "A survey on device-to-device communication in cellular networks," *IEEE Communications Surveys & Tutorials*, vol. 16, no. 4, pp. 1801–1819, 2014.

[6] M. S. Corson, R. Laroia, J. Li, V. Park, T. Richardson, and G. Tsirtsis, "Toward proximity-aware internetworking," *IEEE Wireless Communications*, vol. 17, no. 6, pp. 26–33, 2010.

[7] T. Peng, Q. Lu, H. Wang, S. Xu, and W. Wang, "Interference avoidance mechanisms in the hybrid cellular and device-to-device systems," in *proceedings of the IEEE 20th International Symposium on Personal, Indoor and Mobile Radio Communications*, 2009, pp. 617–621.

[8] M. N. Tehrani, M. Uysal, and H. Yanikomeroglu, "Device-to-device communication in 5G cellular networks: challenges, solutions, and future directions," *IEEE Communications Magazine*, vol. 52, no. 5, pp. 86–92, 2014.

[9] K. Doppler, J. Manssour, A. Osseiran, and M. Xiao, "Innovative concepts in peer-to-peer and network coding," *Celtic Telecommunication Solutions*, vol. 16, p. 09, 2008.

[10] K. Doppler, M. Rinne, C. Wijting, C. B. Ribeiro, and K. Hugl, "Device-to-device communication as an underlay to LTE-advanced networks," *IEEE Communications Magazine*, vol. 47, no. 12, pp. 42–49, 2009.

[11] A. Asadi, Q. Wang, and V. Mancuso, "A survey on device-to-device communication in cellular networks," *IEEE Communications Surveys & Tutorials*, vol. 16, no. 4, pp. 1801–1819, 2014.

[12] C.-H. Yu, K. Doppler, C. Ribeiro, and O. Tirkkonen, "Performance impact of fading interference to device-to-device communication underlaying cellular networks," in *proceedings of the IEEE 20th International Symposium on Personal, Indoor and Mobile Radio Communications*, 2009, pp. 858–862.

[13] J. Hong, S. Park, H. Kim, S. Choi, and K. B. Lee, "Analysis of device-to-device discovery and link setup in LTE networks," in *proceedings of the IEEE 24th Annual International Symposium on Personal, Indoor, and Mobile Radio Communications*, 2013, pp. 2856–2860.

[14] C. Xu, L. Song, Z. Han, D. Li, and B. Jiao, "Resource allocation using a reverse iterative combinatorial auction for device-to-device underlay cellular networks," in *proceedings of the IEEE Global Communications Conference*, 2012, pp. 4542–4547.

[15] L. Wei, R. Q. Hu, Y. Qian, and G. Wu, "Enable device-to-device communications underlaying cellular networks: challenges and research aspects," *IEEE Communications Magazine*, vol. 52, no. 6, pp. 90–96, 2014.

[16] C. Xu, L. Song, Z. Han, Q. Zhao, X. Wang, X. Cheng, and B. Jiao, "Efficiency resource allocation for device-to-device underlay communication systems: A reverse iterative combinatorial auction based approach," *IEEE Journal on Selected Areas in Communications*, vol. 31, no. 9, pp. 348–358, 2013.

[17] B. Kaufman, J. Lilleberg, and B. Aazhang, "Spectrum sharing scheme between cellular users and ad-hoc device-to-device users," *IEEE Transactions on Wireless Communications*, vol. 12, no. 3, pp. 1038–1049, 2013.

[18] Y. Pei and Y.-C. Liang, "Resource allocation for device-to-device communications overlaying two-way cellular networks," *IEEE Transactions on Wireless Communications*, vol. 12, no. 7, pp. 3611–3621, 2013.

[19] H. Min, W. Seo, J. Lee, S. Park, and D. Hong, "Reliability improvement using receive mode selection in the device-to-device uplink period underlaying cellular networks," *IEEE Transactions on Wireless Communications*, vol. 10, no. 2, pp. 413–418, 2011.

[20] C. Ma, G. Sun, X. Tian, K. Ying, H. Yu, and X. Wang, "Cooperative relaying schemes for device-to-device communication underlaying cellular networks," in *proceedings of the IEEE Global Communications Conference*, 2013, pp. 3890–3895.

[21] N. C. Beaulieu and X. Jiandong, "A novel fading model for channels with multiple dominant specular components," *IEEE Wireless Communications Letters*, vol. 4, no. 1, pp. 54–57, 2015.

[22] W. Sun, E. G. Ström, F. Brännström, Y. Sui, and K. C. Sou, "D2D-based V2V communications with latency and reliability constraints," in *proceedings of the IEEE Globecom Workshops*, 2014, pp. 1414–1419.

[23] X. Yang, L. Liu, N. Vaidya, and F. Zhao, "A vehicle-to-vehicle communication protocol for cooperative collision warning," in *proceedings of the First Annual International Conference on Mobile and Ubiquitous Systems: Networking and Services*, 2004, pp. 114–123.

[24] I. F. Akyildiz, A. Kak, and S. Nie, "6G and beyond: The future of wireless communications systems," *IEEE Access*, vol. 8, pp. 133 995–134 030, 2020.

[25] A. Tassi, M. Egan, R. J. Piechocki, and A. Nix, "Modeling and design of millimeter-wave networks for highway vehicular communication," *IEEE Transactions on Vehicular Technology*, vol. 66, no. 12, pp. 10 676–10 691, 2017.

[26] A. Ghosh, T. A. Thomas, M. C. Cudak, R. Ratasuk, P. Moorut, F. W. Vook, T. S. Rappaport, G. R. MacCartney, S. Sun, and S. Nie, "Millimeter-wave enhanced local area systems: A high-data-rate approach for future wireless networks," *IEEE Journal on Selected Areas in Communications*, vol. 32, no. 6, pp. 1152–1163, 2014.

[27] J. Wang, M. Wu, and F. Zheng, "The codebook design for MIMO precoding systems in LTE and LTE-A," in *proceedings of the 6th International Conference on Wireless Communications Networking and Mobile Computing*, 2010, pp. 1–4.

[28] L. Lei, Z. Zhong, C. Lin, and X. Shen, "Operator controlled device-to-device communications in LTE-advanced networks," *IEEE Wireless Communications*, vol. 19, no. 3, pp. 96–104, 2012.

[29] M. J. Yang, S. Y. Lim, H. J. Park, and N. H. Park, "Solving the data overload: Device-to-device bearer control architecture for cellular data offloading," *IEEE Vehicular Technology Magazine*, vol. 8, no. 1, pp. 31–39, 2013.

[30] P. Phunchongharn, E. Hossain, and D. I. Kim, "Resource allocation for device-to-device communications underlaying LTE-advanced networks," *IEEE wireless communications*, vol. 20, no. 4, pp. 91–100, 2013.

[31] C.-H. Yu, K. Doppler, C. B. Ribeiro, and O. Tirkkonen, "Resource sharing optimization for device-to-device communication underlaying cellular networks," *IEEE Transactions on Wireless Communications*, vol. 10, no. 8, pp. 2752–2763, 2011.

[32] C.-H. Yu, O. Tirkkonen, K. Doppler, and C. Ribeiro, "On the performance of device-to-device underlay communication with simple power control," in *proceedings of the IEEE 69th Vehicular Technology Conference*, 2009, pp. 1–5.

[33] Y. Zhang, Y. Yang, and L. Dai, "Energy efficiency maximization for device-to-device communication underlaying cellular networks on multiple bands," *IEEE Access*, vol. 4, pp. 7682–7691, 2016.

[34] Y. Yang, Y. Zhang, K. Shi, and J. Li, "Optimal power control for energy efficiency of device-to-device communication underlaying cellular networks," in *proceedings of the IEEE 14th International Conference on Industrial Informatics*, 2016, pp. 1028–1031.

[35] Y. Liu, "Optimal mode selection in D2D-enabled multibase station systems," *IEEE Communications Letters*, vol. 20, no. 3, pp. 470–473, 2016.

[36] H. Wang and X. Chu, "Distance-constrained resource-sharing criteria for device-to-device communications underlaying cellular networks," *Electronics letters*, vol. 48, no. 9, pp. 528–530, 2012.

[37] M. Zulhasnine, C. Huang, and A. Srinivasan, "Efficient resource allocation for device-to-device communication underlaying LTE network," in *proceedings of the IEEE 6th International Conference on Wireless and Mobile Computing, Networking and Communications*, 2010, pp. 368–375.

[38] P. Janis, V. Koivunen, C. Ribeiro, J. Korhonen, K. Doppler, and K. Hugl, "Interference-aware resource allocation for device-to-device radio underlaying cellular networks," in *proceedings of the IEEE 69th Vehicular Technology Conference*, 2009, pp. 1–5.

[39] Y. Cheng, Y. Gu, and X. Lin, "Combined power control and link selection in device-to-device enabled cellular systems," *IET Communications*, vol. 7, no. 12, pp. 1221–1230, 2013.

[40] R. Chithra, R. Bestak, and S. K. Patra, "Orthogonal MIMO precoding schemes for device-to-device communication in LTE networks," in *proceedings of the 38th International Conference on Telecommunications and Signal Processing*, 2015, pp. 1–5.

[41] P. Jänis, V. Koivunen, C. B. Ribeiro, K. Doppler, and K. Hugl, "Interference-avoiding MIMO schemes for device-to-device radio underlaying cellular networks," in *proceedings of the IEEE 20th International Symposium on Personal, Indoor and Mobile Radio Communications*, 2009, pp. 2385–2389.

[42] H. Min, J. Lee, S. Park, and D. Hong, "Capacity enhancement using an interference limited area for device-to-device uplink underlaying cellular networks," *IEEE Transactions on Wireless Communications*, vol. 10, no. 12, pp. 3995–4000, 2011.

[43] C. Ma, W. Wu, Y. Cui, and X. Wang, "On the performance of successive interference cancellation in D2D-enabled cellular networks," in *proceedings of the IEEE Conference on Computer Communications*, 2015, pp. 37–45.

[44] Y. Nam, J. So, and J. Kim, "Interference mitigation scheme for device-to-device MIMO communications underlaying a cellular network," *KSII Transactions on Internet and Information Systems*, vol. 11, no. 4, pp. 1841–1865, 2017.

[45] G. D. Swetha and G. R. Murthy, "D2D communication as an underlay to next generation cellular systems with resource management and interference avoidance," in *proceedings of the International Conference on Wireless Communications, Signal Processing and Networking*, 2017, pp. 1348–1352.

[46] N. P. Kuruvatti, R. Hernandez, and H. D. Schotten, "Interference aware power management in D2D underlay cellular networks," in *proceedings of the IEEE AFRICON*, 2019, pp. 1–5.

[47] Y. Hassan, F. Hussain, S. Hossen, S. Choudhury, and M. M. Alam, "Interference minimization in D2D communication underlaying cellular networks," *IEEE Access*, vol. 5, pp. 22 471–22 484, 2017.

[48] M. Elnourani, S. Deshmukh, and B. Beferull-Lozano, "Reliable multicast D2D communication over multiple channels in underlay cellular networks," in *proceedings of the IEEE 31st Annual International Symposium on Personal, Indoor and Mobile Radio Communications*, 2020, pp. 1–6.

[49] S. Gupta, A. Trivedi, and P. Pawar, "An approach for improving performance of underlay D2D communication," in *proceedings of the Conference on Information and Communication Technology (CICT)*, 2018, pp. 1–5.

[50] P. Bao, G. Yu, and R. Yin, "Novel frequency reusing scheme for interference mitigation in D2D uplink underlaying networks," in *proceedings of the 9th International Wireless Communications and Mobile Computing Conference*, 2013, pp. 491–496.

[51] X. Li, N. Qin, and T. Sun, "Interference coordination for FD-MIMO cellular network with D2D communications underlaying," *China Communications*, vol. 15, no. 12, pp. 75–88, 2018.

[52] M. Milisic, M. Hamza, and M. Hadzialic, "Outage and symbol error probability performance of l-branch maximal-ratio combiner for generalized κ- μ fading," in *proceedings of the 50th International Symposium ELMAR*, vol. 1. IEEE, 2008, pp. 231–236.

[53] D. T. T. Ba Cao Nguyen, Xuan Nam Tran and L. T. Dung, "Full-duplex amplify-and-forward relay system with direct link: Performance analysis and optimization," *Physical Communication*, vol. 37, 2019.

[54] L. W. Wei and S. X. Shao, "Outage probability of device-to-device MIMO relay systems with imperfect channel estimation," *IEIE Transactions on Smart Processing and Computing*, vol. 2, no. 2, pp. 67–76, 2013.

[55] U. Uyoata and M. E. Dlodlo, "Relay assisted device-to-device communication: Approaches and issues," *CoRR*, vol. abs/1810.07799, 2018.

[56] J.-Y. Pan and M.-H. Hsu, "Relay selection of relay-assisted device-to-device and uplink communication underlying cellular networks," in *proceedings of the International Conference on Computing, Networking and Communications*, 2017, pp. 980–985.

[57] W. Wang, J. Zhao, and H. Qu, "Outage probability analysis for two-way amplify-and-forward mobile relay assisted device-to-device communication in rayleigh fading channel," in *Journal of Physics: Conference Series*, vol. 2218, no. 1. IOP Publishing, 2022, p. 012005.

[58] I. Singh and N. P. Singh, "Coverage and capacity analysis of relay-based device-to-device communications underlaid cellular networks," *Engineering Science and Technology, an International Journal*, vol. 21, no. 5, pp. 834–842, 2018.

[59] S. Zhang and Y. Peng, "D2D communication relay selection algorithm based on game theory," *Procedia Computer Science*, vol. 166, pp. 563–569, 2020.

[60] M. Botsov, M. Klügel, W. Kellerer, and P. Fertl, "Location dependent resource allocation for mobile device-to-device communications," in *proceedings of the IEEE Wireless Communications and Networking Conference*, 2014, pp. 1679–1684.

[61] M. H. Zafar, I. Khan, and M. O. Alassafi, "An efficient resource optimization scheme for d2d communication," *Digital Communications and Networks*, vol. 8, no. 6, pp. 1122–1129, 2022. [Online]. Available: https://www.sciencedirect.com/science/article/pii/S2352864822000232

[62] A. Masmoudi, S. Feki, K. Mnif, and F. Zarai, "Efficient radio resource management for D2D-based LTE-V2X communications," in *proceedings of the IEEE/ACS 15th International Conference on Computer Systems and Applications*, 2018, pp. 1–6.

[63] R. Zhang, X. Cheng, Q. Yao, C.-X. Wang, Y. Yang, and B. Jiao, "Interference graph-based resource-sharing schemes for vehicular networks," *IEEE Transactions on Vehicular Technology*, vol. 62, no. 8, pp. 4028–4039, 2013.

[64] Y. Ren, F. Liu, Z. Liu, C. Wang, and Y. Ji, "Power control in D2D-based vehicular communication networks," *IEEE Transactions on Vehicular Technology*, vol. 64, no. 12, pp. 5547–5562, 2015.

[65] Z. Liu, J. Su, Y.-a. Xie, Y. Yuan, Y. Yang, and X. Guan, "Distributed robust power control in two-tier vehicle networks under uncertain channel environments," *Digital Communications and Networks*, 2022.

[66] N. Du, C. Zhou, and X. Ma, "A novel subchannel and power allocation algorithm in V2V communication," *Wireless Communications and Mobile Computing*, vol. 2021, 2021.

[67] R. Zhang, X. Cheng, L. Yang, and B. Jiao, "Interference-aware graph based resource sharing for device-to-device communications underlaying cellular networks," in *proceedings of the IEEE Wireless Communications and Networking Conference*, 2013, pp. 140–145.

[68] S. Amari and R. Misra, "Closed-form expressions for distribution of sum of exponential random variables," *IEEE Transactions on Reliability*, vol. 46, no. 4, pp. 519–522, Dec 1997.

[69] A. Papoulis and S. U. Pillai, *Probability, random variables, and stochastic processes*. Tata McGraw-Hill Education, 2002.

[70] A. Jeffrey and D. Zwillinger, *Table of Integrals, Series, and Products*. Academic Press, 2000, vol. 6.

[71] *Technical Specification of LTE; Evolved Universal Terrestrial Radio Access (E-UTRA); Physical channels and Modulation*, 3GPP TS 36.211 version 11.3.0 Release 11, 07 2013.

[72] C. Hucher and P. Sadeghi, "Embracing asynchronism: Achieving cooperative diversity using zigzag interference cancellation," *IEEE Transactions on Wireless Communications*, vol. 11, no. 9, pp. 3240–3249, 2012.

[73] X. Ma, R. Yin, G. Yu, and Z. Zhang, "A distributed relay selection method for relay assisted device-to-device communication system," in *proceedings of the IEEE 23rd International Symposium on Personal, Indoor and Mobile Radio Communications*, 2012, pp. 1020–1024.

[74] Y. Ni, S. Jin, W. Xu, Y. Wang, M. Matthaiou, and H. Zhu, "Beamforming and interference cancellation for D2D communication underlaying cellular networks," *IEEE Transactions on Communications*, vol. 64, no. 2, pp. 832–846, 2016.

[75] H. Ghavami and S. S. Moghaddam, "Outage probability for underlaying device to device communications," in *proceedings of the 8th International Symposium on Telecommunications*. IEEE, 2016, pp. 353–358.

[76] B. Kumbhani and R. S. Kshetrimayum, "Outage probability analysis of spatial modulation systems with antenna selection," *Electronics Letters*, vol. 50, no. 2, pp. 125–126, 2014.

[77] M. Milisic, M. Hamza, and M. Hadzialic, "BEP/SEP and outage performance analysis of L-branch maximal-ratio combiner for $\kappa-\mu$ fading," *International Journal of Digital Multimedia Broadcasting*, 2009.

[78] L. V. Nguyen, B. C. Nguyen, X. N. Tran, and L. T. Dung, "Closed-form expression for the symbol error probability in full-duplex spatial modulation relay system and its application in optimal power allocation," *Sensors*, vol. 19, no. 24, 2019. [Online]. Available: https://www.mdpi.com/1424-8220/19/24/5390

[79] D.-T. Do, M.-S. V. Nguyen, and B. M. Lee, "Outage performance improvement by selected user in D2D transmission and implementation of cognitive radio-assisted NOMA," *Sensors*, vol. 19, no. 22, 2019. [Online]. Available: https://www.mdpi.com/1424-8220/19/22/4840

[80] K. Gomadam, V. R. Cadambe, and S. A. Jafar, "A distributed numerical approach to interference alignment and applications to wireless interference networks," *IEEE Transactions on Information Theory*, vol. 57, no. 6, pp. 3309–3322, 2011.

[81] M. Abramowitz and I. A. Stegun, *Handbook of Mathematical Functions with Formulas, Graphs, and Mathematical Tables*. New York: Dover, 1972.

[82] A. Goldsmith, *Wireless Communications*. Cambridge University Press, 2005.

[83] Y. Ren, F. Liu, Z. Liu, C. Wang, and Y. Ji, "Power control in D2D-based vehicular communication networks," *IEEE Transactions on Vehicular Technology*, vol. 64, no. 12, pp. 5547–5562, 2015.

[84] A. Olutayo, H. Ma, J. Cheng, and J. F. Holzman, "Level crossing rate and average fade duration for the Beaulieu-Xie fading model," *IEEE Wireless Communications Letters*, vol. 6, no. 3, pp. 326–329, 2017.

[85] A. Olutayo, J. Cheng, and J. Holzman, "Asymptotically tight performance bounds for selection diversity over Beaulieu-Xie fading channels with arbitrary correlation," in *proceedings IEEE International Conference on Communications*, 2017, pp. 1–6.

[86] ——, "Asymptotically tight performance bounds for equal-gain combining over a new correlated fading channel," in *proceedings of the 15th Canadian Workshop on Information Theory*, 2017, pp. 1–5.

[87] J. Hu, Z. Zhang, L. Wu, J. Dang, and G. Zhu, "Outage analysis of AF-based mixed Beaulieu-Xie and Gamma-Gamma transmission systems," in *proceedings of the 11th International Conference on Wireless Communications and Signal Processing*, 2019, pp. 1–5.

[88] H. S. Silva, D. B. T. Almeida, W. J. L. Queiroz, I. E. Fonseca, A. S. R. Oliveira, and F. Madeiro, "Cascaded double Beaulieu-Xie fading channels," *IEEE Communications Letters*, vol. 24, no. 10, pp. 2133–2136, 2020.

[89] M. B. Tsegay, K. Dhaka, and R. Bhattacharjee, "Performance analysis of a relay-assisted D2D underlay cellular network," in *proceedings of the National Conference on Communications*, 2022, pp. 397–401.

[90] J. Hu, Z. Zhang, J. Dang, L. Wu, and G. Zhu, "Performance of decode-and-forward relaying in mixed Beaulieu-Xie and $\mathcal{M}$ dual-hop transmission systems with digital coherent detection," *IEEE Access*, vol. 7, pp. 138 757–138 770, 2019.

[91] H. Bateman, *Higher Transcendental Functions*. New York, USA: McGraw-Hill, 1953, vol. 1.

[92] G. Fodor, E. Dahlman, G. Mildh, S. Parkvall, N. Reider, G. Miklós, and Z. Turányi, "Design aspects of network assisted device-to-device communications," *IEEE Communications Magazine*, vol. 50, no. 3, pp. 170–177, 2012.

[93] W. Sun, E. G. Ström, F. Brännström, K. C. Sou, and Y. Sui, "Radio resource management for D2D-based V2V communication," *IEEE Transactions on Vehicular Technology*, vol. 65, no. 8, pp. 6636–6650, 2016.

[94] M. Botsov, M. Klügel, W. Kellerer, and P. Fertl, "Location dependent resource allocation for mobile device-to-device communications," in *proceedings of the IEEE Wireless Communications and Networking Conference*, 2014, pp. 1679–1684.

[95] L. Liang, S. Xie, G. Y. Li, Z. Ding, and X. Yu, "Graph-based radio resource management for vehicular networks," in *proceedings of the IEEE International Conference on Communications*. IEEE, 2018, pp. 1–6.

[96] L. Liang, G. Y. Li, and W. Xu, "Resource allocation for D2D-enabled vehicular communications," *IEEE Transactions on Communications*, vol. 65, no. 7, pp. 3186–3197, 2017.

[97] P. S. Bithas, G. P. Efthymoglou, and A. G. Kanatas, "Intervehicular communication systems under co-channel interference and outdated channel estimates," in *proceedings of the IEEE International Conference on Communications*, 2016, pp. 1–6.

[98] H. Ilhan, "Performance analysis of cooperative vehicular systems with co-channel interference over cascaded Nakagami-m fading channels," *Wireless Personal Communications*, vol. 83, 07 2015.

[99] G. T. Pitsiladis, D. Papanikolaou, A. D. Panagopoulos, and C. Antoniou, "Vehicle-to-vehicle communication: End-to-end performance evaluation in dense propagation environments," in *proceedings of the 9th European Conference on Antennas and Propagation*. IEEE, 2015, pp. 1–5.

[100] Y. Alghorani and M. Seyfi, "On the performance of reduced-complexity transmit/receive-diversity systems over MIMO-V2V channel model," *IEEE Wireless Communications Letters*, vol. 6, no. 2, pp. 214–217, 2017.

[101] *Wolfram Research Inc., Mathematica Edition [Online].* Source link: https://functions.wolfram.com/HypergeometricFunctions/HypergeometricU/.

[102] P. Ioannou, *Automated Highway Systems.* Springer US, 2013.

List of Publications

National and International Conferences

- Mahari B.Tsegay, Kalpana Dhaka, and Ratnajit Bhattacharjee, "**Interference Cancellation in Multiple D2D Underlaying LTE Cellular Networks**," in *proceedings of the 4th International Conference on Computer, Communication and Signal Processing*, Chennai, India, 2020, pp. 1-5.
- Mahari B.Tsegay, Kalpana Dhaka, and Ratnajit Bhattacharjee, "**Performance Analysis of a Relay-Assisted D2D Underlay Cellular Network**," in *proceedings of the National Conference on Communications*, Mumbai, India, 2022, pp. 397-401.
- Mahari B.Tsegay, Kalpana Dhaka, and Ratnajit Bhattacharjee, "**Performance analysis of D2D-based V2V Communication System**," (in preparation).

International Journals

- Mahari B.Tsegay, Kalpana Dhaka, and Ratnajit Bhattacharjee, "**Performance Analysis of Underlay DF Relay System under Beaulieu-Xie Fading**," (in preparation).